INTERNATIONAL ATOMIC ENERGY AGENCY
UNITED NATIONS EDUCATIONAL, SCIENTIFIC AND CULTURAL ORGANIZATION
INTERNATIONAL CENTRE FOR THEORETICAL PHYSICS
I.C.T.P., P.O. BOX 586, 34100 TRIESTE, ITALY, CABLE: CENTRATOM TRIESTE

H4.SMR/473-18

COLLEGE ON NEUROPHYSICS

"Neural correlates of behaviour, development, plasticity and memory"

1-19 October 1990

Functional reorganization of primary somatosensory cortex in adult owl monkeys after behaviorally controlled tactile stimulation

W. J. Jenkins, Michael M. Merzenich, Marlene T. Ochs
Terry Allard and Eliana Guic-Robles
University of California
San Francisco, California USA

M M. MERZENICH

JOURNAL OF NEUROPHYSIOLOGY
Vol. 63, No. 1, January 1990. *Printed in U.S.A.*

Functional Reorganization of Primary Somatosensory Cortex in Adult Owl Monkeys After Behaviorally Controlled Tactile Stimulation

WILLIAM M. JENKINS, MICHAEL M. MERZENICH, MARLENE T. OCHS, TERRY ALLARD, AND ELIANA GUÏC-ROBLES
Coleman Laboratory, University of California at San Francisco, San Francisco, California 94143-0732

SUMMARY AND CONCLUSIONS

1. Multiple microelectrode maps of the hand representation within and across the borders of cortical area 3b were obtained before, immediately after, or several weeks after a period of behaviorally controlled hand use. Owl monkeys were conditioned in a task that produced cutaneous stimulation of a limited sector of skin on the distal phalanges of one or more fingers.

2. Analysis of microelectrode mapping experiment data revealed that *1*) stimulated skin surfaces were represented over expanded cortical areas. *2*) Most of the cutaneous receptive fields recorded within these expanded cortical representational zones were unusually small. *3*) The internal topography of representation of the stimulated and immediately surrounding skin surfaces differed greatly from that recorded in control experiments. Representational discontinuities emerged in this map region, and "hypercolumn" distances in this map sector were grossly abnormal. *4*) Borders between the representations of individual digits and digit segments commonly shifted. *5*) The functionally defined rostral border of area 3b shifted farther rostralward, manifesting either an expansion of the cutaneous area 3b fingertip representation into cortical field 3a or an emergence of a cutaneous input zone in the caudal aspect of this normally predominantly deep-receptor representational field. *6*) Significant lateralward translocations of the borders between the representations of the hand and face were recorded in all cases. *7*) The absolute locations—and in some cases the areas or magnifications—of representations of many skin surfaces not directly involved in the trained behavior also changed significantly. However, the most striking areal, positional, and topographic changes were related to the representations of the behaviorally stimulated skin in every studied monkey.

3. These experiments demonstrate that functional cortical remodeling of the S1 koniocortical field, area 3b, results from behavioral manipulations in normal adult owl monkeys. We hypothesize that these studies manifest operation of the basic adaptive cortical process(es) underlying cortical contributions to perception and learning.

INTRODUCTION

One of the key features of the study of behavior and its underlying neural mechanisms is an understanding of the dynamic properties of the nervous system that normally allow behavior to adapt in response to experience. Biologists and psychologists have long assumed that plasticity must be an inherent, lifelong property of the nervous system. A major research focus until recently has been on the role of early experience in the developing nervous system. One consequence of these important studies has been the emergence of the general view that beyond a critical period(s) in development, the nervous system becomes a fixed system not amenable to structural or substantial functional changes in response to experience. That view is currently being challenged.

Neocortical representations of the body surface in adult primates reorganize in response to alterations in the patterns of activation of sensory elements within the skin. Several classes of surgical manipulations in the periphery have been used to produce altered patterns of sensory input. One group of recent experiments indicates that when a subset of these sensory elements is silenced by either restricted deafferentation or amputation, there is an extensive reorganization or "remapping" of the remaining active inputs (Kelahan and Doetsch 1984; Merzenich et al. 1983a,b, 1984b; Rasmusson 1982; Wall et al. 1984, 1986). In those studies, neurons everywhere across a large cortical region, including both the former zone of representation of the transected, nonregenerating nerve(s) and an extensive surrounding cortical zone, acquire new, effective excitatory afferent inputs. Several consistent features of this emergent representation of the skin have been observed. First, within these new maps, the internal topographic representations are usually orderly. Microelectrode penetration sequences across the horizontal dimension of the cortex commonly reveal a continuously shifting overlap of cutaneous receptive fields. Second, many of the newly emergent receptive fields do not overlap with receptive fields defined for neurons at those same locations before the peripheral deprivation. That is, some skin surfaces come to be overtly represented at entirely new cortical locations. Third, for some specific skin surfaces, the cortical territory of representation within the reorganized cortical zone is enlarged. Fourth, the relationship between the cortical area of representation and the size of receptive fields recorded for specific skin surfaces is roughly inverse. That is, as the cortical magnification increases for specific skin surfaces, those skin surfaces come to be represented in a finer grain.

A second related class of experiments has explored the consequences of plastic surgical manipulation of skin that greatly alters its spatiotemporal patterns of input (Clark et al. 1986, 1988). Normal behavioral uses of the hand produce substantially independent temporal and spatial patterns of activation of sensory primary afferents innervating adjacent fingers. Interestingly, borders between adjacent

digits in the area 3b cortical representation of the hand in adult owl monkeys are normally very abrupt. As a rule, in this species, receptive fields for closely placed recording sites across digit representation borders are located on either one digit or another–but rarely on both–digits. When two digits are surgically fused to produce a "syndactyly" by a procedure that minimizes peripheral nerve damage, behavioral use of the hand produces now-synchronized patterns of activation within a large group of sensory afferents innervating both of the two fused digits. Apparently as a consequence, the normally abrupt representational border between these two digits is eliminated (Clark et al. 1988). In such monkeys, all neurons in a wide cortical band occupying approximately one-third of the cortical area within area 3b representing the two fused digits came to respond to stimulation of the skin on both digits.

Substantial alterations in the topographies of cortical representations are also observed after the transfer of an innervated patch of skin from one digit to another (Clark et al. 1986). In these "neurovascular island transfer" experiments, there is a novel temporal and spatial coactivation of the island skin with the newly surrounding skin. After such island transfers, novel RF's are created that encompass both island skin and joined neighboring skin. In addition, new topographic relationships emerge in the cortical representation of the manipulated hand such that the overt representation of some skin surfaces are translocated within area 3b. More recently, island transfers spanning several intermediate digits indicate that reorganizational translocations are possible over 2- to 3-mm distances within cortical area 3b (Merzenich et al. 1988). In both the syndactyly and neurovascular island transfer studies, control experiments indicate that these effects are central in origin and not the result of peripheral nerve sprouting or mechanical coupling artifact.

We have suggested that the alterations of the mapped distributions of effective excitatory sensory inputs after these surgical manipulations provide strong evidence that cortical representational maps in adults are "use dependent" (Clark et al. 1988; Jenkins et al. 1987, 1990; Merzenich et al. 1983a–1984b; 1987; 1988). According to this view, thalamocortical and potentially corticocortical connections provide inputs from broader regions of the skin than is evident in the effective excitatory inputs defined by conventional extracellular electrophysiological recordings (see Merzenich et al. 1988; also see Garraghty and Sur 1987; Hicks and Dykes 1983; Snow et al. 1988; Zarzecki et al. 1982, 1983). Corticocortical connections also have extensive long-range focal collateralization both within and between the architectonic areas of primary somatic sensory cortex (De Felipe et al. 1986).

These and related studies in other sensory and motor cortical areas suggest that the effective excitatory inputs evident in the discharges of cortical neurons represent only a small functionally effective subset of inputs derived from a far larger, largely masked anatomic repertoire. An "input selection" or "input filtering" process presumably underlies receptive-field determination and the functional dynamism observed in cortical maps. The results of the surgical manipulations described above suggest that alterations in the temporal correlation and amounts of activity across distributed inputs are critical factors in this input selection or input filtering process. By this view, an electrophysiologically derived cortical map of the skin surface can be thought to represent the cumulative effects of the history of behaviorally important spatiotemporal patterns of skin stimulation.

The present experiments were designed to test the reorganizational potential of cortical area 3b in normal adult owl monkeys. We used behavioral conditioning techniques to produce large amounts of tactile stimulation restricted to a limited patch of skin. Such restricted tactile stimulation is presumed to produce high activity levels in a subset of thalamocortical afferents extending across a cortical sector larger than the cortical region overtly representing this patch of skin before stimulation. Furthermore, the applied tactile stimulation would induce nearly synchronous activity across this limited afferent subset. At the same time, other thalamocortical afferents that derive their inputs from regions of the hand not engaged in the behavioral task would have relatively lower levels of activity. Activity-dependent temporal coactivation of afferents has previously been implicated in reorganization in retinotectal maps (e.g., Schmidt and Edwards 1983; Wilshaw and von der Malsburg 1975), has been argued to be the basis for ocular dominance column formation in visual cortex (Chapman et al. 1986; Reiter et al. 1986; Stryker et al. 1982, 1986a,b), and constitutes an integral property of several neural network models of cortical function (e.g., see Edelman et al. 1978, 1981, 1984; Frohn et al. 1987; Grajski 1989; Pearson et al. 1987; Singer 1985, 1987; Takeuchi and Amari 1979; von der Malsburg et al. 1973, 1982). As a consequence of such behaviorally controlled tactile stimulation, the quantities of synchronous or nearly synchronous neural activity in subpopulations of afferents terminating in the same cortical zone could be substantially altered. If the process(es) by which cortical receptive fields and the details of cortical topographic representations operate dynamically throughout life, then this behaviorally controlled differential stimulation should alter cortical-map topography in normal adult owl monkeys. That has been found to be the case.

Preliminary results from a part of this study have been reported previously (Jenkins et al. 1984, 1987; Merzenich et al. 1988).

METHODS

Surgical and recording procedures

These studies were conducted with six feral adult owl monkeys. Although their exact age was unknown, they were judged to be adult by their weights (~1 kg) and their full complement of adult dentition (Hershkovitz 1977). All animals were neurologically intact and had no previous experimental use.

In physiological studies, animals were initially anesthetized with halothane (1.5%) in a 75% NO_2-25% O_2 gas mixture to allow for placement of a venous catheter. They were subsequently anesthetized with pentobarbital sodium (initial dose at 28 mg/kg iv) and maintained at a surgical level of anesthesia with iv supplementation. Heart rate and blood pressure were monitored. Lactated Ringer solution with 5% dextrose was given at the rate of ~2 ml/h, adjusted if indicated by cardiovascular system monitoring. Temperature was maintained at 38°C. The cortical mapping procedures employed in these studies have been described in several

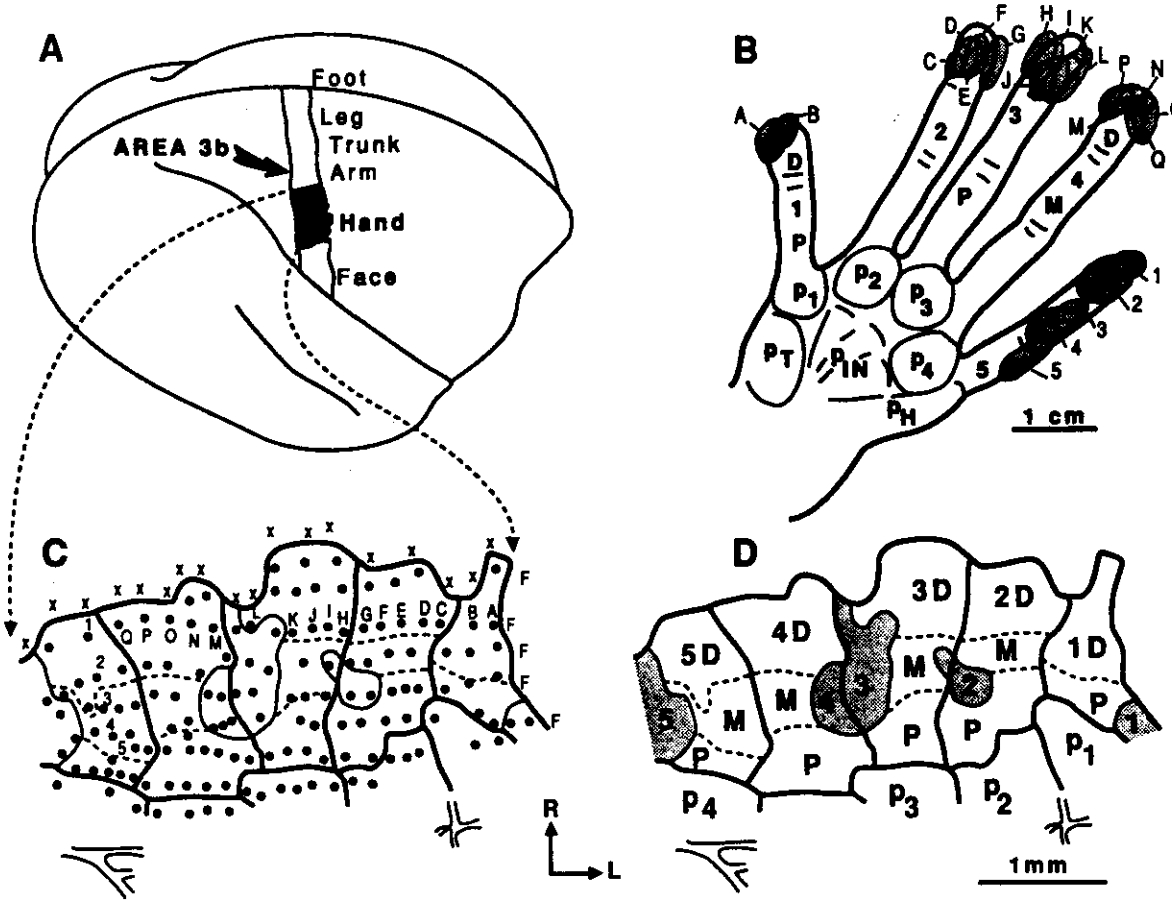

FIG. 1. Location and topographic representation of the hand within area 3b in a normal adult owl monkey. *A*: lateral view of the right neocortex. Approximate location of area 3b is outlined. Large cutaneous representation of the hand is indicated by stippling and is located medial to the representation of the face and lateral to that of the remainder of the body surface representation. *B*: outline of the glabrous hand surface in a normal adult owl monkey, with 2 typical sequences of receptive fields (from sites 1–5 and A–Q in *C*) drawn. Large numbers 1–5 denote the digits (e.g., 1 = thumb; D, M, and P are distal, middle, and proximal phalanges, respectively); p_{1-4} are the palmar pads at the base of the digits; p_H is the hypothenar eminence; p_T is the thenar eminence; and p_{IN} refers to the 3 insular pads. *C*: locations of 174 penetration sites from which the topographic representation of the hand surfaces shown in *D* were reconstructed. Numbers 1–5 and letters A–Q adjacent to penetration sites indicate locations at which the cutaneous receptive fields shown in *B* were obtained. Lines are boundaries between the territories of representation of different hand surfaces shown in *D*. Note that the map has been rotated 90° counterclockwise with respect to *A*. *D*: diagrammatic illustration of the representation of hand surfaces. Stippled zones indicate dorsal (hairy) skin on the digits. Solid lines outline territories of representation of the digits and palmar pads. Broken lines mark the borders between phalangeal representational zones. Distal digit tips are represented along the rostral margin of area 3b. More proximal portions of the digits and palm are represented at successively more caudal locations within area 3b.

earlier reports (Merzenich et al. 1983a,b, 1984b, 1987; Stryker et al. 1987). Briefly, the monkey was placed in a stereotaxic head holder and the hand representation zone in area 3b exposed by a parietal craniotomy and dural resection. A photograph of the brain surface vasculature was taken, and a 35–40× print made for siting microelectrode penetrations. The exposed cortex was bathed in a shallow well of sterile liquid silicone (dimethyl polysiloxane) throughout the course of the experiment.

Parylene C–coated tungsten electrodes with impedances of 1–2 MΩ at 1 kHz were used for recording neural responses. Electrode penetrations in each experiment were approximately normal to the cortical surface and were parallel to each other. Each electrode penetration site was marked on the brain photograph. Receptive fields were determined for neurons or small clusters of neurons in the middle cortical layers (~600–1,000 μm in depth) with the use of fine handheld blue glass probes to produce just-visible indentations of the skin. The tips of these probes were hemispherical in shape with a diameter of ~0.5 mm. All fields were carefully drawn to scale on enlarged hand photographs. In exemplary fields, the field boundaries were also explored with the use of suprathreshold nylon monofilament von Frey hairs (Stoelting pressure aesthesiometer, No. 18011) that apply indenting stimuli at a relatively constant, predetermined force. The most commonly used von Frey hair was 0.2 mm diameter with a 0.5-g bending force and 15.92 g/mm² bending pressure.

In experiments in which two (and in 1 monkey, 3) maps were derived in the same animal, all but the final electrophysiological recordings were conducted with the use of strict sterile procedures. In these special preparations, the removed bone flap was refrigerated in sterile Ringer solution; at the end of these recording experiments, the dura was resutured and the bone flap replaced with the use of stainless steel sutures. Antibiotics were administered before and for several days after surgery as a prophylactic. Analgesics were administered through the brief recov-

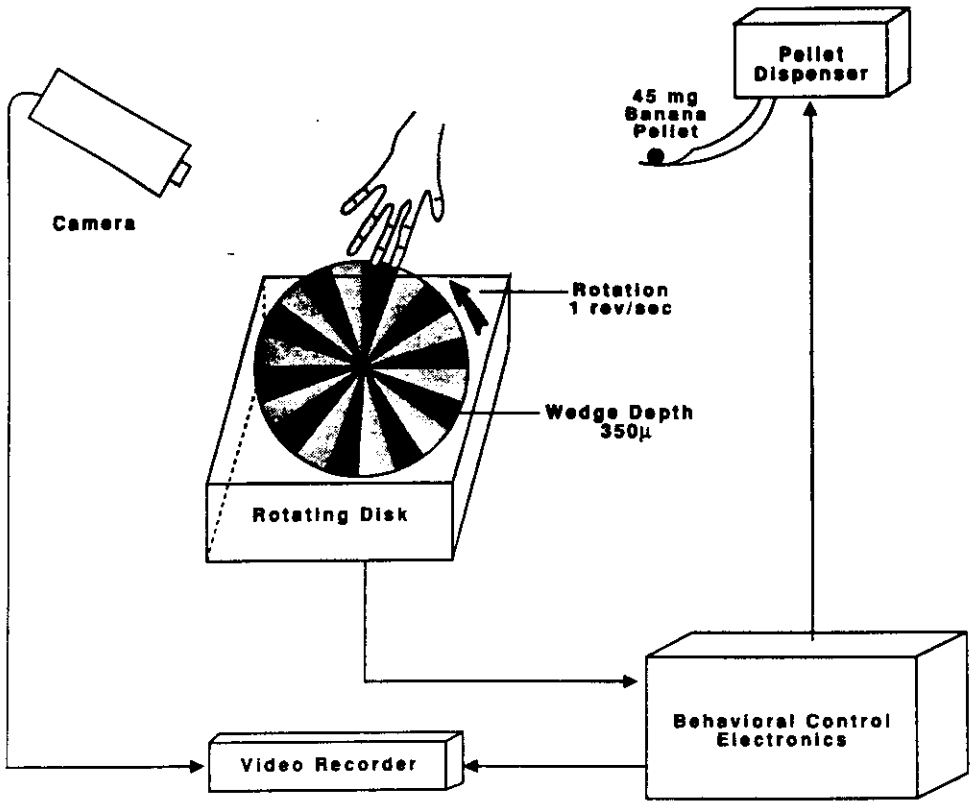

FIG. 2. Behavioral apparatus that required the monkey to maintain contact with a rotating stimulus disk for ~10–15 s per banana pellet reward. Only the distal aspect of the distal segment of ≥1 digits contacted the disk. Ten wedge-shaped groves 350 μm deep were machined into the metal disk. Disk, in most experiments, was continuously rotating at 1 rev/s, providing the contacted digital skin with edges moving across the digit at a rate of 20 Hz.

ery period. All procedures were conducted within an approved recovery surgical facility. Recovery was uneventful in every experimental case.

As has been noted in earlier studies (Merzenich et al. 1983a,b), the initial time-limited sterile mapping procedure had no obvious effect on the responsiveness of cortical neurons. No surface damage was seen at the time of the second exposure of the hand representation. Vascular details recorded in the initial procedure provided a clear reference in the second.

Data analysis

The details of construction of hand representation maps have been described elsewhere (Merzenich et al. 1987) and are described in RESULTS. Briefly, hand representation maps were drawn by outlining cortical areas over which receptive fields were centered over given skin surfaces. The delimiting lines in these maps were drawn between penetration sites with receptive fields centered on different labeled skin areas (see Fig. 1). Where receptive fields overlapped onto different skin surfaces, the line position was biased to reflect the extent of that overlap. The degree of error inherent in defining the representational areas was small (see Merzenich et al. 1987 and Stryker et al. 1987 for a discussion of the sources and dimensions of errors in mapping by the use of these procedures). The possible errors in the measurement of representational area associated with the spacing of the microelectrode grid were very small compared with the plasticity observed in this study (see Stryker et al. 1987).

In all cases except *OM 2*, one map was derived either before initiation of behavioral training or immediately after the behavior, and a second map was derived either immediately after the behavior or several weeks after cessation of the experimental behavioral task. Thus, in five monkeys, maps derived at these different times allow each animal to serve as its own control. All measurements of cortical area and receptive-field size were derived with use of a computerized planimeter.

Behavioral apparatus and procedures

The tactile stimulus delivery device illustrated in Fig. 2 consisted of a 12.8-cm-diam aluminum disk that had been machined to produce an alternating pattern of raised and lowered surfaces. The pattern consisted of 20 pie-shaped wedges that alternated in depth by 350 μm. This disk was attached to a gear motor that was rotated at the rate of 1 rev/s. The disk and the motor were housed in a small metal enclosure from which a portion of the rotating disk protruded. The disk and motor were mounted in a frame on the animal's home cage that allowed for adjustments in the location of the disk relative to the front of the cage.

Animals were given free access to water and a vitamin C–enriched drink in their home cages. During extended periods of controlled tactile stimulation, food delivery was contingent on appropriate performance on the behavioral task. Initially, 24-h food-deprived monkeys were trained to make contact with the nonrotating aluminum disk. An electronic contact circuit between the disk and the animal's home cage allowed for the detection of finger contact with the disk, and brief contact resulted in the automated (Gerbands D-1) delivery of a 45-mg banana-flavored food pellet (Bio-Serv F0059). The pellets appeared in a small pellet chute (BRS/LVE RPC-001) mounted at the front of the cage on the left-hand side of the centrally located disk apparatus. Retrieval of the pellets occurred by use of one or both hands or, more commonly, by the monkey licking the pellet out of the chute while keeping the hand and arm extended toward the disk apparatus. The nutritional content of the food pellets was comparable with the primate chow fed to other monkeys in our colony. The contact duration necessary for the delivery of a food pellet was gradually increased to 15 s. At this point in training, the position of the disk was progressively moved farther away from the front of the cage until the monkey could only contact the disk surface with the tips of one or two of the longest digits. At this stage, the dc motor was switched on and the disk rotated at the rate of 1 rev/second. Because of the increased difficulty in main-

taining contact with the disk, the contact duration necessary for pellet delivery was reduced to ~1 s. The increased difficulty of this task was because of the fact that the animal had to regulate contact pressure to maintain reliable finger contact with the disk; and excessive finger pressure resulted in the digits being carried along the path of disk rotation and eventually breaking disk contact. Monkeys gradually learned to regulate contact pressure, and the minimum contact duration was gradually increased to 15 s once more. Naive monkeys were trained to the final behavioral contingencies over the course of ~10 days. The rotating disk was continuously available to the monkey and, therefore, allowed the animals to obtain as many pellets as they cared to work for. These procedures resulted in ~600 banana pellets being delivered within a 24-h period.

The total disk contact time and the total number of delivered banana pellets were recorded daily. The monkey's hand contact was also videotaped during periods of disk contact. Analysis of the videotape recordings revealed that all of these monkeys used a single hand exclusively in this behavioral task. After the first few days, for each individual monkey, the motor patterns and skin surfaces stimulated during disk contact appeared the same throughout the course of behaviorally controlled tactile stimulation.

In two cases, a smooth, nonrotating disk was substituted for the wedge-patterned rotating disk over one training period. All other behavioral contingencies were identical for these monkeys.

RESULTS

Before describing the topographic representations of the surfaces of the hands in experimental cases, it is useful to review briefly the normal pattern of representation of the hand in area 3b in adult owl monkeys. Figure 1 illustrates the results of a typical area 3b mapping experiment from a normal (preexperimental behavior) adult owl monkey. A lateral view of the neocortex illustrating the location of area 3b within anterior parietal cortex in this monkey is shown in Fig. 1*A*. The location of the large cutaneous representation of the hand within this cortical area is indicated by stippling; it is located medial to the zone of representation of the face and lateral to the representation of the remainder of the body surface representation. The typical microelectrode map of the zone of representation of the fingers in cortical area 3b derived in this adult owl monkey is illustrated at the *bottom* of Fig. 1. At the *left* (*C*), parallel microelectrode penetration sites within the hand representation of area 3b are indicated by filled dots; penetrations across the rostral border of the cutaneous representation, in which neurons are driven only by higher threshold tactile stimulation and joint manipulation, are marked by Xs. In penetrations marked by Fs, receptive fields were exclusively on the skin surfaces of the face. Two typical sequences of glabrous receptive fields defined for neurons in the middle cortical layers at a series of cortical sites are shown in Fig. 1*B*. They illustrate the normal, orderly shifting-overlap topography of receptive-field sequences defined within closely spaced rows of penetrations across area 3b. Note that in lateral-to-medial penetration sequences (A–Q in Fig. 1, *B* and *C*), there was an orderly progression of cutaneous receptive-field locations across the radial-to-ulnar (1st digit-to-4th digit) surfaces of the hand digits. In rostral-to-caudal sequences, receptive fields shift in an orderly sequence from distal to proximal along the digits (in this example, down *digit 5*). Glabrous digit tips are represented along the extreme rostral border of area 3b in this monkey; the remainder of the digits are represented more caudally.

The borders defined between the cortical representation of adjacent digits were always sharp. With few exceptions, receptive fields defined for neurons flanking these representational discontinuities had receptive fields exclusively on the skin of one of the two adjacent digits. A similarly sharp functional boundary was defined between the representation of the radialmost surfaces of the hand and the face and between the cutaneous and higher threshold representations within cortical areas 3b and 3a, respectively. Again, all along these borders, receptive fields exclusively represented skin of either the hand or the face or were driven selectively by light tactile or by high threshold "deep" inputs, respectively. A topographic representation of these data is shown in Fig. 1*D*. Boundaries between areas 3b and 3a are drawn midway between penetrations in which cutaneous receptive fields were defined and penetrations at which only higher threshold, noncutaneous stimuli evoked neural activity. These high-threshold sites were defined by manual manipulation (to provide an adequate stimulus for joint or muscle afferents) or by vigorous tapping. At a small number of penetration sites rostral to the cutaneous area 3b representation, not even very vigorously applied stimuli evoked neural activity. These fields were interspersed with the deep response fields of functionally defined field 3a and hence were included within it in the following drawings.

In contrast to functional discontinuities observed between adjacent digits, receptive fields continuously shifted down the long axes of digits and across most of the representation of the palm. In the topographic drawing in Fig. 1*D*, boundaries between zones of representation of digit segments or palmar surfaces mark the lines over which equal parts of receptive fields fell on the two adjacent skin surfaces.

The observed cortical representation of the hand dorsum is indicated by stippling in the reconstructed map of the hand illustrated in Fig. 1*D*. These small islands of dorsum representation were embedded in the larger representation of glabrous digital skin surfaces. The representation of dorsal digits in this hand map was fragmented and incomplete, as is often the case (see Merzenich et al. 1987).

The hand representations within area 3b defined in all normal mapping experiments in this, as in earlier studies (Kaas et al. 1984; Merzenich et al. 1978, 1983a,b, 1987), share several common features. *1*) There was a single, complete representation of the glabrous hand surface in area 3b. *2*) The most distal aspects of the digits (the skin under the projecting fingernails) were represented along or near the functionally defined 3b-3a (cutaneous-deep) border. *3*) The more proximal digit skin surfaces were represented in topographic sequence in progressively more caudal portions of area 3b. *4*) The radial aspect of the hand (e.g., *digit 1*) was represented in the lateral part of the hand representation adjacent to the representation of the face. *5*) The more ulnar aspects of the hand were represented in topographic order in progressively more medial parts of area 3b. *6*) The cortical area devoted to the representation of each distal phalanx was always greater than the cortical

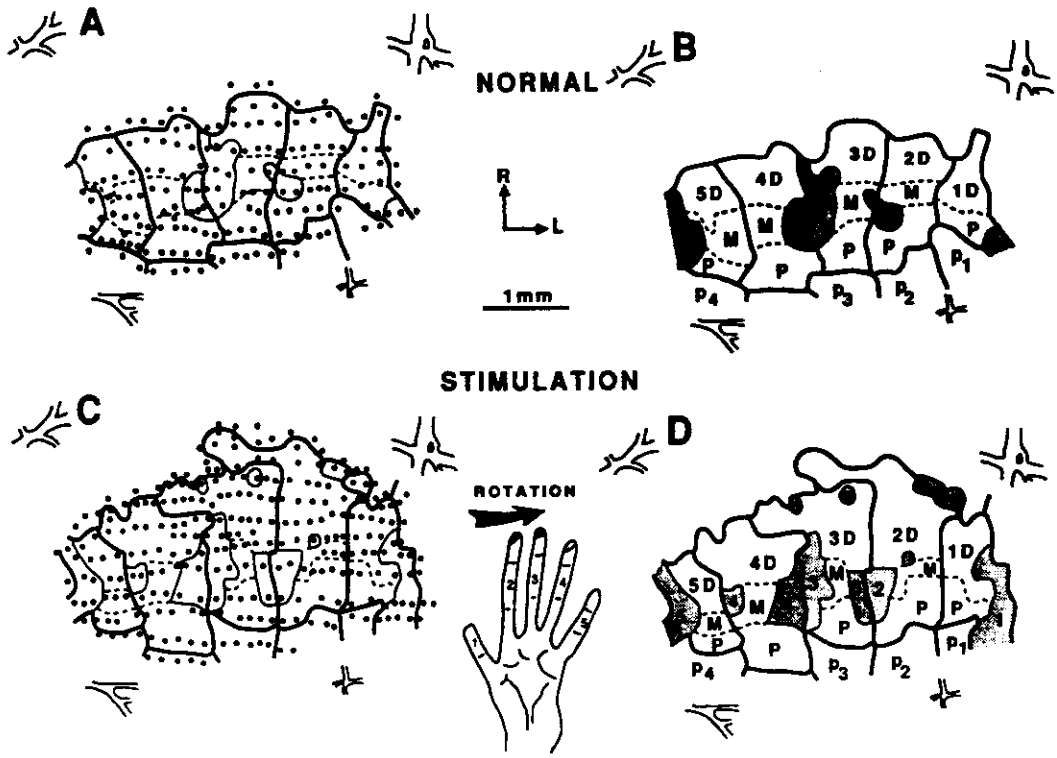

FIG. 3. *A*: penetration grid in and across the borders of the hand representation within area 3b in a normal adult owl monkey. *B*: reconstruction of the hand representation in area 3b for *OM 1* before differential stimulation. Map labels as in Fig. 1. *C*. penetration grid for a mapping experiment conducted 109 days after daily differential stimulation on the rotating disk, totaling ~1.5 h/day. *D*: poststimulation reconstruction of the hand representation. Skin surfaces differentially stimulated during the disk contact behavior are indicated in black on the hand inset at the *bottom center*. Skin surfaces on the tips of *digits 2* and *3* and occasionally the tip of *digit 4* were stimulated in the behavior in this monkey. Cortical representation of the stimulated skin surfaces expanded greatly in all such experiments (compare the distal aspects of *digits 2, 3,* and *4* in *B* and *D*).

area of representation of either the middle or proximal phalanx. *7*) The internal topographic order was maintained throughout the field, with very few receptive fields out of topographic sequence. *8*) The dorsal surfaces of *digit 1* were represented in the most lateral aspect of these maps and the dorsum of *digit 5* along the medial aspect of the glabrous representation. *9*) These and other dorsal skin surfaces were represented in a number of small, fragmented, discontinuous patches embedded in a much larger glabrous digital skin representation. *10*) The functionally defined borders within the cortical representation between adjacent digits were always sharp.

Reorganization of cortical representations after differential stimulation of restricted skin surfaces

The principal results recorded in this experimental series were that *1*) differentially stimulated skin surfaces had expanded cortical representations; *2*) the observed cutaneous receptive fields within these expanded cortical representational zones were often unusually small; *3*) the details of topographic representation of digit tips and subjacent skin on the proximal aspect of the distal phalanx and on the middle phalanx of differentially stimulated digits were unusual, with abnormal receptive-field overlap distances and with breaks in topography; *4*) there were unequivocal shifts in the representational borders between individual digits and digit segments; *5*) there were shifts in the functionally defined rostral 3b-3a (cutaneous-deep) border, reflecting an apparent expansion of the cutaneous hand representation; *6*) there were shifts in the borders between the representations of the hand and face, or between the representations of *digit 5* dorsum and glabrous skin, consistent with an overall expansion of the territory of cortex occupied by the representation of the digits; and *7*) there were substantial differences in representation of skin surfaces not directly involved in the behavior.

ENLARGEMENT OF THE CORTICAL REPRESENTATION OF STIMULATED SKIN. The results of two detailed microelectrode mapping experiments conducted before and immediately after differential tactile stimulation for *OM 1* are shown in Fig. 3. The locations of the 176 electrode penetration sites within and across the borders of the hand representation for this normal adult owl monkey before differential stimulation are shown in Fig. 3*A*. The overlying solid and dashed lines define the various borders between the zones of representation of specific skin surfaces. A reconstruction of the hand representation within area 3b from this normal adult owl monkey is shown in Fig. 3*B*. Note that the areal extents of cortical representation of the distal phalanges (labeled 1–5d) are of similar size. The cortical area representing the individual distal phalanges ranged from 0.28 to 0.48 mm^2 (also see Table 1).

TABLE 1. *Cortical areas and receptive field sizes*

Cortical Area, mm²					Receptive Field, mm²				
Digit 1	*Digit 2*	*Digit 3*	*Digit 4*	*Digit 5*	*Digit 1*	*Digit 2*	*Digit 3*	*Digit 4*	*Digit 5*
OM 1									
					No disk experience; map 1				
0.28	0.32	0.48	0.42	0.29	8.478 ± 3.598	7.345 ± 2.16	11.531 ± 4.234	8.658 ± 2.416	6.171 ± 2.519
					After 109 days of rotating disk; map 2				
0.36	0.92	0.64	0.53	0.23	6.894 ± 2.515	4.676 ± 2.181	4.995 ± 3.09	9.379 ± 6.107	6.654 ± 2.976
Map 2 as a percentage of map 1					*p*				
129	288	133	126	79	0.2626	0.0041	0.0001	0.7099	0.8609
OM 3									
					After 52 days of rotating disk; map 1				
0.56	0.69	1.24	0.67	0.40	19.595 ± 6.267	16.012 ± 8.908	8.981 ± 4.585	7.545 ± 4.031	14.562 ± 5.787
					80 days after terminating rotating disk; map 2				
0.62	0.67	0.71	0.66	0.44	13.665 ± 4.056	12.509 ± 7.989	11.217 ± 4.451	13.165 ± 4.786	11.659 ± 5.176
Map 1 as a percentage of map 2					*p*				
90	103	175	102	91	0.0016	0.1028	0.0526	0.0001	0.2198
OM 4									
					After 103 days of rotating disk; map 1				
0.46	0.60	1.03	0.66	0.36	7.961 ± 5.323	8.381 ± 4.166	6.866 ± 5.744	10.345 ± 5.107	10.058 ± 2.841
					31 days after terminating rotating disk; map 2				
0.48	0.58	0.38	0.51	0.33	10.085 ± 5.321	7.68 ± 4.71	8.781 ± 2.96	11.527 ± 7.776	5.849 ± 2.626
Map 1 as a percentage of map 2					*p*				
96	103	271	129	109	0.2677	0.588	0.2394	0.5478	0.0049
OM 5									
					No disk experience; map 1				
0.44	0.41	0.43	0.43	n.a.	7.578 ± 3.129	6.941 ± 2.231	8.369 ± 3.318	8.573 ± 2.956	
					After 74 days of static flat disk; map 2				
0.28	0.39	0.49	0.29	n.a.	6.404 ± 1.538	7.942 ± 3.37	6.953 ± 4.676	11.008 ± 8.084	
Map 2 as a percentage of map 1					*p* Map 1 vs. map 2				
64	95	114	67	n.a.	0.2747	0.2418	0.2541	0.3251	
					After 278 days of rotating disk; map 3				
n.a.	n.a.	0.77	0.47	n.a.	n.a.	6.949 ± 2.703	6.2 ± 3.079	5.912 ± 2.405	n.a.
Map 3 as a percentage of map 1					*p* Map 1 vs. map 3				
n.a.	n.a.	179	109	n.a.	n.a.	0.9918	0.0165	0.0046	n.a.

TABLE 1. *(Continued)*

Cortical Area, mm²					Receptive Field, mm²				
Digit 1	*Digit 2*	*Digit 3*	*Digit 4*	*Digit 5*	*Digit 1*	*Digit 2*	*Digit 3*	*Digit 4*	*Digit 5*
OM 6									
					After 580 days of rotating disk; map 1				
0.53	0.90	1.22	0.41	0.32	8.318 ± 3.843	5.352 ± 3.54	3.806 ± 1.545	7.869 ± 4.628	11.552 ± 3.447
					63 days after terminating rotating disk; map 2				
0.43	0.60	0.54	0.78	0.24	10.254 ± 5.73	11.675 ± 6.559	13.954 ± 5.924	11.971 ± 4.369	8.763 ± 2.37
Map 1 as a percentage of map 2					*p*				
123	150	226	53	133	0.3086	0.0001	0.0001	0.0135	0.0656

Values for receptive field are means ± SD. n.a., not applicable. Analysis of variance procedures were used to calculate *p* values.

The skin surfaces stimulated during 109 days of daily differential stimulation on the rotating disk lasting ~1.5 h/day are indicated in black on the hand *inset* (*bottom center*). Analysis of the videotapes obtained during disk contact indicates that the distal radial glabrous aspect of the distal phalanx of *digit 2* was always stimulated by the rotating disk. The distal glabrous aspect of the distal phalanx of *digit 3* was stimulated >50% of the time. The stippled skin surface on the distal phalanx of *digit 4* was stimulated <20% of the time. No other skin surfaces were directly stimulated during disk contact.

The penetration grid consisting of 264 recording sites for the mapping experiment conducted immediately after 109 days of daily differential stimulation on the rotating disk lasting ~1.5 h/day is shown in Fig. 3*C*. A reconstruction of the hand representation from this normal adult owl monkey after differential stimulation, principally of the distal aspect of *digit 2*, is shown in Fig. 3*D*. Note that the representations of the distal phalanges are no longer of similar size. The areal extents of cortical representation of the distal phalanges (labeled 1–5d) in this poststimulation map ranged from 0.23 to 0.92 mm². The largest absolute change in cortical representational area occurred for the most heavily stimulated (and 1st-stimulated) phalanx. Within area 3b, before tactile stimulation, the glabrous distal phalanx of *digit 2* was exclusively represented within a 0.32-mm² cortical zone; and, immediately after 109 days of tactile stimulation, it was represented within a 0.92-mm² cortical zone. This represents nearly a threefold increase in the cortical area representing the glabrous surface of this phalanx. Less striking changes in cortical representational area were seen for the other differentially stimulated skin surfaces. There was ~33% increase in the representational area of the distal phalanx of *digit 3*, and ~25% increase in the representational area of the distal phalanx of *digit 4*.

Reconstructions of area 3b hand representations for cases *OM 3, 4, 5*, and *6* are shown in Figs. 4 and 5. For cases *OM 3, 4*, and *6*, the first electrophysiological mapping experiments were conducted immediately after a period of behaviorally controlled disk stimulation. The hand *inset* for each case indicates the approximate skin surface stimulated by disk contact. For cases *OM 3, 4*, and *6*, a second mapping experiment was conducted after several weeks during which time there was no access to disk stimulation. *OM 5* was mapped before initiation of the behavioral task (Figure 5, *top left*) and again after several weeks of behaviorally controlled stimulation with a rotating disk (Figure 5, *bottom left*). In each case, the representational zone of the stimulated skin surfaces was greater immediately after controlled stimulation with the rotating disk as compared with the control maps. For each case, there was a distal phalanx on one digit that was always stimulated during disk contact. For those phalanges, the area of representation was 1.76–2.71 times larger than the area of representation observed in the control mapping experiments (see Table 1 for a summary).

An additional experiment was conducted in *OM 5* and *OM 2*. In these two cases, a nonrotating flat disk was substituted for the usual disk. All behavioral procedures were identical to those employed with the grooved rotating disk. Unlike the task with the rotating disk, no regulation of contact force was necessary for successful completion of a rewarded sequence, nor was there repetitive tactile stimulation during disk contact. Comparisons between the normal map and the map obtained immediately after several weeks of experience indicate little change in the areas of representation for the skin surfaces that contacted the static disk (for *OM 5* see Fig. 5 *top* and *middle left*). For *OM 5, digit 2* and *3* distal phalanges were 0.95 and 1.13 times normal, respectively. For *OM 2*, a mapping experiment was conducted only after disk training, because this animal did not recover from surgery, which was complicated by an undiagnosed chronic glomerulonephritis of unknown etiology. The results from this single mapping experiment did not suggest any unusual representational topography or differential enlargement of the behaviorally engaged skin surfaces.

CORTICAL MAGNIFICATION AS AN INDEX OF REPRESENTATIONAL CHANGE. One method of comparing the relative sizes of cortical representations is by calculating a "cortical magnification" factor. Cortical magnification is defined as

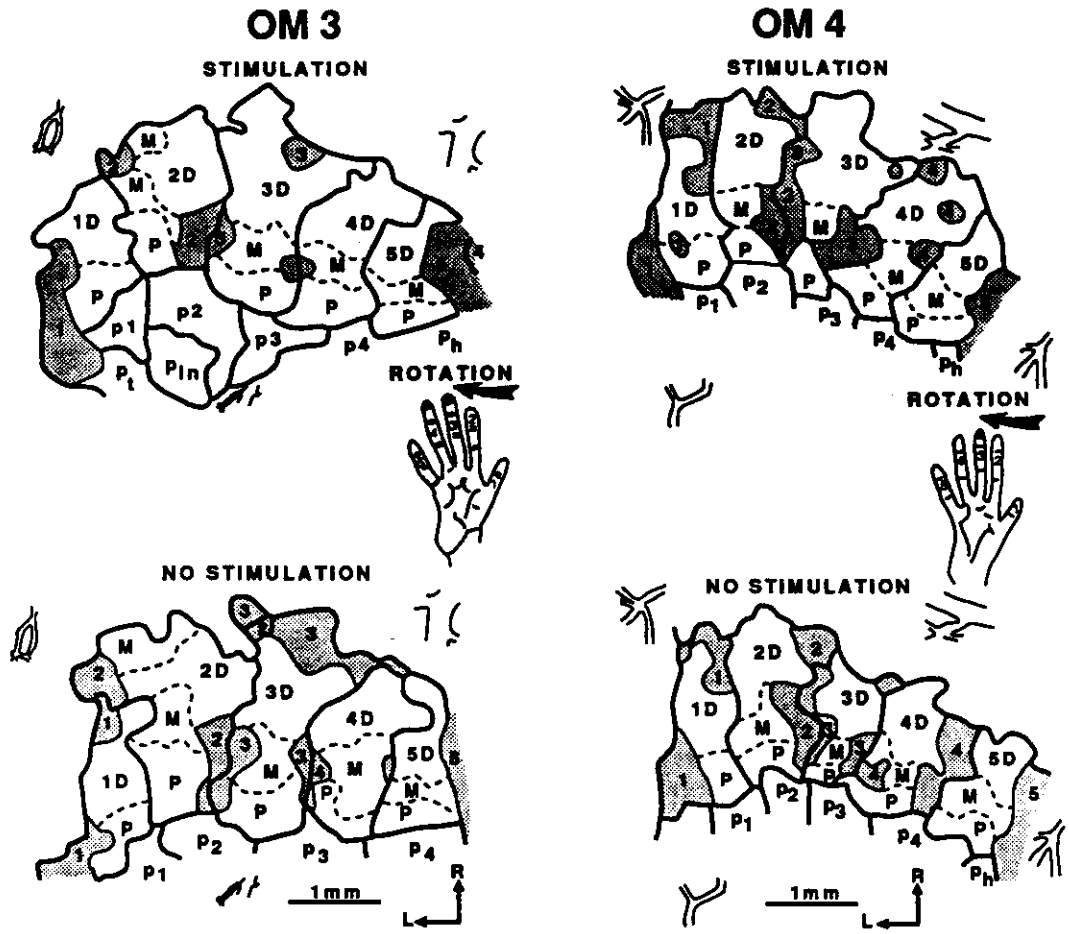

FIG. 4. Reconstructions of the hand representation for *OM 3* and *OM 4* immediately after differential stimulation with a rotating disk (*top*) and after 80 and 31 subsequent days without differential stimulation, respectively (*bottom*). Locations of the skin surfaces stimulated during disk contact are indicated in black on the hand figurines. Note that the cortical representations of the stimulated distal phalanges of *digit 3* in *OM 3* occupied a larger cortical area immediately after disk stimulation (*top left*) as compared with the map obtained 80 days later (*bottom left*). Similarly, the cortical representation of the stimulated distal phalanx of *digit 3* in *OM 4* occupied a larger cortical area immediately after disk stimulation (*top right*) as compared to the map obtained 31 days later (*bottom right*).

the cortical area of representation divided by the skin surface area. That is, cortical magnification is the proportional quantity defined as cortical area per unit hand-surface area. For the present purpose, we have calculated the cortical magnification factor of each phalanx by the use of the cortical areas of representation defined in normal- and differential-stimulation mapping experiments. Areal estimates of various skin surfaces were obtained from reconstructions based on multiple-perspective photographs of the hand (also see Sur et al. 1980). These cortical magnification factors for *OM 1* are depicted in Fig. 6, *top*, and for *OM 6* in Fig. 6, *bottom*. A linear transformation of cortical magnification factors (i.e., $\times 10^3$) was performed to facilitate ordinate labeling. The open symbols depict the cortical magnification factors for the glabrous phalanges on the basis of the cortical areas of representation defined in the "normal" mapping experiment (*OM 1*) or after a period of no stimulation (*OM 6*). The closed symbols depict the cortical magnification factors obtained on the basis of the poststimulation mapping experiments. Note that, for *OM 1* (Fig. 6, *top*), there has been a substantial increase in the cortical magnification factor for the distal phalanx of *digit 2*; progressively smaller increases were found for the distal phalanges of *digits 3* and *4*. Similar results were seen in *OM 6* (Fig. 6, *bottom*) and in all other cases immediately after behaviorally controlled stimulation with the rotating disk. Note also that, in these mapping experiments, little change in cortical magnification was observed for the representations of any other phalanges.

CHANGES IN RECEPTIVE-FIELD SIZES. In addition to the observed expanded cortical representation of the differentially stimulated skin, the cutaneous receptive fields within these cortical zones of representation were often unusually small. All of the defined glabrous cutaneous receptive fields located on the distal digit phalanges from two mapping experiments for *OM 1* are illustrated in Fig. 7. In the normal mapping experiment, the size of distal phalangeal receptive fields (Fig. 7, *top*) were not significantly different across digits [$F(4, 38) = 1.875$, $P = 0.1349$]. The mean receptive-field area on individual phalanges ranged from 7.3 to 11.5 mm^2.

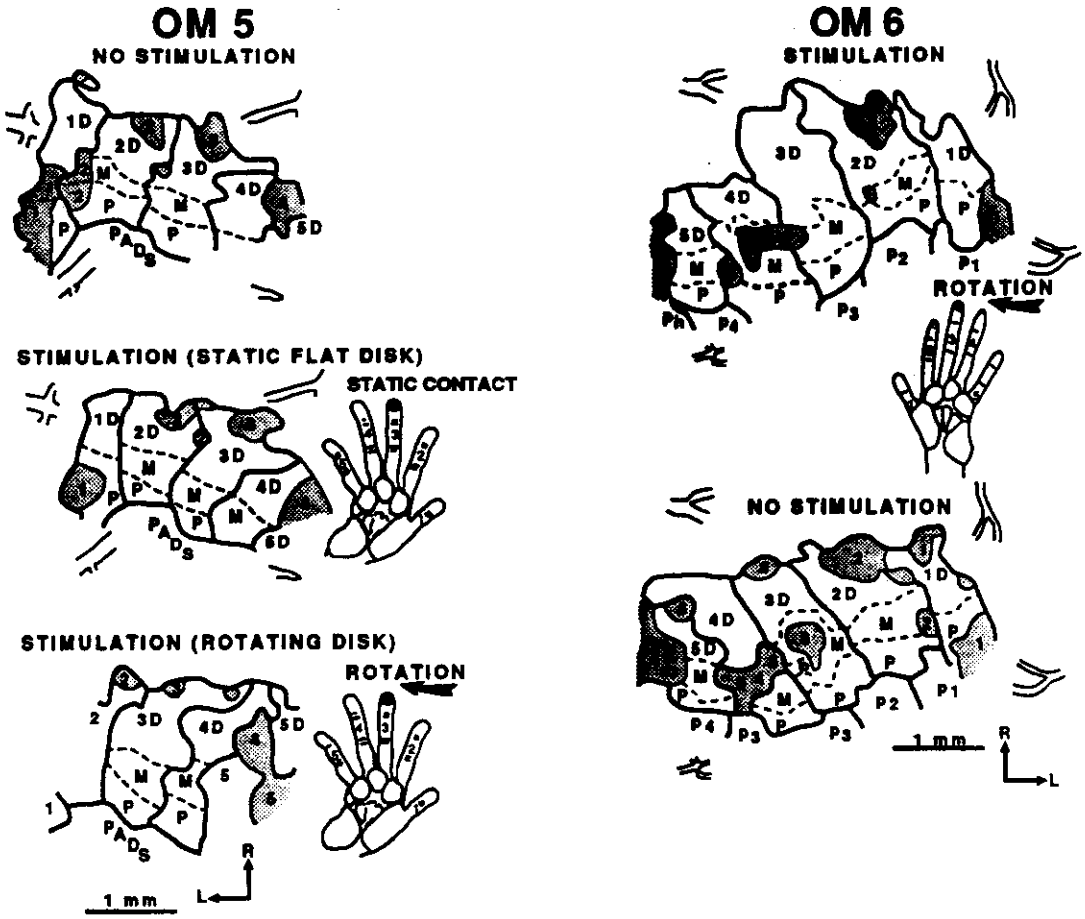

FIG. 5. Reconstruction of the hand representation within area 3b for *OM 5* is illustrated on the *left* before behavioral training (*top*), immediately after behaviorally controlled stimulation with the use of a static flat disk (*center*), and immediately after differential stimulation with a rotating disk (*bottom*). Hand representation within area 3b for *OM 6* is illustrated on the *right* immediately after differential stimulation with a rotating disk (*top*) and 63 days later (*bottom*). For each of the stimulation experiments, the location of the skin surfaces consistently stimulated during disk contact are indicated in black and by stippling for occasional disk contact on the hand figurines. Note that, for both cases, the cortical representation of the stimulated distal phalanx of *digit 3* occupied a larger cortical area immediately after disk stimulation as compared with the representation defined either before stimulation (*OM 5*) or that obtained 63 days later (*OM 6*). Note also that, after stimulation provided by the static flat disk, little obvious task-related alteration in the cortical representation of the hand was recorded.

Significant differences were observed in receptive-field sizes across the digits in the second mapping experiment [$F(4, 101) = 6.918$, $P < 0.0001$]. In the poststimulation mapping experiment, the distal phalangeal receptive fields were significantly smaller [$F(1, 104) = 22.95$, $P < 0.0001$] on the most heavily stimulated skin surfaces (*digits 2* and *3*; Fig. 7, *middle*). The mean receptive-field area on individual phalanges in this poststimulation mapping experiment ranged from 4.7 to 9.9 mm^2. Figure 7, *bottom*, is a histogram of the mean receptive-field area in square millimeters (bars indicate 1 SD). Receptive fields on the distal phalanges of *digits 2* and *3* were significantly smaller in the poststimulation map compared with the normal map for these two skin surfaces [digit 2, $F(1, 35) = 9.42$, $P < 0.005$; digit 3, $F(1, 44) = 32.54$, $P < 0.0001$]. In another case (*OM 5*) in which a normal and a poststimulation map were obtained, similar significant changes in receptive-field sizes were recorded. Receptive-field sizes on the other distal phalanges were not significantly different between the normal and poststimulation mapping experiments in these two owl monkeys.

In other owl monkeys in which the poststimulation map was obtained first and a subsequent map was obtained several weeks after a period of no disk stimulation, similar changes in receptive-field sizes were seen, except for case *OM 4*. All glabrous receptive fields located on the distal phalanges obtained from the two mapping experiments for *OM 6* are depicted in Fig. 8. Immediately after disk stimulation (Fig. 8, *top*), significant differences were observed in receptive-field size across the distal phalanges [$F(4, 103) = 16.278$, $P < 0.0001$]. The distal phalangeal receptive fields were significantly smaller [$F(1, 106) = 33.578$, $P < 0.0001$] on the stimulated skin surfaces (*digits 2, 3,* and *4*). The mean receptive-field area on individual distal phalanges in this poststimulation mapping experiment ranged from 3.8 to 11.6 mm^2. In the mapping experiment after a period of no disk stimulation (Fig. 8, *middle*), the sizes of distal phalangeal receptive fields were not significantly different

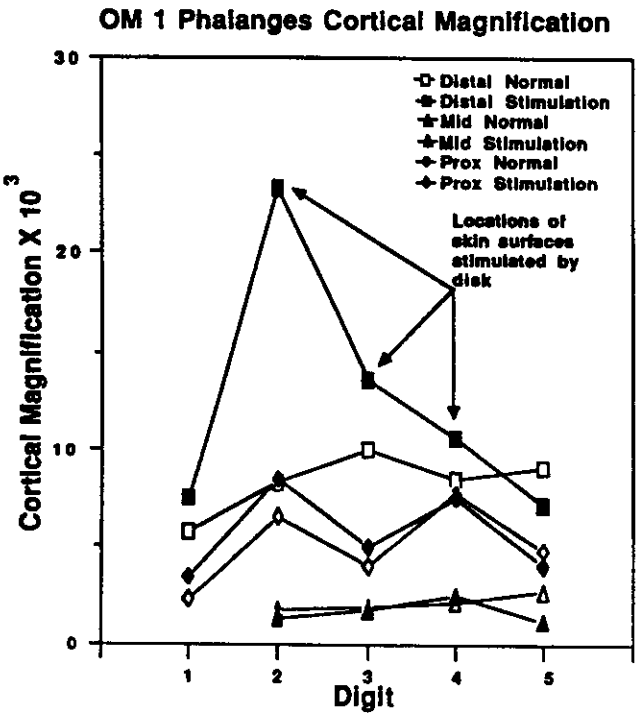

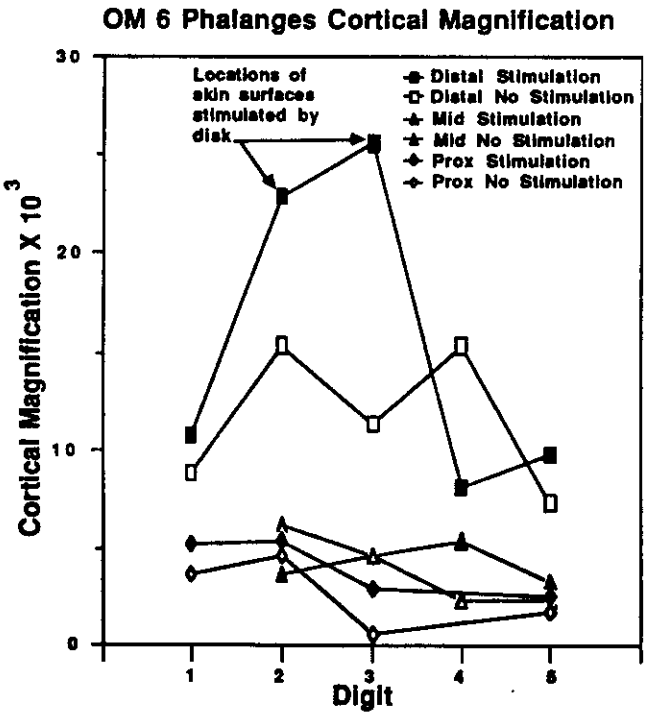

FIG. 6. Cortical magnification (cortical area of representation/skin surface area) ×1,000 of the glabrous representation of all 5 digits for normal and poststimulation middle, distal, and proximal phalanges for *OM 1* (*top*) and *OM 6* (*bottom*). Note that the magnification of the representation of each phalangeal surface is relatively constant across the 5 fingers in both monkeys at these 2 stages of life, except for the striking increase in the magnification of representation of the stimulated phalanges. Arrows indicate the locations of skin surfaces stimulated by disk contact.

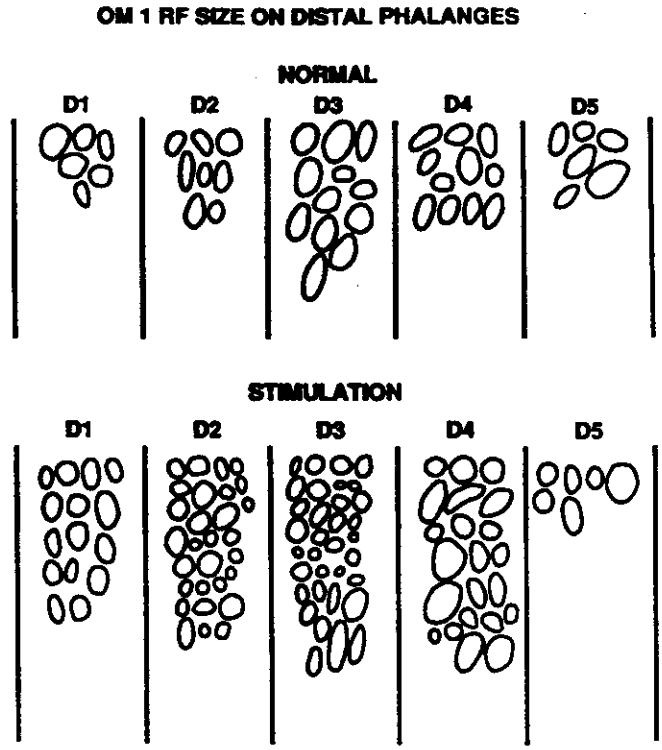

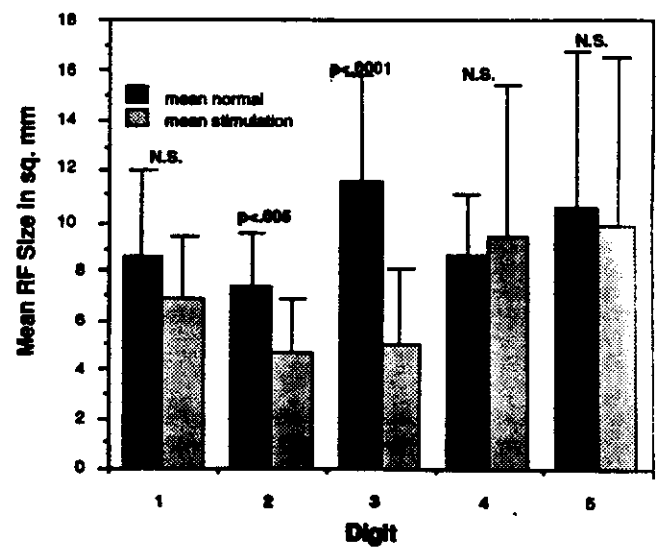

FIG. 7. Receptive fields from the distal phalanges of a normal monkey (*OM 1*) are outlined at the *top* (Normal). Receptive fields from the poststimulation map are shown in the *middle* (Stimulation). Receptive fields from both experiments are drawn to the same scale. These data are summarized at the *bottom*, where the bars indicate mean receptive-field size in square millimeters in the normal map (black) and after differential stimulation (gray). Error bars indicate standard deviations. Receptive fields representing skin surfaces heavily engaged (distal phalanges on *digits 2* and *3*) in these differential stimulation behaviors in area 3b are significantly smaller [*digit 2*, $F(1, 35) = 9.416$, $P < 0.005$; *digit 3*, $F(1, 44) = 32.54$, $P < 0.001$] than those recorded in the same representational zones before the behavior.

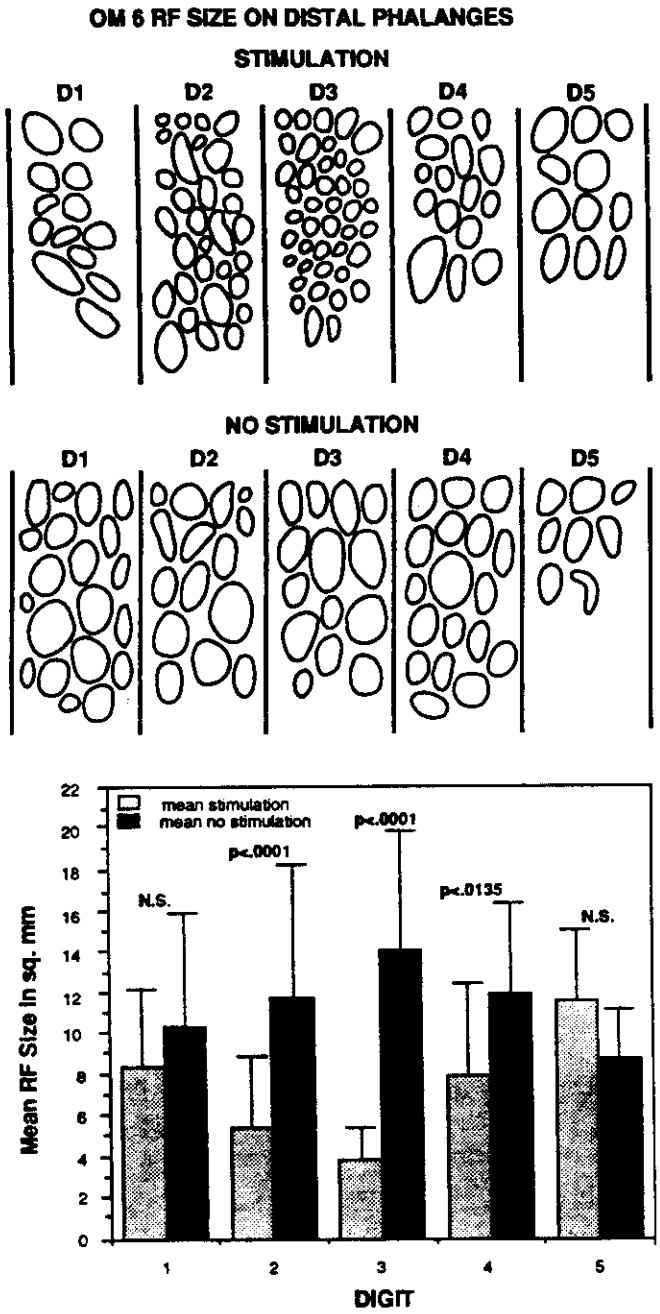

FIG. 8. Receptive fields from the distal phalanges of *OM 6* from the poststimulation map are outlined at the *top* (Stimulation). Receptive fields from a 2nd map, obtained after 63 days without disk stimulation, are outlined in the *middle* (No Stimulation). Receptive fields from both experiments are drawn to the same scale. These data are summarized at the *bottom*, where the bars indicate mean receptive-field size in square millimeters in the no-stimulation condition (black) and after differential stimulation (gray). Error bars indicate the standard deviation. Receptive fields in area 3b located on skin surfaces engaged in disk contact are significantly smaller [*digit 2*, $F(1, 42) = 17.413$, $P < 0.0001$; *digit 3*, $F(1, 52) = 101.113$, $P < 0.0001$; *digit 4*, $F(1, 31) = 6.861$, $P < 0.0136$] than those recorded after a period of no differential stimulation.

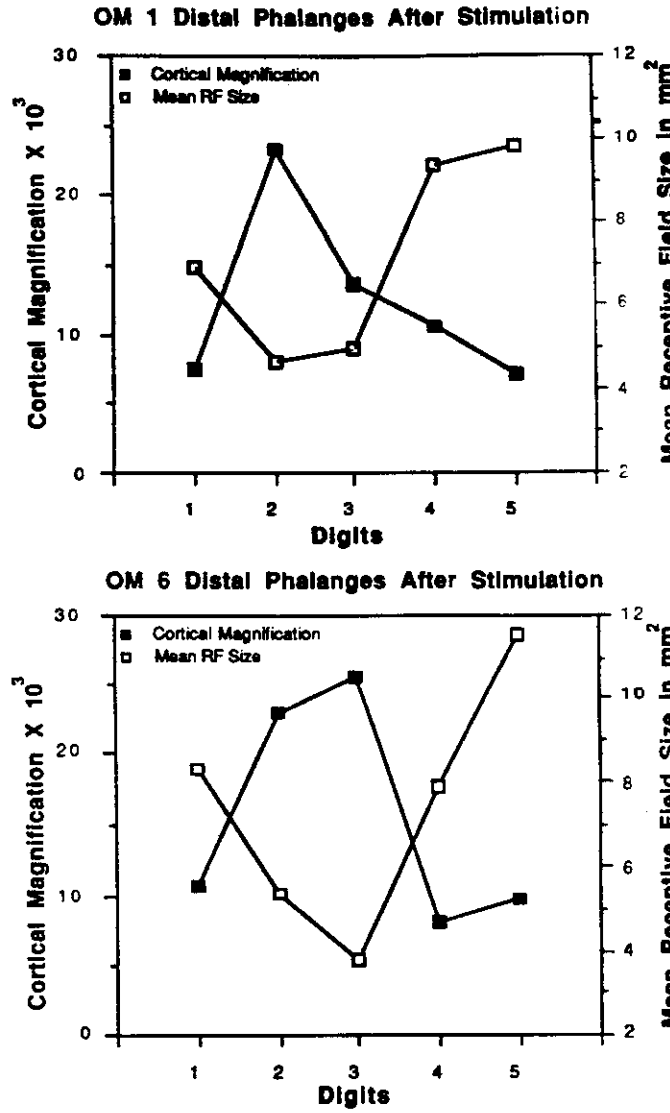

FIG. 9. Cortical magnification (black squares) for distal phalanges obtained after differential stimulation is plotted for *OM 1* (*top*) and *OM 6* (*bottom*; ordinate is on the left axis). Note that cortical magnification has been linearly transformed by a factor of 1,000. Mean receptive-field size in square millimeters plotted for these same skin surfaces obtained after differential stimulation is also plotted (ordinate on the right axis). It can be seen that in both exemplary cases these 2 functions are roughly inversely related. That is, as cortical representations of these struck surfaces expanded, they came to be represented in finer grain.

across digits [$F(4, 69) = 1.528$, $P = 0.2038$]. The mean receptive-field area on individual distal phalanges ranged from 8.8 to 13.9 mm^2. Figure 8, *bottom*, shows a histogram of the mean receptive-field area in square millimeters for these two mapping experiments (bars indicate 1 SD). Receptive fields on the distal phalanges of *digits 2, 3*, and *4* were significantly smaller in the poststimulation map compared with the no-stimulation map [*digit 2*, $F(1, 42) = 17.413$, $P < 0.0001$; *digit 3*, $F(1, 52) = 101.113$, $P < 0.0001$; *digit 4*, $F(1, 31) = 6.861$, $P = 0.0135$]. In one case (*OM 4*), no significant differences in receptive-field sizes for the stimulated phalanges were seen when the poststimulation data was compared with the no-stimulation data. Perhaps this can be accounted for by the fact that the shortest interval between mapping experiments (31 days) occurred in this case. These data suggest that the cortical area of representation and receptive field size are not strictly coupled. Recall that substantial enlargements in cortical

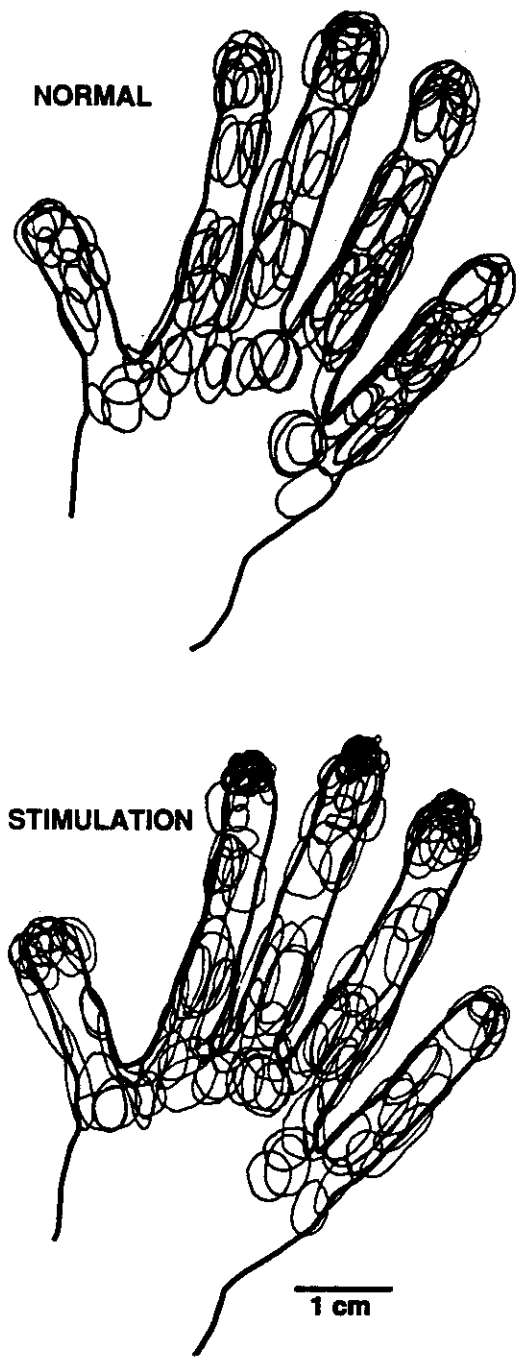

FIG. 10. All glabrous receptive fields identified for recording sites within area 3b for *OM 1* before differential stimulation (Normal, *top*) and after differential stimulation (Stimulation, *bottom*). Note the large number of receptive fields identified for skin locations (distal phalanges of digits *2*, *3*, and *4*) stimulated during the trained behavior.

area of representation of the stimulated skin surfaces were observed for *OM 4* (see Fig. 4).

RELATIONSHIPS BETWEEN CORTICAL MAGNIFICATION AND RECEPTIVE-FIELD SIZE. It has previously been suggested that there is an inverse relationship between cortical magnification and receptive-field size within areas 3b and 1 (Sur et al. 1980). A rough inverse relationship between cortical magnification and receptive-field size on the distal phalanges was observed in the poststimulation mapping experiment for *OM 1*. In Fig. 9 (*top*), the black squares indicate the cortical magnification (scale on the left ordinate), and the open squares indicate the mean receptive-field size (scale on the right ordinate) for each of the five distal phalanges. The distal phalanx (*digit 2*) with the largest cortical magnification (0.02337) had the smallest mean receptive-field size (4.676 mm^2). The distal phalanx (*digit 5*) with the smallest cortical magnification (0.00706) had the largest mean receptive-field size (9.852 mm^2). A similar relationship between cortical magnification and mean receptive-field size was also seen in *OM 5*. Recall that in this monkey, like OM 1, the poststimulation mapping experiment was preceded by a normal mapping experiment a number of weeks earlier.

The relationship between cortical magnification and mean receptive-field size in a second case (*OM 6*), in which the first mapping experiment was initiated after disk stimulation, is shown in Fig. 9 (*bottom*). Once again, it is clear that cortical magnification and mean receptive-field size are roughly inversely related. The distal phalanx on *digit 3* was always stimulated during disk contact. This distal phalanx had the largest cortical magnification (0.02562) and the smallest mean receptive-field size (3.806 mm^2). In two

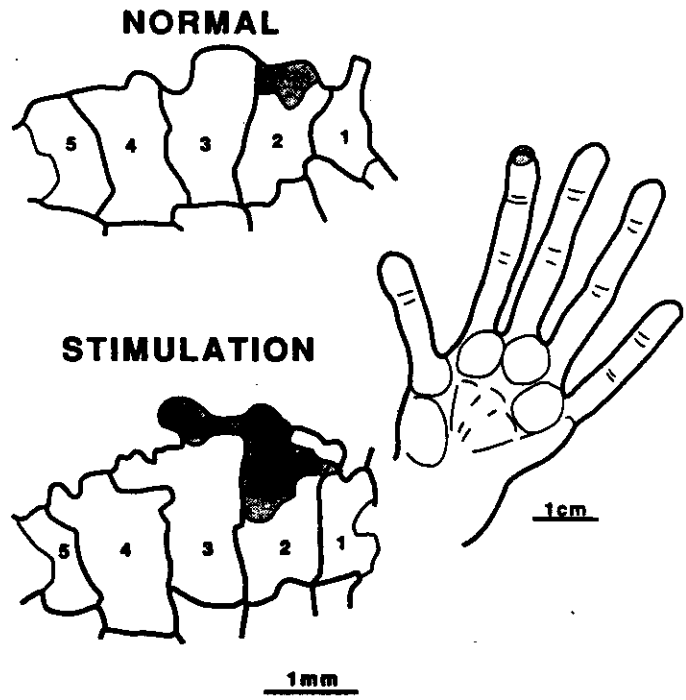

FIG. 11. Outlines of the area 3b cortical territories representing the surfaces of the digits for *OM 1* before differential stimulation (Normal, *top*) and after differential stimulation (Stimulation, *bottom*). Most of the differentially stimulated skin surface on *digit 2* is indicated by stippling in the hand drawing at the *right*. Zones of representation of the struck skin surface on the distal phalanx of *digit 2* are stippled in both drawings, i.e., in this zone, all defined receptive fields overlapped onto this heavily stimulated surface. Note that after a period of differential digit tip stimulation in this monkey—as in other monkeys studied with this paradigm—there was a substantial enlargement of its territory of representation. In this monkey, most of the gain in territory was from across the area 3b-3a border as defined functionally before the initiation of this digital stimulation behavior.

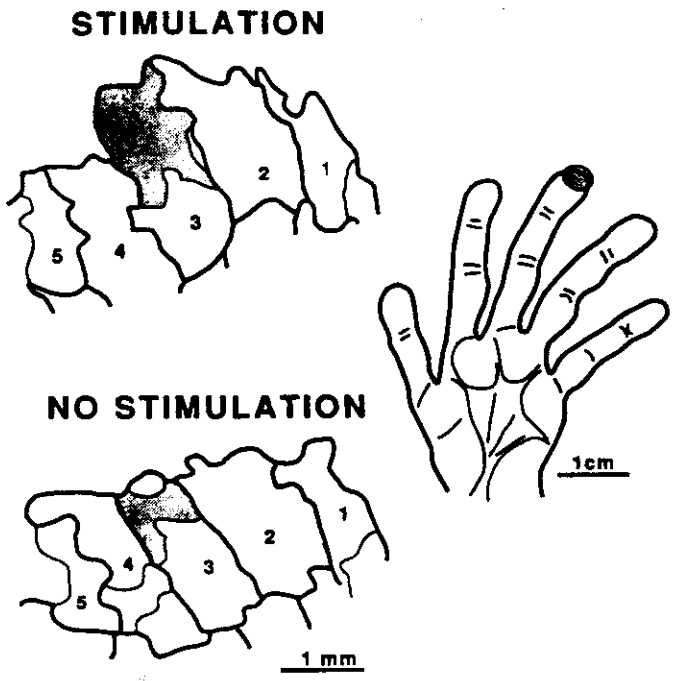

FIG. 12. Outlines of the area 3b cortical territories representing the surfaces of the digits for *OM 6* after differential stimulation (Stimulation, *top*) and long after differential stimulation (No Stimulation, *bottom*). Note that, after a period of differential digit tip stimulation in this monkey, there was a substantial enlargement of its territory of representation.

other cases (*OM 3* and *OM 4*) where the first map was obtained after disk stimulation, the largest cortical magnification and small mean receptive-field sizes were also seen for the stimulated skin surfaces. However, this relationship was not as striking as in other cases, and some exceptions were evident. Thus, for example, in *OM 3* where the distal phalanx of *digit 3* (it was always stimulated during disk contact) exhibited the largest cortical magnification, a slightly smaller mean receptive-field size was seen for the distal phalanx of *digit 4*, which was usually stimulated during disk contact.

STIMULATION SITE SPECIFICITY FOR OBSERVED CHANGES. Thus far, we have considered the effects of stimulation of individual distal phalanges on receptive-field sizes and cortical magnifications. The stimulated skin surface on *digit 2* in *OM 1* directly engages no more than ~20% of the surface of the phalanx. The question arises: is there a preferential enlargement of these limited stimulated skin surfaces within the cortical representational zone of the distal phalanx? The locations of all of the glabrous cutaneous receptive fields defined in the two mapping experiments are shown in Fig. 10. The receptive fields defined before differential stimulation were relatively uniformly distributed across each of the distal phalanges (Fig. 10, *top*). However, in the map obtained after differential stimulation, most of the receptive fields defined for the behaviorally engaged distal phalanges were centered over the stimulated skin surfaces (Fig. 10, *bottom*). This result is most apparent for *digit 2*, the most differentially stimulated digit, where 87% of the defined receptive fields included differentially stimulated skin. We have considered the possibility that this result might reflect a sampling bias in the location of the recording sites used to define the distal phalanges. However, in both mapping experiments, the locations of recording sites within the representational zone of each distal phalanx were evenly distributed spatially. Furthermore, the number of penetrations when corrected for distal phalanx representational area indicate that each distal phalanx in a given mapping experiment was defined by penetrations of similar density. For example, if we divide the cortical area of representation of each phalanx by the number of penetrations located within that zone, we have an index of mapping density. For the poststimulation mapping experiment, this resulted in 0.024, 0.030, 0.022, 0.024, and 0.033 mm^2/penetration for digits 1–5, respectively (0.026 ± 0.0046, mean ± SD). Thus the large number of receptive fields on digits *2*, *3*, and *4*, which included skin surfaces stimulated in the behavioral task, is not simply the result of a spatial sampling bias. A similar, nearly uniform mapping density also applied for all other poststimulation cases.

These results suggest that not only has there been an expansion of the distal phalanges of the behaviorally engaged digits but also that this representational enlargement occurred specifically for the stimulated skin. The enlargement of the cortical area representing the stimulated skin surface of the distal phalanx of *digit 2* in *OM 1* and *digit 3* in *OM 6* is shown in Figs. 11 and 12, respectively. In the hand *insets* (Figs. 11 and 12, *right*) the consistently stimulated skin surfaces are approximated by the stippled region on the distal aspect of *digits 2* or *3*. A reconstruction of the cortical representation of the hand in area 3b obtained before (*top*) and after (*bottom*) differential stimulation is shown in Fig. 11. For *OM 6*, the stimulation map was obtained first (*top*), and a second map (*bottom*) was obtained after a period without disk access. The cortical zones over which these differentially stimulated skin surfaces were represented at these two epochs in the monkeys' lives are indicated by stippling in both drawings. Within these stippled zones, all defined receptive fields included at least a portion of this heavily stimulated skin surface. The cortical area of representation of these skin surfaces has increased by nearly 500%. These data, as well as those from other studied cases, indicated that the expansion of cortical representation is occurring specifically for the stimulated skin surfaces.

ALTERATIONS IN THE DETAILS OF CORTICAL-MAP TOPOGRAPHY. As a result of this expanded cortical representation, striking changes should be apparent in the internal topography of the cortical zones representing the stimulated phalanges. Recall that, in 3b maps of the hand representation in normal adult owl monkeys, there is an orderly shift from distal to proximal in the location of receptive fields for rostral-to-caudal sequences of electrode penetration sites (e.g., Fig. 1, *B* and *C*, 1–5). (For an extensive treatment of this feature of the internal topography of area 3b representations, see Merzenich et al. 1987.) Two caudal-to-rostral sequences of penetration sites and associated receptive fields for the poststimulation mapping experiment in *OM 1* are shown in Fig. 12. The caudal-to-rostral sequence of penetration sites labeled 1–6 (Fig. 13*A*) on the palm and *digit 5* had receptive fields that illustrate a nor-

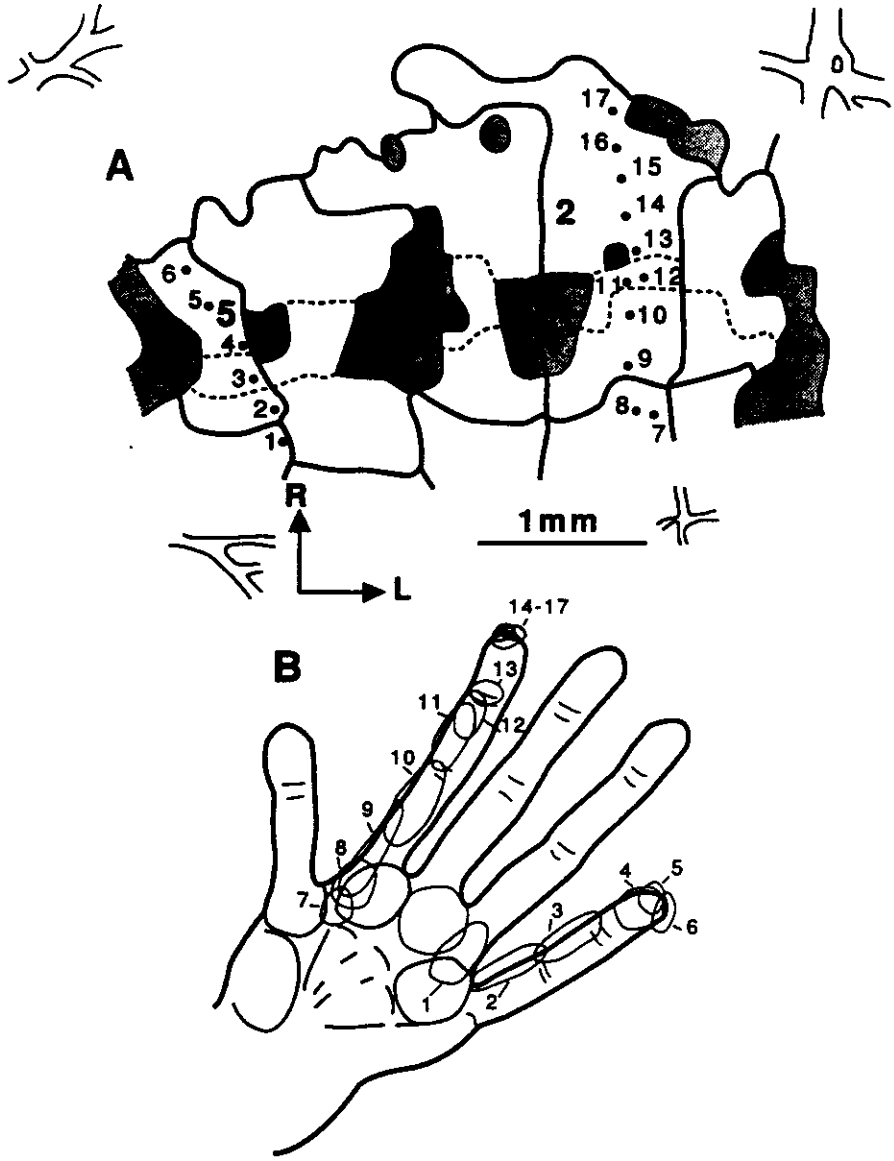

FIG. 13. Caudal-to-rostral sequences of recording sites within area 3b (*top*) and corresponding receptive fields (*bottom*) defined after behaviorally controlled differential stimulation for *OM 1*. Caudal-to-rostral sequence of penetration sites labeled 1–6 had receptive fields that illustrate a normal gradual shift from proximal to distal in receptive-field locations. Electrode penetrations sites and their associated receptive fields in the sequence labeled 7–17 indicate a striking change in the internal topography of the representation of *digit 2*. A normal gradual shift in receptive-field locations from the palm to the proximal aspect of the distal phalanx was observed for sites 7–13. Note that there was an abrupt jump in the location of the next receptive field in sequence (14) despite only a small shift (125 μm) in the location of the recording site. Note also that, for additional movements in the locations of subsequent recording sites (15–17), the locations of those receptive fields closely overlapped with one another.

mal gradual shift from proximal to distal in receptive-field locations (Fig. 13*B*). This example also illustrates that small discontinuities in receptive-field sequences (see RFs 3 and 4) were occasionally observed in regions not directly stimulated by the disk or in sequences from normal maps. In contrast, inspection of the electrode penetration sites and their associated receptive fields in the sequence labeled 7–17 (Fig. 13, *A* and *B*) indicates a striking change in the internal topography of the representation of *digit 2*. The sequence of penetration sites 7–13 shows a normal gradual shift in receptive-field locations from the palm to the proximal aspect of the distal phalanx of *digit 2*. However, the next penetration site in this sequence (14) had a receptive field located on the extreme distal and radial aspect of the distal phalanx of *digit 2*. That is, despite the fact that these two adjacent penetration sites are separated by only ~125 μm, their receptive fields are decidedly nonoverlapping. The other penetration sites in this sequence (15–17) had receptive fields that were also located over the skin stimulated during disk contact on the extreme distal aspect of the distal phalanx of *digit 2*. Rostral-to-caudal sequences all across the distal phalanx representation of *digit 2* and, to a lesser extent, across *digits 3* and *4* exhibited a discontinuity between the representation of the stimulated and other nearby skin surfaces. For each of these digits, these nonoverlapping representational boundaries marked the boundary of representation of the skin surfaces stimulated directly during disk contact.

The existence of a break in the topographic sequence of representation of the stimulated skin surfaces was a feature common to all poststimulation mapping experiments. Another example of this unusual map feature is illustrated in Fig. 14 for *OM 6*. A caudal-to-rostral sequence of penetration sites labeled 1–8 (Fig. 14*A*) on the palm and *digit 1* had receptive fields that illustrate a normal gradual shift from proximal to distal in receptive-field locations (Fig. 14*B*). This normal gradual shift was usually seen in each case for digits not stimulated by disk contact. In the penetration sequence labeled 9–19 (Fig. 14, *A* and *B*), it can be seen that, once again, there is an abrupt shift in the orderly

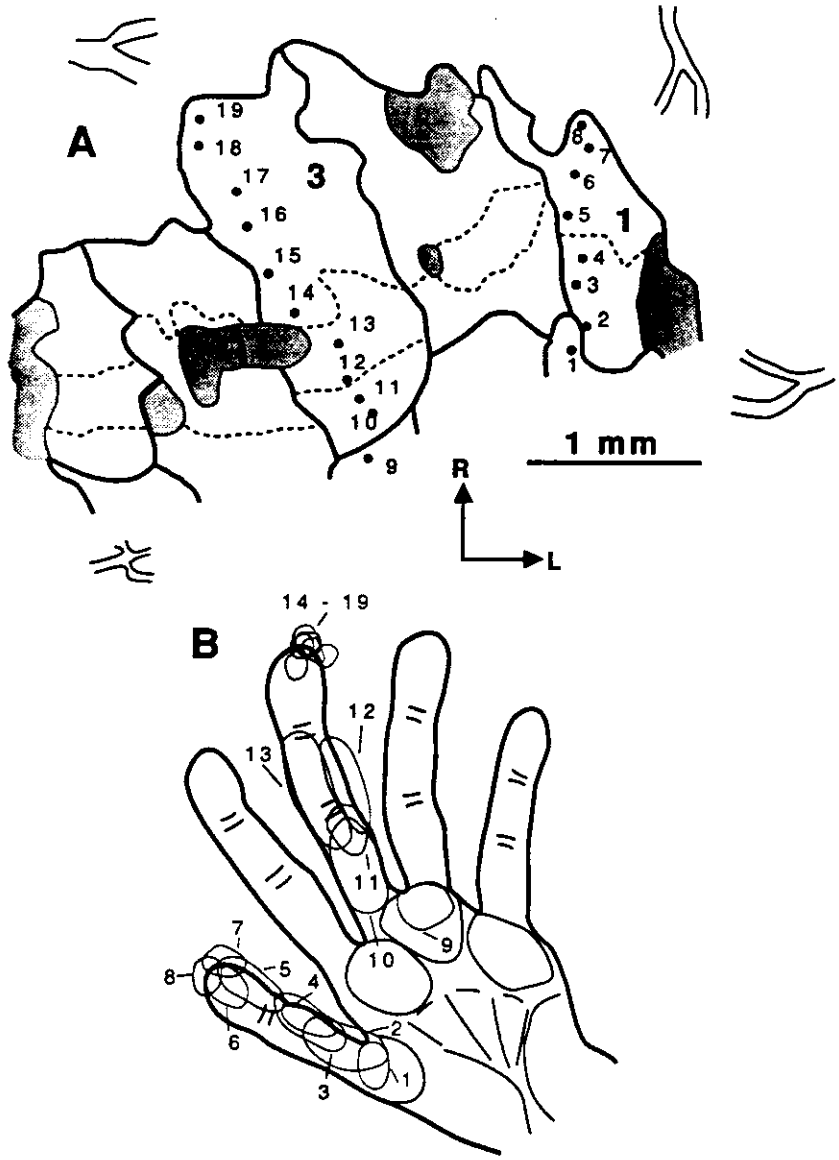

FIG. 14. Caudal-to-rostral sequences of recording sites within area 3b (*top*) and corresponding receptive fields (*bottom*) defined after behaviorally controlled differential stimulation for *OM 6*. Caudal-to-rostral sequence of penetration sites labeled 1–8 had receptive fields that illustrate a typical gradual shift from proximal to distal in receptive-field locations. Penetration sequence from 9–19 again illustrates the typical unusual topography of representation of the stimulated digit. A normal gradual shift in receptive-field locations from the palm to the distal aspect of the middle phalanx of *D3* was seen for sites 9–13. At site 14, there was an abrupt shift in the location of the receptive field to the distal aspect of the distal phalanx of *D3*. For electrode penetrations sites located over the next 1,000+ μm in this sequence (sites 15–19), there was little change in the location of the receptive field.

progression of receptive-field locations at the border of the representation of the stimulated phalanx. In this sequence, which covers ~1,250 μm across the cortical surface, again little change in receptive-field locations was observed. Once again, the cortical zone exhibiting a discontinuity in digital surface representation was seen along the borders of representation of the skin surfaces directly engaged in the behaviorally controlled stimulation. As previously mentioned, occasional smaller discontinuities in receptive-field sequences were observed on unstimulated digits or in control maps. However, these discontinuities were not associated with cortical zones of nonshifting, largely overlapping receptive fields or with systematically smaller receptive-field sizes.

ADJACENT CORTICAL REPRESENTATIONAL ZONES ALTERED BY STIMULATION. One consequence of the expansion of the cortical zones representing skin surfaces stimulated in the behavioral task is a change in topographic relationships with surrounding somatic representations. These changes are illustrated in Fig. 15 for representative skin surfaces (i.e., the distal phalanx of the digit most heavily involved in the task). The illustrations presented for *OM 1, 3, 4*, and *6* are derived from data obtained after differential stimulation with the use of the rotating disk procedures. For comparison, the illustration presented for *OM 5* was derived from data obtained after stimulation with the use of the flat static disk procedure. Each of the cases differentially stimulated by the use of the rotating disk share the following common features with regard to the changes in topographic relationships: *1*) there was a centrally located cortical zone within area 3b that was common to the two representations; *2*) within area 3b, there was a loss of cortical territory to either adjacent digits or the middle phalanx; *3*) within area 3b, there was a gain in cortical territory from either adjacent digits, the middle phalanx, or dorsum representation; and *4*) there was a gain in functionally defined area 3b that was obtained at the expense of functionally defined area 3a.

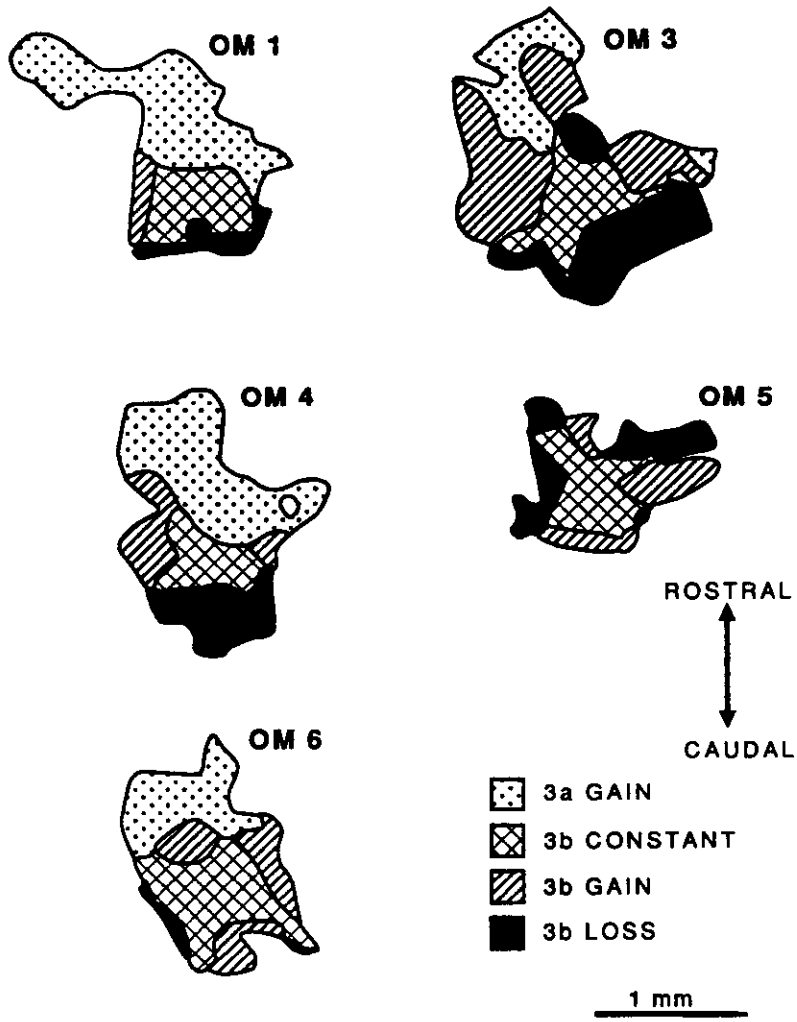

FIG. 15. Changes in the cortical zones of representation of stimulated glabrous distal phalanges. For *OM 1*, the illustrated changes are from a normal map and a subsequent poststimulation map. For *OM 3*, *4*, and *6*, the illustrated changes are from a poststimulation map as compared with a subsequent map after a period of several weeks without access to the behavioral apparatus. For *OM 5*, the illustrated changes are from a normal map and a subsequent map obtained after a period of controlled stimulation with the use of a static flat disk. Stippled zone indicates a cortical gain from functionally defined area 3a. Cross-hatched region indicates a constant cortical zone within these 2 maps that represent these phalanges. Diagonal lines indicate a cortical gain from other skin surfaces within functionally defined area 3b. Black zone indicates a loss in cortical representation from functionally defined area 3b for the stimulated phalanx. Note that, for all cases, there were positive changes in the cortical zone of representation of the stimulated phalanx that included gains in territory from functionally defined area 3a (except *OM 5*) and 3b, as well as some more limited area 3b loss. Note that, for all cases except *OM 5*, the net result was an increase in the area of cortex within functionally defined 3b representing the stimulated phalanx. For *OM 5*, there was no gain in cortical territory from the adjacent functionally defined area 3a. There was little net effect on the size of the representational zone as a consequence of the observed changes in cortical zones of representation of the distal phalanx for *OM 5*.

The net effect of these alterations in topographic relationships was a gain in area of the cortical zone representing differentially stimulated skin surfaces. The topographic changes observed after exposure to the static flat disk (Fig. 15, *OM 5*) were similar to those seen in the other cases, except that there was no gain in territory from functionally defined area 3a. The net effect of these alterations in topographic relationships on the area of cortex representing the skin surface that contacted the static disk was insignificant.

It is important to point out that the aforementioned changes in representational topography necessarily indicate that there is an alteration of topographic relationships for other skin surfaces on the hand. Three examples of these changes for a distal phalanx not directly engaged in disk contact are shown in Fig. 16. In each of these examples, as well as many others, we observed changes that were qualitatively similar to those seen for stimulated skin surfaces. That is, between the two representations, there was usually *1*) a central common zone, *2*) a loss within area 3b, *3*) a gain within area 3b, and sometimes *4*) a gain or loss in territory from functionally defined cortical field 3a. However, unlike stimulated skin surfaces, the net effect on the cortical area of representation was usually negligible.

CHANGES ACROSS THE AREA 3a-3b BORDER. As previously stated, in every poststimulation experiment, there were unequivocal changes in location of the functionally defined 3a-3b border. This somewhat surprising result is summarized in Fig. 17. There, for each of the five illustrated examples, the dashed line represents the functionally defined 3a-3b border along the rostral margin of 3b obtained either before disk stimulation (*OM 1* and *5*) or after a several-week period without disk stimulation (*OM 3*, *4*, and *6*). The solid line represents the functionally defined 3a-3b border obtained immediately after disk stimulation training. Recall that lines defining the borders between various skin surfaces or functionally defined cortical areas are drawn by interpolating between adjacent recording sites. Therefore it is reasonable that some small variation in the exact location of these borders may occur as a result of differences in the exact locations of sampled recording sites between any two mapping experiments. However, most of the changes along the rostral 3a-3b border cannot be explained by such an artifact in methodology. For example, the stippled regions in Fig. 17 represent the cortical regions over which the recording sites from the two mapping experiments directly overlapped spatially and for which no

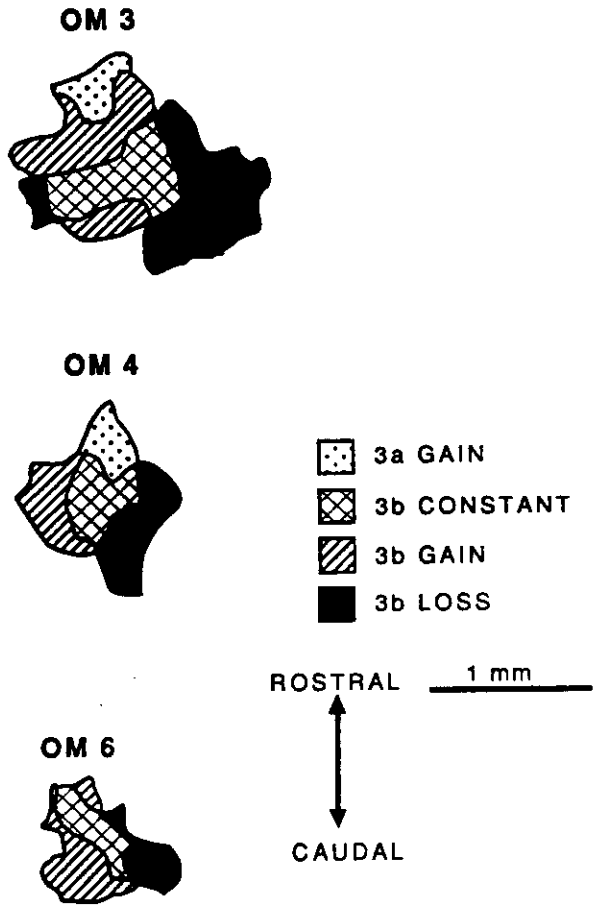

FIG. 16. Changes in the cortical zones of representation of nonstimulated glabrous distal phalanges. For *OM 3* (*digit 2*), *OM 4* (*digit 5*), and *OM 6* (*digit 5*), the illustrated changes are from a poststimulation map as compared with a subsequent map after a period of several weeks without access to the behavioral apparatus. Various patterned fills are as indicated in Fig. 14. Note that, in spite of the fact that there were changes in the absolute locations of the cortical zones of representation of distal phalanges not specifically engaged in the behavioral task, there was little net effect on the sizes of their cortical representation.

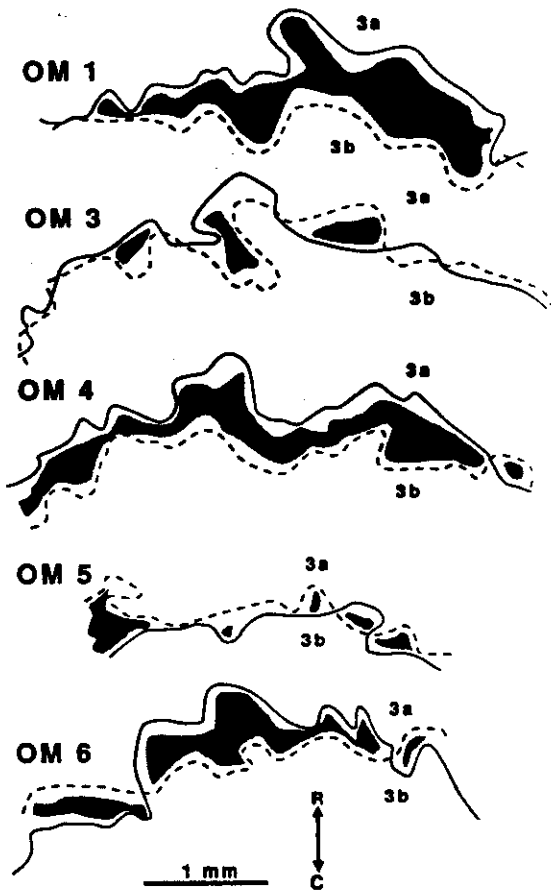

FIG. 17. In each of the 5 illustrated examples, dashed line represents the functionally defined 3a-3b border along the rostral margin of 3b obtained either before disk stimulation (*OM 1* and *5*) or after a several-week period without disk stimulation (*OM 3*, *4*, and *6*). Solid line represents the functionally defined 3a-3b border obtained immediately after disk stimulation training. Recall that lines defining the borders between various skin surfaces or functionally defined cortical areas are drawn by interpolating between adjacent recording sites. Stippled areas represent the cortical regions over which the recording sites from the 2 mapping experiments directly overlapped and for which no interpolation applies. That is, these recorded representational borders minimally and unequivocally shifted by the extents indicated by the stippled area.

interpolation was used. That is, they represent a conservative estimate of the cortical region over which neurons exhibited changes from 3a to 3b response properties or vice versa. Note that, for *OM 1*, *3*, *4*, and *6*, there is a substantial region over which the functionally defined border has shifted, resulting in an expansion of the defined area 3b representation. Of particular interest is the fact that the largest caudal-to-rostral expansion occurred in the region immediately adjacent to the stimulated skin surfaces. The most striking example of this can be seen in the *bottom* of Fig. 17 for *OM 6*. There, the cutaneous/deep border has been translocated rostrally adjacent to the stimulated distal phalanges and translocated caudally adjacent to the distal phalanges not directly stimulated during disk contact. Note also that for *OM 5*, in which the disk was not rotating and had a smooth surface, little change was observed in the location of the functionally defined 3a-3b border.

CHANGES ACROSS THE HAND/FACE BORDER. Changes in the functionally defined hand/face border were also observed. Figure 18 presents a summary of these results. Again, the dashed line represents the functionally defined hand-face border along the lateral margin of the hand representation within area 3b obtained either before disk stimulation (*OM 1* and *5*) or after a several-week period without disk stimulation (*OM 3*, *4*, and *6*). The solid line represents the functionally defined hand-face border obtained immediately after disk stimulation training. The stippled area represents the cortical regions over which the recording sites from the two mapping experiments overlapped spatially. Three of the cases exposed to the rotating-disk stimulation (*OM 1*, *3*, and *4*) show clear evidence of a lateral translocation of the hand-face border. The largest translocation was seen in *OM 3*, where there was as much as a 600-μm lateral displacement of the hand-face border with the use of the more conservative measure. No significant change in the hand-face border was observed for *OM 6*. Interestingly, *OM 5*, which had been stimulated with the static flat disk, also exhibited a shift in the hand-face

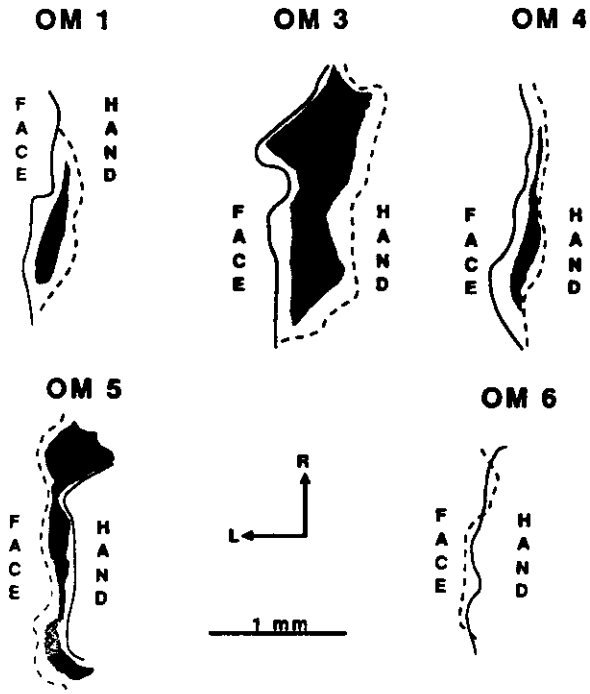

FIG. 18. In each of the 5 illustrated examples, dashed line represents the functionally defined hand-face border along the lateral margin of the hand representation within area 3b obtained either before disk stimulation (*OM 1* and *5*) or after a several-week period without disk stimulation (*OM 3*, *4*, and *6*). Solid line represents the functionally defined hand-face border obtained immediately after disk stimulation training. Stippled area represents the cortical regions over which the recording sites from the 2 mapping experiments overlapped directly. For *OM 1*, *3*, *4*, and *6*, stimulation was with the rotating disk. For *OM 5*, stimulation was accomplished with a static flat disk.

border. However, unlike other cases, the hand-face border in this case was translocated medially by as much as 200 μm, again with the use of a conservative estimate.

DISCUSSION

The disproportionately large representation of the heavily stimulated skin surface resulted in substantial translocations of the sites of representation of surrounding skin surfaces. Significant shifts in the cortical locations of the functional area 3b-area 3a border and in the location of the hand-face border were recorded. Across the mapped sector of area 3b, the topographic order of defined receptive fields was altered. Surprisingly, except for the representation of the nonstimulated surfaces of the distal phalanx of the same digit, the enlargement of the cortical representation of behaviorally engaged hand surfaces did not result in a substantial underrepresentation of surrounding skin surfaces. That was apparently a consequence of the long-distance "borrowing" of representational territory, which was a striking feature of these experimental cases.

Interestingly, in two special cases in which the behavioral task required minimal attention because the stimulandum was not moving, no significant representational enlargement of the behaviorally engaged skin surfaces was recorded. It is not possible to determine, at this point, if this lack of representational plasticity in these two special cases was because of the static nature of the stimulandum and/or because of the relatively low level of attention requisite for the monkey to successfully perform this simpler task—or to some other differences in the features of the stimulus provided by disk contact.

Some implications

INPUT-SELECTING PROCESSES CONSTITUTE FUNDAMENTAL OPERATIONS OF THE NORMAL ADULT NEOCORTEX. These studies demonstrate that the receptive fields of cortical neurons can be altered and the representational topographies of cortical fields modified by use throughout life. We have earlier summarized a large body of evidence that suggests that *1*) this representational plasticity involves alterations in the effectiveness of in-place afferent inputs (see Clark et al. 1988; Jenkins et al. 1987, 1989; Merzenich et al. 1985, 1987, 1988). *2*) The coincidence of afferent inputs plays a powerful role in reshaping cortical receptive fields and representational topographies (Clark et al. 1988; Merzenich et al. 1988; Yun et al. 1987). *3*) Input effectivenesses are likely modulated as a function of behavioral state (see Merzenich et al. 1988), and *4*) Use-driven alteration of cortical representations accounts for most of the great normal variability in the details of cortical representations recorded in adult monkeys (Merzenich et al. 1987).

These present results are consistent with these earlier findings and hypotheses. First, representational translocations recorded in these experiments are recorded over cortical distances of up to 600–700 μm, i.e., within the limits of the spreads of divergent-convergent anatomic inputs (Garraghty and Sur 1987; Snow et al. 1988) and within "distance limits" defined in earlier reported experiments conducted in this cortical area in owl monkeys (Merzenich et al. 1983a,b, 1985). Although their possible contributions are difficult to rule out completely, no sprouting or movement of afferent input arbors would be required to explain representational translocations on this scale.

Second, this behaviorally controlled stimulation resulted in increased amounts of nearly coincident stimulation of small digital skin patches. Most of the small receptive fields in the expanded zones of representation of these small skin surfaces were limited to these small, nearly simultaneously excited skin zones. These results are therefore consistent with a growing body of evidence suggesting that the quantities of temporally coincident or nearly coincident inputs play a major role in shaping cortical receptive fields and representational topographies (see Clark et al. 1988; Merzenich et al. 1988).

Third, dramatic changes were recorded in monkeys performing a behavioral task—maintaining light contact with a ridged, moving disk—that required their close "attention." By contrast, little or no task-related changes in the hand representational zone was recorded in monkeys performing a simpler task—maintaining contact with a static surface—that required little attention on their part. These data are consistent with the view, generated largely by functional studies of other cortical areas (Diamond and Weinberger 1986; Spitzer et al. 1988; Weinberger and Diamond 1988; Woody et al. 1972; but see Yun et al. 1987), that the effectivenesses of afferent inputs for generating

representational change are modulated as a function of behavioral state.

At the same time, differences in the quantities of sensory input may also contribute to observed differences between static and rotating disk cases. Although initial contact with either disk would excite virtually all cutaneous mechanoreceptors, static pressure on a flat surface excites only SA mechanoreceptors in monkeys. These receptors are innervated by only 25% of the large-diameter myelinated cutaneous afferents in the median nerve (Darian-Smith and Kenins 1980). By contrast, maintained contact on a moving disk with ridged surface features periodically (at 20 HZ) excites all cutaneous mechanoreceptors. Furthermore, both RA and SA mechanoreceptors fire at significantly higher rates when moving edges cross their fields than when smooth surfaces contact their fields because they are most sensitive to "curvature gradients" (Johnson and Lamb 1981; LaMotte and Srinivasan 1987a,b; Srinivasan and LaMotte 1987). The relative contributions of firing rates and population size of cutaneous afferents versus attentional factors to the observed map differences are not separable in these experiments.

Fourth, these simple behaviors contributed to an idiosyncratic remodeling of the area 3b representation of the hand, different in each of these monkeys, different from all others studied, and related specifically to one of a number of behaviorally important hand uses. Presumably any behaviorally important hand use requiring subtle sensory feedback or discrimination would have impacts on the details of this (and many other) cortical representation(s). These studies provide further evidence that the strikingly individual representational details of hand representations in different adult monkeys (Merzenich et al. 1985, 1987) have been shaped by each monkey's unique experiential history.

CHANGES ALONG THE AREA 3a-AREA 3b BORDER. There was a significant extension of the cutaneous representation of the behaviorally stimulated digital surfaces into presumptive area 3a in four behavioral cases (*OM 1, 3, 4*, and *6*; Fig. 17). The deep input representation in functionally defined area 3a extended significantly into area 3b in three studied monkeys (*OM 3, 5*, and *6*; Fig. 17). These changes in the functionally defined 3b-3a border are especially interesting in *OM 6*, in which the cutaneous representation of the behaviorally engaged digit tips expanded >500 μm into functionally defined area 3a, while at the same time the deep representation adjacent to the cutaneous representation of nonengaged digits appeared to move up to several hundred micrometers into functionally defined area 3b.

We have explored the area 3b-3a border in >60 normal adult owl monkeys. In the great majority, progressing rostrally, receptive fields at the extreme digit tips, under cover of the fingernails or in the fingernail beds, were followed by recording sites in which no cutaneous responses could be recorded. The hand area of this latter zone, presumptive area 3a, has been mapped in entirety in several adult monkeys. It is ~2 mm wide rostrocaudally. Neurons within it often respond vigorously to tapping unrestrained fingers. However, when joint movement is disallowed, very few or no sites respond to light tactile stimulation in this zone. This is consistent with the observation that muscle spindle and other deep receptor inputs predominate in this cortical area (Hore et al. 1976; Jones and Porter 1980; Lucier et al. 1975; Phillips et al. 1971).

At the same time, in some normal cases, cutaneous receptive fields have been recorded in area 3a. Pacinian input responses are occasionally recorded along the 3b-3a border —although we cannot usually assign them unequivocally to either field 3b or 3a. Relatively large cutaneous fields innervating the dorsal surfaces of the digits or extending over one or more fingertips have also been recorded rostral to the small-field digit tip representation in some monkeys. Although these receptive fields are cutaneous by our definition (i.e., they respond to light indenting of the skin when the digit joints are stabilized), they usually resemble high-threshold tapping response fields in the sense that their defined receptive fields commonly extend over the surfaces of more than one digit. The finding of occasional large-field cutaneous responses in cortical area 3a is consistent with the finding that 3a receives anatomic inputs ultimately arising from purely cutaneous nerves (Heath et al. 1976; Oscarsson et al. 1966).

Given these observations, is the functional border of areas 3a and 3b truly plastic? Electrophysiological data are consistent with the functional 3b representation expanding into area 3a. There is nothing in the small receptive-field responses or representational topography to distinguish clearly the most rostral response sites from the more caudal ones. The skin on the extreme fingertip under the fingernail is represented in the rostral aspect of this zone. By these criteria, the 3b-stimulated skin representation has enlarged to occupy now a significant sector that was formerly functionally 3a. A presumption might be that this plasticity would require a significant anatomic overlap of input arbors and output destinations of neurons in a relatively broad 3a-3b transitional zone.

On the other hand, nearly the same results could have been obtained if a caudal sector of 3a was converted from a large-field, multiple-digit deep representational zone to a small-field, single-digit cutaneous representational zone. It is difficult to eliminate this second possibility. Indeed, the emergence of a large cutaneous overrepresentation of a stimulated fingertip in a cortical field that provides critical sensory inputs to motor cortex might have important implications for control of a behavior in which the animal has to regulate very closely skin position in relation to a moving surface. Whether this is the case or not, the topography and selected effective cortical inputs have been dramatically altered in two functionally defined cortical fields. In either event, all sign of normally large deep multiple-digit receptive fields has been lost over this zone. This presumably requires topographic adjustment elsewhere in field 3a.

If an emergence of a functional 3a zone with small cutaneous receptive fields is occurring in these monkeys, then the net changes in representation occurring in functional area 3b are more modest than those recorded in Table 1. However, the unmistakable changes in topography and the distorted representation of the limited, struck digit tip surfaces would still apply to area 3b alone. Moreover, in one monkey (*OM 3*), net positive changes are almost entirely

attributable to enlargement of the digit tip representation into functional area 3b alone.

In recent experiments not reported herein, we have directed training to proximal digit segments, in part to eliminate this possible confusion along the 3b-3a border. In those studies, training has resulted in a severalfold increase in the representation of the behaviorally engaged skin within area 3b, as well as alterations in the response properties over large sectors of area 3a (Recanzone et al. 1989).

OTHER CHANGES IN REPRESENTATION. Other representational changes were observed in these experiments. Some unstimulated digital surfaces on either the distal, middle, or proximal phalanges exhibited unpredictable gains or losses in cortical representation immediately after stimulation when compared with control maps. For example, the distal phalanx of *digit 1* in case *OM 1* had a 29% increase (see Table 1), whereas *digits 1* and *5* in case *OM 3* had a 10% smaller cortical representation. In these instances, the absolute cortical territorial gains or losses were not great (e.g., 0.08 mm^2 for *digit 1* in *OM 1*). Moreover, significant gains in cortical territory were not always observed for some skin surfaces stimulated by disk contact. For example, the cortical representation of the distal phalanx of *digit 4* in *OM 3* only increased by 6%, whereas changes in the territories of representation of other engaged digital surfaces in this case were great. Similarly, the representation of the distal phalanx of *digit 4* in *OM 6* was actually smaller immediately after disk stimulation. A much smaller skin region on this digit was only occasionally stimulated in the behavior. On the other hand, representations of other more frequently stimulated digits in the same case increased greatly.

Several factors may have contributed to these results. First, there are aspects of behavior that resulted in differential stimulation of various skin surfaces of the hand that were not controlled in these experiments. For example, even though all of the monkeys commonly retrieved banana pellets with their tongue, they were occasionally also observed retrieving pellets with their hands. In addition, no attempt was made to control other hand use before, during, or after behavioral training on the disk. Undoubtedly, these monkeys had idiosyncratic patterns of hand use for food retrieval, locomotion, grooming, and other behaviors that, given the present data, would be expressed in control or experimental maps. Furthermore, these behavioral patterns of hand use may well have been perturbed by behavioral training. Second, although it is not possible to determine the effects of selective attentional factors in these studies, it is interesting to note that, when multiple digits were engaged in contacting the rotating disk, the first-struck digit always exhibited the largest change in cortical representation. Finally, some of the variation in cortical representational territory is because of measurement error. These measurement errors, given a fixed statistical criterion, are affected by both the number of sites used to estimate the area of representation and the absolute size of the cortical area to be estimated. The end result, given the relatively constant spatial sampling of these studies, is that smaller cortical regions of representation are subject to greater measurement errors (Merzenich et al. 1987). Small changes in representation, especially for smaller outlined map sectors, are sometimes not statistically significant.

AN HYPOTHESIS: USE-DRIVEN ALTERATIONS IN NEOCORTICAL REPRESENTATIONS MANIFEST CORTICAL CONTRIBUTIONS TO USE-DRIVEN IMPROVEMENTS IN PERCEPTUAL JUDGMENTS AND ACQUISITION OF SKILL. The view that the adult nervous system, in particular the neocortex, exhibits physiological plasticity in response to historical patterns of sensory input is a premise on which most of the nineteenth-century physiologists and psychologists based their notions of the modifiability of behavior through experience. William James (1890) summarized this view by stating that practiced behaviors must ". . . leave their traces in the paths which they take. [They] . . . deepen old paths or . . . make new ones. . . . [The] . . . whole plasticity of the brain sums itself up in two words when we call it 'an organ' in which currents pouring in from the sense organs make with extreme facility paths which do not easily disappear."

Early psychophysicists clearly recognized that experience on a particular sensory discrimination resulted in marked improvement in the discriminability of all kinds of sensory stimuli (for a review, see Anderson 1981; Gibson 1953). For the early psychologists "this fact was so familiar that few . . . have even recognized it as needing an explanation" (James 1890). It was also recognized historically that this improvement in perceptual judgments with practice or experience was an important feature of human cognition that was largely an "inexplicable fact." Contemporary psychophysicists have largely ignored this problem and have commonly considered measurements of discrimination capacity along a single physical dimension to reflect a stable sensory function. Any variations or improvements in discriminability have been viewed as because of changes in "motivation," "attention," "criterion," "familiarity," with, or "learning" the specific requirements or contingencies of the specific behavioral task used to measure discrimination capacity. Certainly these variables do affect measurements of discrimination capacity. However, it has been clear for more than a century that even the fundamental resolving capacity of the perceptual machinery improves with experience, with gains in acuity achieved over a practiced skin surface not applicable to a nearby, untrained skin surface (Dresslar 1894; Jones et al. 1973; Vierck and Jones 1970; Volkmann 1858).

The data from the present experiments suggest that extensive stimulation to a restricted patch of skin under behaviorally controlled stimulation is "locally expressed" in the functional representation of that skin surface within area 3b. Gains in acuity and/or sensitivity would be expected to result from practiced performance of this task.

Whatever the correct interpretation as to the contributions to area 3a and 3b to these changes, it is clear that the topography and selected effective cortical inputs have been dramatically altered in two functionally defined cortical fields. In any event, all sign of normally large deep multiple-digit receptive fields has been lost over a substantial area 3a zone. These changes along the 3a-3b border presumably require topographic adjustment elsewhere in both fields 3a and 3b.

All of these studies imply that there should be clear evidence of physiological changes at the neuron level that can account for these improvements in perceptual and motor capacities. As a monkey performs the simple behavioral task described in this report over a period of a few to many weeks, a dramatic representational alteration reflecting this specific hand use was recorded within the cortical areas 3b and 3a. It is reasonable to hypothesize that *1*) these representational changes have operational (behavioral) consequences for these monkeys; and *2*) these representational changes manifest the area 3b and 3a contributions to the successful performance of this behavioral task, and to alteration of the ability to perform other tasks, given this special experience.

Area 3b is almost certainly the least alterable, by use, of somatosensory cortical representations (see Jenkins and Merzenich 1987; Merzenich et al. 1987, 1988). Performance of a simple repetitive task like this one must result in reorganizational changes within many cortical areas excited differentially by these special, repetitive, sequenced motor and sensory events. It appears reasonable to hypothesize that use-driven changes in the many areas necessarily engaged by any such task collectively constitute the cortical contributions to the acquisition of skill and perceptual capacity in developing and adult mammals. These ideas are consistent with the view that the nervous system and cerebral cortex in particular are capable of selfregulation and adaptive reorganization, as previously expressed by Lashley (1930, 1933, 1951) and Hebb (1949).

Our behavioral experiments now turn toward a more direct consideration of a determination of the significance of behaviorally driven cortical representational changes in studies in which we can track performance gains in parallel with alterations in cortical representational details and suprathreshold neuronal response characteristics.

We thank G. Recanzone and Drs. Michael Stryker and Randy Nudo for their critical comments on the manuscript.

This work was supported by National Institute of Neurological and Communicative Disorders and Stroke Grant NS-10414 and the Coleman Fund.

Address for reprint requests: W. M. Jenkins, U-499, Box 0732, University of California at San Francisco, San Francisco, CA 94143-0732.

Received 12 May 1989; accepted in final form 23 August 1989.

REFERENCES

ALLARD, T., CLARK, S. A., JENKINS, W. M., AND MERZENICH, M. M. Syndactyly results in the emergence of double-digit receptive fields in somatosensory cortex in adult owl monkeys. *Soc. Neurosci. Abstr.* 11: 965, 1985.

ANDERSON, J. R. *Cognitive Skills and Their Acquisition.* Hillsdale, NJ: Erlbaum, 1981.

CHAPMAN, B., JACOBSON, M. D., REITER, H. O., AND STRYKER, M. P. Ocular dominance shift in kitten visual cortex caused by imbalance in retinal electrical activity. *Nature Lond.* 324: 154–156, 1986.

CLARK, S. A., ALLARD, T., JENKINS, W. M., AND MERZENICH, M. M. Cortical map reorganization following neurovascular island skin transfers on the hands of adult owl monkeys. *Soc. Neurosci. Abstr.* 12: 391, 1986.

CLARK, S. A., ALLARD, T., JENKINS, W. M., AND MERZENICH, M. M. Syndactyly results in the emergence of double digit receptive fields in somatosensory cortex in adult owl monkeys. *Nature Lond.* 332: 444–445, 1988.

DARIAN-SMITH, I. AND KENINS, P. Innervation density of mechanoreceptive fibers supplying glabrous skin of the monkey's index finger. *J. Physiol. Lond.* 309: 147–155, 1980.

DE FELIPE, J., CONLEY, M., AND JONES, E. G. Long-range focal collateralization of axons arising from corticocortical cells in monkey sensorymotor cortex. *J. Neurosci.* 6: 3749–3766, 1986.

DIAMOND, D. M. AND WEINBERGER, N. M. Classical conditioning rapidly induces specific changes in frequency receptive fields of single neurons in secondary and ventral ectosylvian auditory cortical fields. *Brain Res.* 372: 357–360, 1986.

DRESSLAR, F. B. Studies in the psychology of touch. *Am. J. Psychol.* 6: 313–368, 1894.

EDELMAN, G. M. Group selection as the basis for higher brain function. In: *Organization of the Cerebral Cortex,* edited by F. O. Schmitt, F. G. Worden, G. Adelman, and S. G. Dennis. Cambridge, MA: MIT Press, 1981, p. 51–100.

EDELMAN, G. M. AND FINKEL, L. H. Neuronal group selection in the cerebral cortex. In: *Dynamic Aspects of Neocortical Function,* edited by G. M. Edelman, W. E. Gall, and W. M. Cowan. New York: Wiley, 1984, p. 653–695.

EDELMAN, G. M. AND MOUNTCASTLE, V. B. *The Mindful Brain.* Cambridge, MA: MIT Press, 1978.

FROHN, H., GEIGER, G., AND SINGER, W. A self-organizing neural network sharing features of the mammalian visual system. *Biol. Cybern.* 55: 333–343, 1987.

GARRAGHTY, P. E., PONS, T. P., SUR, M., AND KAAS, J. H. The arbors of axons terminating in middle cortical layers of somatosensory area 3b in owl monkeys. *Somatosens. Motor Res.* 6: 401–411, 1989.

GARRAGHTY, P. E. AND SUR, M. The morphology of single physiologically identified thalamocortical axons innervating somatosensory cortex in macaque monkeys. *Soc. Neurosci. Abstr.* 13: 471, 1987.

GIBSON, E. J. Improvement in perceptual judgments as a function of controlled practice or training. *Psychol. Bull.* 50: 401–484, 1953.

GRAJSKI, K. A. AND MERAENICH, M. M. Neural network simulation of peripheral cutaneous nerve section and regeneration in adult owl monkeys. *Soc. Neurosci. Abstr.* 15: 961, 1989.

HEATH, C. J., HORE, J., AND PHILIPS, C. G. Inputs from low threshold muscle and cutaneous afferents of hand and forearm to areas 3a and 3b of baboon's cerebral cortex. *J. Physiol. Lond.* 257: 199–227, 1976.

HEBB, D. O. *The Organization of Behavior: A Neuropsychological Theory.* New York: Wiley, 1949.

HERSHKOVITZ, P. *Living New World Monkeys (Platyrrhini).* Chicago, IL: Univ. of Chicago Press, 1977.

HICKS, T. P. AND DYKES, R. W. Receptive field size for certain neurons in somatosensory cortex is determined by GABA-mediated intracortical inhibition. *Brain Res.* 274: 160–164, 1983.

HORE, J., PRESTON, J. B., DURKOVIC, R. G., AND CHENEY, P. D. Responses of cortical neurons (areas 3a and 4) to ramp stretch of hindlimb muscles in the baboon. *J. Neurophysiol.* 39: 484–500, 1976.

JAMES, W. *The Principles of Psychology.* New York: Henry Holt and Co., 1890.

JENKINS, W. M., MERZENICH, M. M., AND OCHS, M. T. Behaviorally controlled differential use of restricted hand surfaces induce changes in the cortical representation of the hand in area 3b of adult owl monkeys. *Soc. Neurosci. Abstr.* 10: 665, 1984.

JENKINS, W. M. AND MERZENICH, M. M. Reorganization of neocortical representations after brain injury: a neurophysiological model of the bases of recovery from stroke. In: *Progress in Brain Research,* edited by F. J. Seil, E. Herbert, and B. M. Carlson. Amsterdam: Elsevier, 1987, vol. 71, p. 249–266.

JENKINS, W. M., MERZENICH, M. M., AND RECANZONE, G. Neocortical representational dynamics in adults: implications for neuropsychology. *Neuropsychologia.* In press.

JOHNSON, K. O. AND LAMB, G. D. Neural mechanisms of spatial tactile discrimination: neural patterns evoked by braille-like dot patterns in the monkey. *J. Physiol. Lond.* 310: 117–144, 1981.

JONES, E. G. AND PORTER, R. What is area 3a? *Brain Res. Rev.* 2: 1–43, 1980.

JONES, M. B., VIERCK, C. J., AND GRAHAM, R. B. Line-gap discrimination of the skin. *Percept. Mot. Skills* 36: 563–570, 1973.

KAAS, J. H., MERZENICH, M. M., AND KILLACKEY, H. P. The reorganization of somatosensory cortex following peripheral nerve damage in adult and developing mammals. *Annu. Rev. Neurosci.* 6: 325–356, 1984.

KELAHAN, A. M. AND DOETSCH, G. S. Time-dependent changes in the

functional organization of somatosensory cerebral cortex following digit amputation in adult raccoons. *Somatosens. Res.* 2: 49–81, 1984.

LAMOTTE, R. H. AND SRINIVASAN, M. A. Tactile discrimination of shape: responses of slowly adapting mechanoreceptive afferents to a step stroked across the monkey fingerpad. *J. Neurosci.* 7: 1655–1671, 1987a.

LAMOTTE, R. H. AND SRINIVASAN, M. A. Tactile discrimination of shape: responses of rapidly adapting mechanoreceptive afferents to a step stroked across the monkey fingerpad. *J. Neurosci.* 7: 1672–1681, 1987b.

LASHLEY, K. S. Basic neural mechanisms in behavior. *Psychol. Rev.* 37: 1–24, 1930.

LASHLEY, K. S. Integrative functions of the cerebral cortex. *Physiol. Rev.* 13: 1–42, 1933.

LASHLEY, K. S. The problem of serial order in behavior. In: *Cerebral Mechanisms in Behavior*, edited by L. A. Jefress. New York: Wiley, 1951. p. 112–136.

LISBERGER, S. G. The neural basis for motor learning in the vestibulo-ocular reflex in monkeys. *Trends Neurosci.* 11: 147–152, 1988.

LUCIER, G. E., RÖEGG, D. C., AND WIESANDANGER, M. Responses of neurones in motor cortex and in area 3a to controlled stretches of forelimb muscles in cebus monkeys. *J. Physiol. Lond.* 251: 833–853, 1975.

MERZENICH, M. M. Sources of intraspecies and interspecies cortical map variability in mammals: conclusions and hypotheses. In: *Comparative Neurobiology: Modes of Communication in the Nervous System*, edited by G. M. Edelman, W. E. Gall, and W. M. Cowan. New York: Wiley, 1985, p. 138–157.

MERZENICH, M. M., JENKINS, W. M., AND MIDDLEBROOKS, J. C. Observations and hypotheses on special organizational features of the central auditory nervous system. In: *Dynamic Aspects of Neocortical Function*, edited by G. M. Edelman et al. New York: Wiley, 1984a, p. 397–424.

MERZENICH, M. M., KAAS, J. H., SUR, M., AND LIN, C. S. Double representation of the body surface within cytoarchitectonic areas 3b and 1 in "SI" in the owl monkey (*Aotus trivirgatus*). *J. Comp. Neurol.* 181: 41–74, 1978.

MERZENICH, M. M., KAAS, J. H., WALL, J. T., NELSON, R. J., SUR, M., AND FELLEMAN, D. Topographic reorganization of somatosensory cortical areas 3b and 1 in adult monkeys following restricted deafferentation. *Neuroscience* 8: 33–55, 1983a.

MERZENICH, M. M., KAAS, J. H., WALL, J. T., SUR, M., NELSON, R. J., AND FELLEMAN, D. J. Progression of change following median nerve section in the cortical representation of the hand in areas 3b and 1 in adult owl and squirrel monkeys. *Neuroscience* 10: 639–665, 1983b.

MERZENICH, M. M., NELSON, R. J., STRYKER, M. P., CYNADER, M. S., SCHOPPMANN, A., AND ZOOK, J. M. Somatosensory cortical map changes following digit amputation in adult monkeys. *J. Comp. Neurol.* 224: 591–605, 1984b.

MERZENICH, M. M., NELSON, R. J., KAAS, J. H., STRYKER, M. P., JENKINS, W. M., ZOOK, J. M., CYNADER, M. S., AND SCHOPPMANN, A. Variability in hand surface representations in areas 3b and 1 in adult owl and squirrel monkeys. *J. Comp. Neurol.* 258: 281–296, 1987.

MERZENICH, M. M., RECANZONE, G., JENKINS, W. M., ALLARD, T., AND NUDO, R. J. Cortical representational plasticity. In: *Neurobiology of Neocortex*, edited by P. Rakic and W. Singer. New York: Wiley, 1988; p. 41–67.

OSCARSSON, O., ROSÉN, I., AND SULG, I. Organization of neurones in the cat cerebral cortex that are influenced from group I muscle afferents. *J. Physiol. Lond.* 182: 189–210, 1966.

PEARSON, J. C., FINKEL, L. H., AND EDELMAN, G. M. Plasticity in the organization of adult cerebral cortical maps: a computer simulation based on neuronal group selection. *J. Neurosci.* 7: 4209–4223, 1987.

PHILLIPS, C. B., POWELL, T. P. S., AND WIESANDANGER, M. Projection from low threshold muscle afferents of hand and forearm to area 3a of baboon's cortex. *J. Physiol. Lond.* 217: 419–446, 1971.

RASMUSSON, D. D. Reorganization of raccoon somatosensory cortex following removal of the fifth digit. *J. Comp. Neurol.* 205: 313–326, 1982.

RECANZONE, G. H., JENKINS, W. M., HRADEK, G. T., SCHREINER, C. E., GRAJSKI, K. A., AND MERZENICH, M. M. Frequency discrimination training alters topographical representations and distributed temporal response properties of neurons in SI cortex of adult owl monkeys. *Soc. Neurosci. Abstr.* 15: 1223, 1989.

REITER, H. O., WAITZMAN, D. M., AND STRYKER, M. P. Cortical activity blockade prevents ocular dominance plasticity in the kitten visual cortex. *Exp. Brain Res.* 65: 182–188, 1986.

SCHMIDT, J. T. AND EDWARDS, D. L. Activity sharpens the map during the regeneration of the retinotectal projection in goldfish. *Brain Res.* 269: 29–39, 1983.

SINGER, W. Activity-dependent self-organization of the mammalian visual cortex. In: *Models of the Visual Cortex*, edited by D. Rose and G. Dobson. Chichester, UK: Wiley, 1985, p. 123–136.

SINGER, W. Activity-dependent self-organization of synaptic connections as a substrate of learning. In: *The Neural and Molecular Bases of Learning*, edited by J. P. Changeux and M. Konishi. Dahlem Konferenzen. Chichester, UK: Wiley, 1987, p. 301–336.

SNOW, P. J., NUDO, R. J., RIVERS, W., JENKINS, W. M., AND MERZENICH, M. M. Somatotopically inappropriate projections from thalamocortical neurons to the SI cortex of the cat demonstrated by the use of intracortical microstimulation. *Somatosens. Res.* 5: 349–372, 1988.

SPITZER, H., DESIMONE, R., AND MORAN, J. Increased attention enhances both behavioral and neuronal performance. *Science Wash. DC* 240: 338–340, 1988.

SRINIVASAN, M. A. AND LAMOTTE, R. H. Tactile discrimination of shape: responses of slowly and rapidly adapting mechanoreceptive afferents to a step indented into the monkey fingerpad. *J. Neurosci.* 7: 1682–1697, 1987.

STRYKER, M. P. Role of visual afferent activity in the development of ocular dominance columns. *Neurosci. Res. Program Bull.* 20: 540–549, 1982.

STRYKER, M. P. The role of neural activity in rearranging connections in the central visual system. In: *The Biology of Change in Otolaryngology*, edited by R. J. Ruben, T. R. Vandewater, and E. W. Rubel. Amsterdam: Elsevier, 1986a, p. 211–224.

STRYKER, M. P. AND HARRIS, W. A. Binocular impulse blockade prevents the formation of ocular dominance columns in cat visual cortex. *J. Neurosci.* 6: 2117–2133, 1986b.

STRYKER, M. P., JENKINS, W. M., AND MERZENICH, M. M. Anesthetic state does not affect the map of the hand representation within area 3b somatosensory cortex in owl monkey. *J. Comp. Neurol.* 258: 297–303, 1987.

SUR, M., MERZENICH, M. M., AND KAAS, J. H. Magnification, receptive-field area, and "hypercolumn" size in areas 3b and 1 of somatosensory cortex in owl monkeys. *J. Neurophys.* 44: 295–311, 1980.

TAKEUCHI, A. AND AMARI, S. Formation of topographic maps and columnar microstructures in nerve fields. *Biol. Cybern.* 35: 63–72, 1979.

VIERCK, C. J. AND JONES, M. B. Influences of low and high frequency oscillation upon spatio-tactile resolution. *Physiol. Behav.* 5: 1431–1435, 1970.

VOLKMANN, A. W. Über den Einfluss der Übung. *Leipzeg. Berichte, Math.-phys. Classe* 10: 38–69, 1858.

VON DER MALSBURG, C. Self-organization of orientation sensitive cells in the striate cortex. *Kybernetik* 14: 8–100, 1973.

VON DER MALSBURG, C. AND COWAN, J. D. Outline of a theory for the ontogenesis of iso-orientation domains in visual cortex. *Biol. Cybern.* 45: 49–56, 1982.

WALL, J. T. AND CUSICK, C. G. Cutaneous responsiveness in primary somatosensory (S-I) hindpaw cortex before and after partial hindpaw deafferentation in adult rats. *J. Neurosci.* 4: 1499–1515, 1984.

WALL, J. T., KAAS, J. T., SUR, M., NELSON, R. J., FELLMAN, D. J., AND MERZENICH, M. M. Functional reorganization in somatosensory cortical areas 3b and 1 of adult monkeys after median nerve repair: possible relationships to sensory recovery in humans. *J. Neurosci.* 6: 218–233, 1986.

WEINBERGER, N. M. AND DIAMOND, D. M. Dynamic modulation of the auditory system by associative learning. In: *Auditory Function: Neurobiological Bases of Hearing*, edited by G. M. Edelman, W. E. Gall, and W. M. Cowan. New York: Wiley, 1988, p. 485–512.

WILLSHAW, D. J. AND VON DER MALSBURG, C. How patterned neural connections can be set up by self-organization. *Proc. R. Soc. Lond. B Biol. Sci.* 194: 432–445, 1975.

WOODY, C. D. AND ENGEL, J. Changes in unit activity and thresholds to electrical microstimulation at coronal-pericruciate cortex of cat with classical conditioning of different facial movements. *J. Neurophysiol.* 35: 230–241, 1972.

YUN, J. T., MERZENICH, M. M., AND WOODRUFF, T. Alteration of functional representations of vibrissae in the barrel field of adult rats. *Soc. Neurosci. Abstr.* 13: 1596, 1987.

ZARZECKI, P. AND HERMAN, D. Convergence of sensory inputs upon projection neurons of somatosensory cortex: vestibular, neck, head, and forelimb inputs. *Exp. Brain Res.* 50: 408–414, 1983.

ZARZECKI, P. AND WIGGIN, D. M. Convergence of sensory inputs upon projection neurons of somatosensory cortex. *Exp. Brain Res.* 48: 28–42, 1982.

M.M. MERZENICH

FROM: Auditory Function.
G.M. Edelman
W.E. Gall
W.M. Cowan, eds
J. Wiley, New York

Chapter 11

Coding of Temporal Patterns in the Central Auditory Nervous System

CHRISTOPH E. SCHREINER
GERALD LANGNER

ABSTRACT

Complex acoustical signals such as speech or other species-specific sounds can be characterized by their spectral and temporal parameters. The topographic representation of complex signals in the auditory system of mammals is to a large extent based on spectral cues, manifested by the multiple tonotopically organized maps found at all levels of the auditory pathway. The coding of temporal signal aspects in the auditory system has been studied principally with stimulation with amplitude-modulated tones. Modulation transfer functions have been used to describe the temporal filter characteristics of neural elements in the inferior colliculus and auditory cortex. Three levels of organization of temporal information have been distinguished: (1) The average frequency range of temporal variations represented in the time patterns of neural responses of the auditory nerve is higher than in the inferior colliculus, and the encoded temporal range of responses in the inferior colliculus is, on average, substantially higher than in any of several studied cortical fields. Thus fast temporal variations in a signal are represented with high resolution at more peripheral auditory stations; only relatively slower temporal variations are represented at the cortical level. (2) Different auditory cortical fields preferentially respond to slightly different frequency ranges of temporal variation. Thus there is a cortical field-specific treatment of the temporal features of inputs, consistent with some field-specific functional roles of different cortical areas. (3) There is a systematic topographic distribution of neurons with respect to their temporal response characteristics in the central nucleus of the inferior colliculus. Thus the inferior colliculus contains a highly organized topographic representation of acoustic signals based on both *spectral and temporal signal aspects.*

The encoding and representation of the temporal features of complex stimuli will be discussed in light of these findings.

TEMPORAL ENVELOPES OF COMPLEX ACOUSTICAL SIGNALS

Species-specific communication sounds like speech and other natural, complex sounds consist of sequences of a variety of acoustical features, definable in terms of frequency, intensity, and duration. To study the principles and underlying mechanisms of the representation and analysis of these complex signals within the central nervous system, it is analytically useful to select general aspects of sounds, and to explore their parametric representation at different levels of the

auditory system (Bullock, 1977). Studies of the processing of the most important signal parameter—frequency—led to the discovery that the auditory system of mammals resolves and represents frequency, that is, the major divisions of the auditory pathway topographically represent the spectral content of stimuli in their tonotopic organization (e.g., Woolsey and Walzl, 1942; Merzenich and Reid, 1974; Merzenich et al., 1976, 1984; Reale and Imig, 1980; Aitkin et al., 1984).

Besides the spectral content of signals, the temporal patterning of communication sounds constitutes another important information-carrying feature of complex signals. Study of the processing of temporal envelope variations in the frequency analysis channels of tonotopically organized subdivisions of the auditory system should provide insight into the neural representation of complex signals (Nelson et al., 1966; Vartanyan, 1969; Møller, 1972, 1974, 1976; Javel, 1980; Smith and Brachman, 1980; Langner, 1981, 1983).

The temporal range of these envelope changes or modulations of signal amplitude in different frequency channels is wide in many species-specific vocalizations and in speech. Complex communication signals contain envelope periodicities over a range extending from a few events per second to up to several hundred hertz. A sample illustrating the range of modulation frequencies of human speech for different spectral bands is given in Figure 1 (Plomp, 1983). There the distributions of modulation frequencies are shown for a 1-min connected discourse from 10 male speakers. (The parameter is the center frequency of the ⅓-octave carrier frequency band.) The peak of the modulation frequency distribution lies around 3–4 Hz, which corresponds roughly to the sequence rate of words.

The temporal features of vowellike sounds can be characterized by a fundamental frequency and many higher harmonics. Since the auditory system does not resolve the higher frequency components, the temporal features of these signals are comparable and hence coded similarly as those of amplitude-modulated

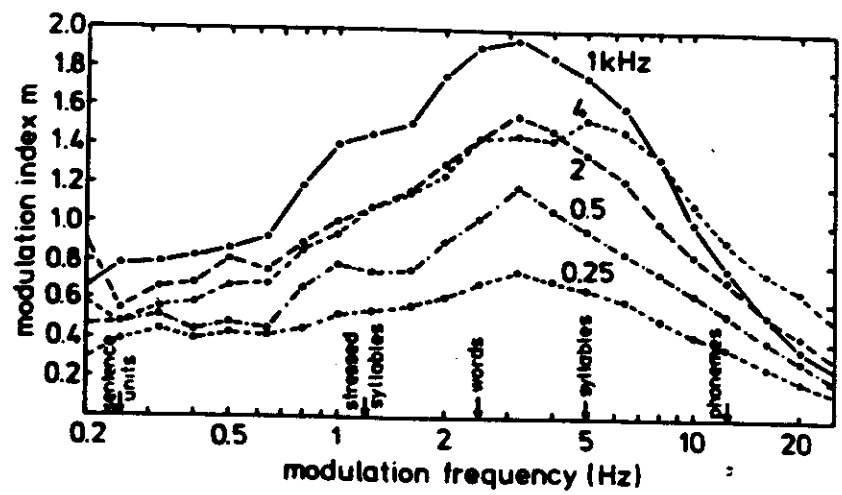

Figure 1. *Modulation index m as a function of the modulation frequency of speech.* The envelope spectra for different ⅓-octave frequency bands from 0.25 kHz to 4 kHz were determined for 1-min fragments of connected speech and averaged for 10 male speakers. (From Plomp, 1983.)

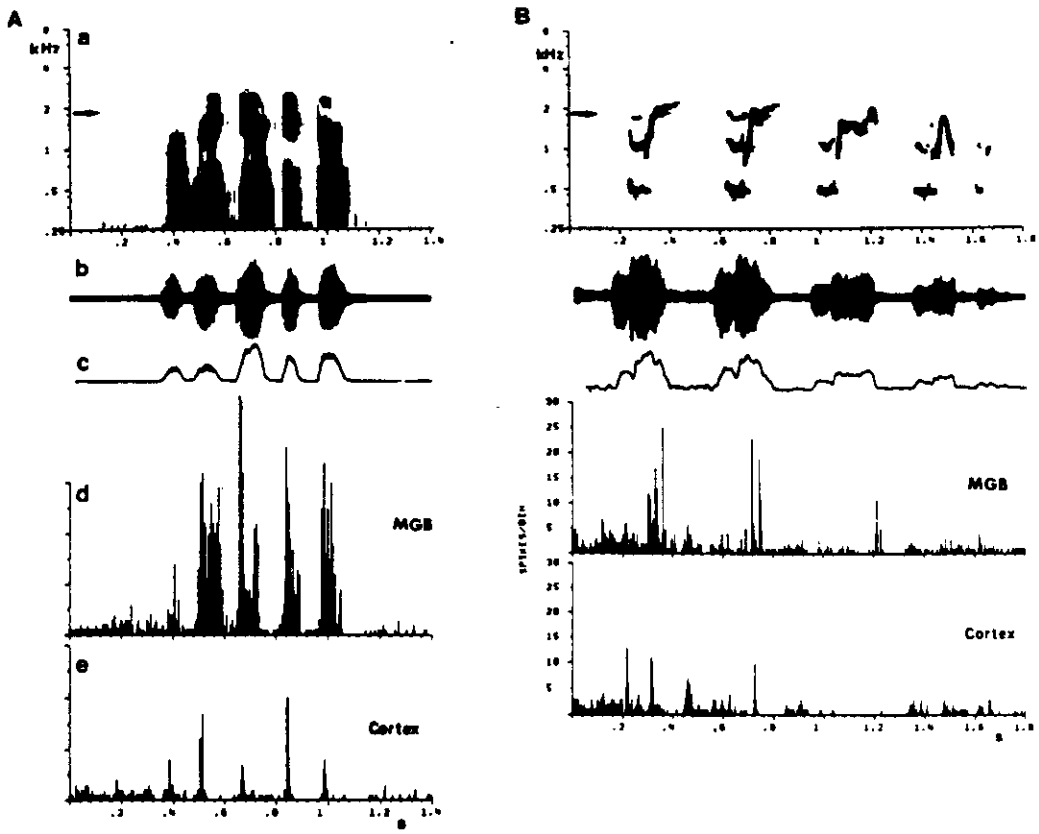

Figure 2. *Responses of a simultaneously recorded thalamocortical neuron pair in an unanesthetized guinea pig to different natural sounds. A*: Repetitive rattling of a guinea fowl. *B*: Grunting of a guinea pig. *Trace a* in both cases represents the sonogram of the natural sound. The overall sound pressure is shown in *trace b* and the envelope of the sounds in *trace c*. In *trace d* the PSTH of a single neuron in the MGB of the guinea pig is shown. The response of a cortical neuron is shown in *trace e*. The PSTHs were constructed from responses to 20 stimulus presentations with a histogram bin width of 2 msec. The CF of both neurons was 1.8 kHz and is indicated in the sonograms by an *arrow*. Cross-correlation of the spontaneous activity of the two units was positive, that is, a certain percentage of cortical spontaneous activity was actually driven by spontaneous activity in the thalamic neurons. (From Creutzfeldt et al., 1980.)

tones. In that sense, the formant frequencies—that is, the spectral peaks of the speech signal—would correspond to the carrier frequencies of amplitude modulations and the fundamental frequency of the vowel would correspond to the modulation frequency. These envelope or modulation frequencies are in the range of 100–400 Hz for normal speech. Other envelope signals—relevant, for example, to musical perception—with frequencies of up to approximately 1200 Hz can be derived that correspond to the existence range of residue or periodicity pitch found in human psychophysics (e.g., Schouten, 1970; Small, 1970; Viemeister, 1979).

The responses of auditory neurons can replicate or follow, to a limited extent, the amplitude fluctuations imposed on a carrier frequency within its spectral receptive field. In Figure 2A and B, two examples of complex signals (a call from

a mynah bird and a call from a guinea pig) are illustrated (Creutzfeldt et al., 1980). The upper traces are the spectrograms of the two natural calls, showing the frequency distribution as a function of time. The next lower traces represent the overall sound pressure and the signal envelope, respectively. Responses of representative single neurons in the medial geniculate body (MGB) and the auditory cortex of an unanesthetized guinea pig to these two calls are shown in the lower two traces of Figure 2 in the form of peristimulus time histograms (PSTHs). From the spectrograms of the calls it can be seen that the modulation frequencies of the envelope at the characteristic frequency (CF) of the two neurons (1.8 kHz, see arrow) cover a wide range—from modulation frequencies of a few hertz, corresponding to the occurrence of major segments of the calls, to about 140 Hz, corresponding to the fundamental frequency of the mynah bird call. (The mynah bird call was used because it contains certain basic acoustical features. The fact that a mynah bird call is most likely not part of a guinea pig's relevant acoustic biotope does not preclude its use in demonstrations of basic neural processes of the guinea pig or other mammals; see Bullock, 1977; Symmes, 1981.)

Whereas the response of a neuron in the MGB to the call followed most of the amplitude fluctuations with high precision, the cortical neuron responded only to those modulations that were slower than about 6 Hz. In other words, the MGB neuron responded to some features in the fine structure of the acoustical signal and the cortical neuron essentially marked the onset of major segments, or transients, in the signal. These differences in the temporal response characteristics of the neurons at these two locations are even more striking when it is pointed out that the two neurons were simultaneously recorded and were synaptically linked, as demonstrated by cross-correlation of the spontaneous activity of the two units (Creutzfeldt et al., 1980).

It is concluded that temporal changes in the frequency or intensity domain found in natural signals include a wide range of modulation frequencies and that different parts of the auditory system can be sensitive to different parts of that temporal range.

TEMPORAL MODULATION TRANSFER FUNCTION

To systematically study the temporal properties or temporal resolution of neurons responding to envelope variations, a parametric description of the responses in the time domain is a prerequisite. The concept of "temporal modulation transfer functions" (tMTF) has been widely used for this purpose (Møller, 1972, 1974, 1976; Viemeister, 1979; Fay, 1980; Langner, 1981, 1983; Schroeder, 1981; Palmer, 1982; Rose and Capranica, 1984). For the following discourse, the tMTF will be defined as the amount of neural activity evoked by amplitude-modulated CF tones as a function of modulation frequency. The amount of evoked neural activity can be expressed in terms of firing rate, or in terms of synchrony of the evoked activity to the stimulus envelope (phase locking to the envelope). Accordingly, two kinds of temporal MTFs can be constructed from the response to amplitude modulated tones. For the "rate MTF," the total firing rate of a neuron or a group of neurons at a given signal level is determined and plotted as a function of the modulation frequency. For the second kind of MTF, the

synchronization of the neural response to the modulation of the carrier signal is determined using vector strength or other related measures (Rose et al., 1967; Johnson, 1980). The "synchronization MTF" is constructed by plotting this synchronization measure as a function of the modulation frequency.

An example of the response of a small group of neurons in the primary auditory cortex of an anesthetized cat to sinusoidally modulated CF tones (CF = 10 kHz; signal level = 50 dB SPL; 100% modulation) is shown in Figure 3. The highest activity of the neurons was evoked by a modulation frequency of about 5 Hz. The derived synchronization MTF and rate MTF for this response are shown in Figure 4A and B. Both kinds of MTF have a similar shape and show a bandpass characteristic with a maximum at about 5 Hz. The modulation frequency corresponding to the highest degree of synchronization and/or highest evoked firing rate at a given location will be called best modulation frequency (BMF) and is the single most important descriptor of the temporal characteristic of central neural responses. Side maxima in the synchronization MTF, and especially in the rate MTF, correspond to stimulation conditions that contain higher harmonics of the BMF.

The temporal MTF provides a good estimate of the filter characteristics of a neuron in the time domain. It can be interpreted as a measure of the receptive field size of a neuron in the time domain. In combination with the filter characteristics in the frequency domain—the spectral receptive field is usually expressed as the frequency tuning curve (FTC)—a basic, relatively complete description of the response properties of a neural element to a wide range of acoustical stimuli can be derived. The coding of a natural call by a neuron and a first-order description of the response by the spectral and temporal filter characteristics of the neuron is illustrated in Figure 5. The upper trace of Figure 5A shows the overall envelope of a guinea pig call (see Figure 2B for spectrogram) and the lower trace shows the response of a single unit in the MGB of an unanesthetized guinea pig (CF = 1 kHz). In Figure 5B, the natural call has been filtered in the frequency domain according to the FTC of that neuron. The upper trace in Figure 5B shows the envelope of the call in the spectral range of 1 kHz after the spectral filtering process. The PSTH of the response of the neuron to this filtered call is shown in the lower trace of Figure 5B. The FTC of the neuron is shown in the left part of Figure 5B.

Comparison of the response to the unfiltered call (Figure 5A) with the response to the spectrally filtered call (Figure 5B) shows that the main features of the response appear to be preserved, although some response peaks are missing in the response to the filtered response. Influences from outside the main excitatory receptive field (e.g., from inhibitory side bands) are clearly represented in the response to the unfiltered signal and will not be considered here. In Figure 5C, the envelope of the natural call was additionally filtered in the temporal domain according to the temporal MTF of the unit depicted in the left-hand part of the figure. The result of this complete spectrotemporal filtering of the natural call is shown in the upper trace of Figure 5C. A comparison of this envelope with the response of the unit to the CF portion of the call (shown in the lower trace of Figure 5B and redisplayed in Figure 5C) reveals a reasonable resemblance of the major features in the model response to the neural response. In other words, a combined spectrotemporal filtering of the input signal with the spectral and

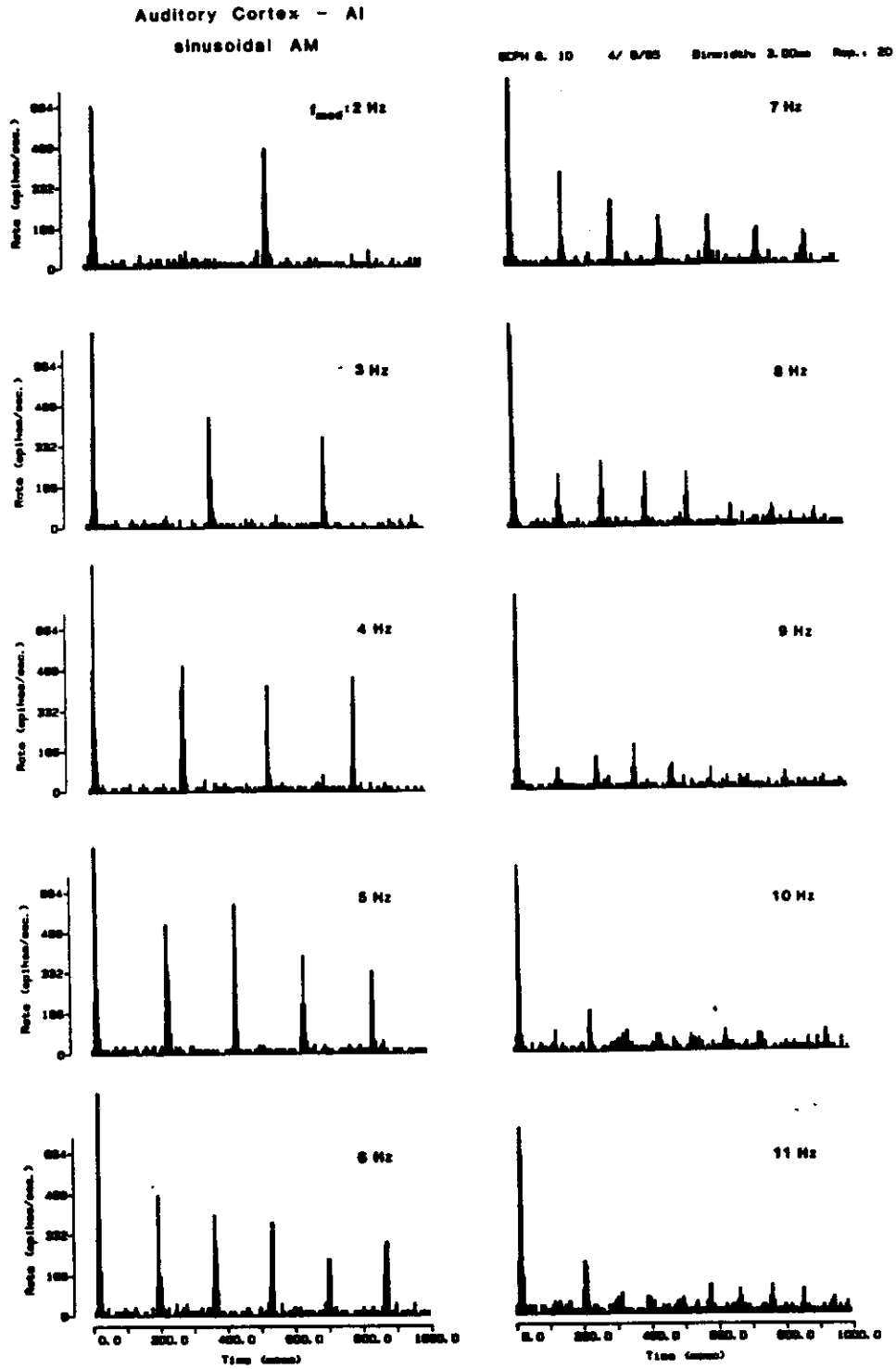
Auditory Cortex – AI
sinusoidal AM
f_{mod}: 2 Hz
7 Hz
3 Hz
8 Hz
4 Hz
9 Hz
5 Hz
10 Hz
6 Hz
11 Hz
Rate (spikes/sec.)
Time (msec)

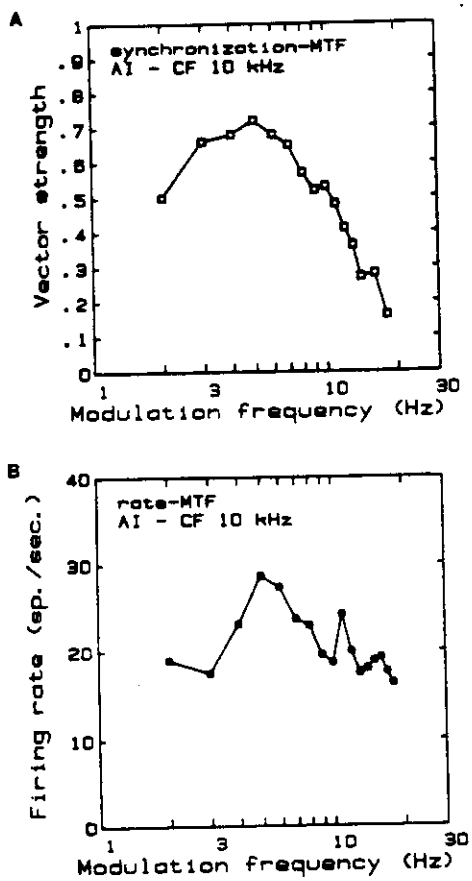

Figure 4. *tMTFs for cortical responses shown in Figure 3. A*: The synchronization MTF was constructed by plotting the vector strength of the response as a function of the modulation frequency. The vector strength is a quantitative measure of the occurrence of spikes in synchrony with the stimulating waveform (phase locking), in this case with the envelope waveform. The peak of the MTF is at 5 Hz (BMF). Small side peaks appear at 10 Hz and 15 Hz. *B*: The rate MTF was constructed by plotting the firing rate as a function of modulation frequency. The BMF was between 5 and 6 Hz. Pronounced side peaks can be seen at 11 Hz and 16 Hz (multiples of the BMF).

temporal receptive fields or the FTC and the MTF of a unit provides a basic description of the actual response of the unit to complex signals. The estimate of the response could presumably be further improved by including in the model features like adaptation, inhibitory side bands and nonlinear input–output functions.

The demonstration that the temporal properties of a unit described by its tMTF can be successfully utilized for the characterization of the overall response properties of neurons leads to the following questions: (1) Is there a systematic organization of the auditory system with regard to signal features of the temporal

Figure 3. *Response of a representative small group of neurons in the primary cortical field (AI) of an anesthetized cat to sinusoidal amplitude modulation of a best frequency tone.* The carrier signal of the modulation was 10 kHz (the units' CF), and the signal level was 50 dB SPL. The modulation depth was 100%. PSTHs for modulation frequencies from 2 to 11 Hz are shown. Twenty stimulus presentations were made in the generation of each PSTH. The bin width of the histograms was 3 msec. Note the narrow temporal region (about 20 msec) within which each response occurred, even with a 2-Hz modulation frequency, that is, responses mark the *onset* of each modulating wave and do not trace the shape of the modulating waveform. The strongest responses for 10- and 11-Hz modulation occurred about 200 msec after the onset response. This interval corresponded well to the BMF of neurons at this recording site of about 5–6 Hz.

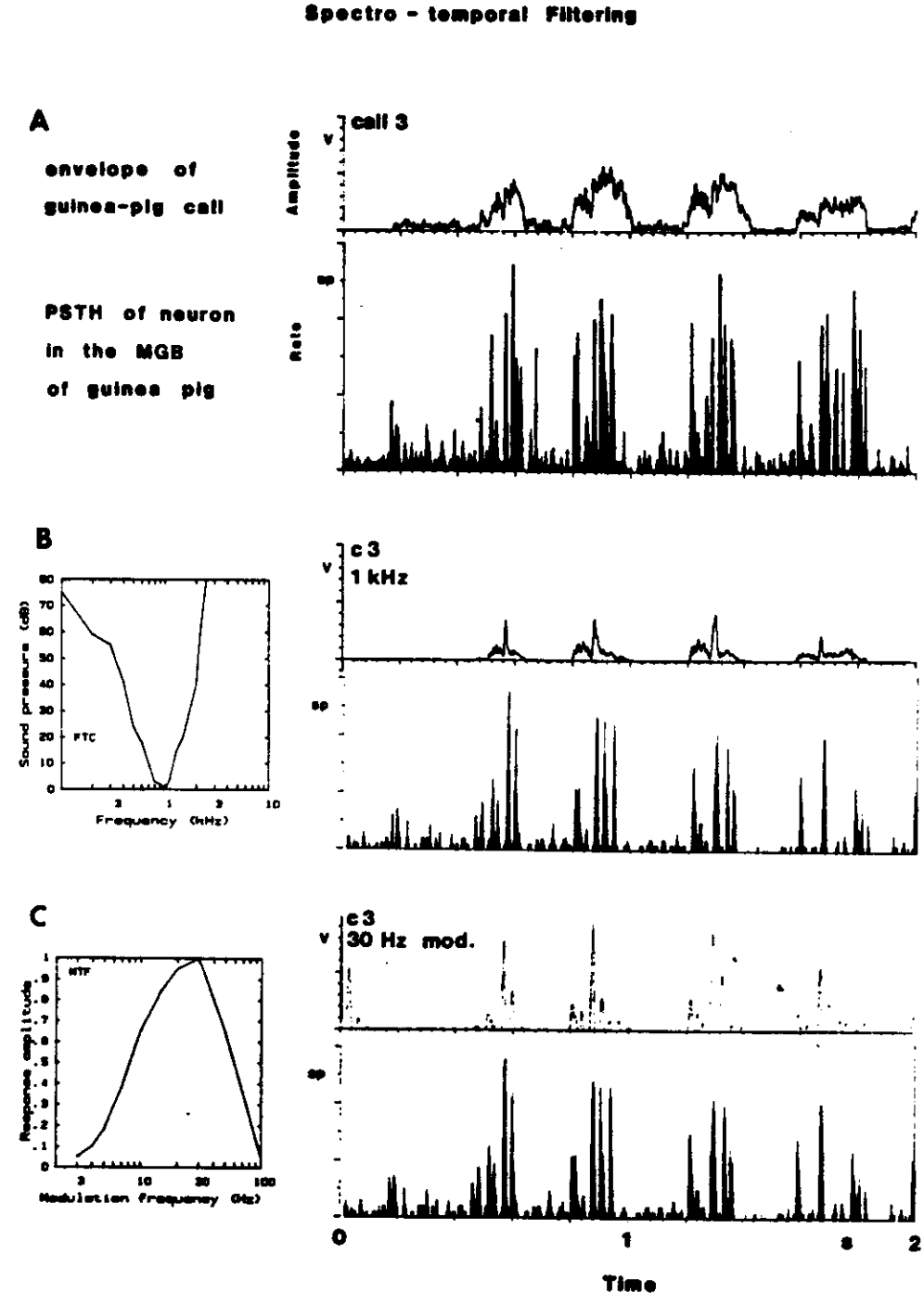
Spectro - temporal Filtering
A
envelope of guinea-pig call
PSTH of neuron in the MGB of guinea pig
call 3
Amplitude
Rate
B
c 3
1 kHz
Sound pressure (dB)
FTC
Frequency (kHz)
C
c 3
30 Hz mod.
MTF
Response amplitude
Modulation frequency (Hz)
Time

domain? (2) If so, how is it related to tonotopic organization in the spectral domain?

A number of investigations have revealed some aspects of the temporal resolution of neurons at different levels of the auditory system. In general, responses in the auditory nerve show a high temporal resolution, that is, the responses follow amplitude modulations over a wide frequency range (Javel, 1980; Smith and Brachman, 1980; Palmer, 1982). Slightly poorer temporal resolution was found in the cochlear nucleus (Møller, 1972, 1974, 1976) and a substantially poorer ability to follow amplitude modulation was seen in the inferior colliculus (IC) (Nelson et al., 1966; Vartanyan, 1969; Gersuni and Vartanyan, 1973; Rees and Møller, 1983) and the auditory cortex (Whitfield and Evans, 1965; Evans, 1974; Creutzfeldt et al., 1980). In contrast, modulation frequencies as high as 1000 Hz are coded by phase-coupled responses at the level of the midbrain in awake birds (Langner, 1981, 1983).

These findings can be summarized in part by stating that there is evidence supporting the hypothesis that overall temporal resolution decreases in successive stations along the ascending auditory pathway. No attempt has previously been made to search on a finer scale for a temporal topographic organization at any auditory system level. The following sections give an overview of some efforts to define in greater detail the distribution of temporal response characteristics within the IC and the auditory cortex of cats.

REPRESENTATION OF AMPLITUDE MODULATION IN THE INFERIOR COLLICULUS OF THE CAT

In the IC of barbiturate-anesthetized cats, the responses of 226 single units and 536 multiple units to sinusoidally amplitude-modulated CF tones were measured (Schreiner and Langner, 1984, 1988; Langner and Schreiner, 1985, 1988; Langner et al., 1987). About 90% of the recording sites were located in the central nucleus of the IC (called the ICC), based on physiological measures such as continual

Figure 5. *Demonstration of combined spectral and temporal filtering of a complex signal by the auditory system of an unanesthetized guinea pig. A*: The *upper trace* shows the signal envelope of a natural guinea-pig call (for sonogram, see Figure 2B). The *lower trace* represents a PSTH of the response to the call obtained from a single neuron in the MGB (20 signal presentations; bin width of 2 msec. *B*: At *left*, the FTC of this unit is shown. The CF of this spectral filter curve is about 1 kHz. The *upper trace* at *right* illustrates the envelope of the natural call after it has been spectrally filtered around 1 kHz, in accordance with the FTC. The response of the neuron to the spectrally filtered call is shown in the PSTH depicted in the *lower trace*. Although some peaks in the response to the filtered call are diminished or have disappeared, the frequency range around the CF of the unit clearly dominates the response characteristic of the unfiltered call. The resemblance between the filtered envelope of the call and the response is weak and is mostly based on similar main segmentations in call and response. *C*: At *left*, the tMTF of the neuron is shown. The CF of the temporal filter curve of this unit is 30 Hz. The *upper trace* shows the envelope of the 1-kHz band of the natural call (shown in *B*) after temporal filtering of the envelope around 30 Hz in accordance with the MTF. (The amplitude in the display of the temporally filtered envelope has been increased by a factor of about two in relation to the envelope amplitudes in *A* and *B*.) The *lower trace* in C redisplays the response of the unit to the 1-kHz band of the natural call (shown in *B*). After spectral and temporal filtering of the natural call, the resulting envelope resembles in many aspects the actual response of the unit to the original call.

CF sequence and tuning sharpness (expressed as Q-10 dB). In the majority of recording sites it was possible to assign a BMF to the response. The relationship between the BMF and CF of the recording sites is shown in Figure 6 (circles = single units; dots = multiple units). No clear systematic relationship between the CF and BMF can be extracted from the scatter diagram except an overall increase of the average BMF with increasing CF. Consequently, the upper limit of encountered BMFs also increases with the CF. The dashed line corresponds to a CF/BMF ratio of 4/1, which gives a fair approximation of the observed upper frequency limit of the BMFs.

A closer systematic relationship between the BMF and CF than indicated by the pooling of all data in Figure 6 was seen in single electrode tracks along the tonotopic gradient of the nucleus. Figure 7 shows the relationship of the CF and BMF of two electrode tracks as a function of the depth of recording sites along the dorsoventral dimension of the IC. The two parallel electrode tracks were separated by about 1 mm. With increasing depth of penetration, the CFs of encountered units increased gradually, in accordance with the tonotopic organization of the nucleus (Merzenich and Reid, 1974). Further, the BMF of the recording locations also showed an overall increase with depth, paralleling the changes in the CF. Whereas the CF essentially increased monotonically with depth, the increase of the BMF for both recording tracks showed two or three discontinuities in its course, marked by steplike decreases in the BMF. However,

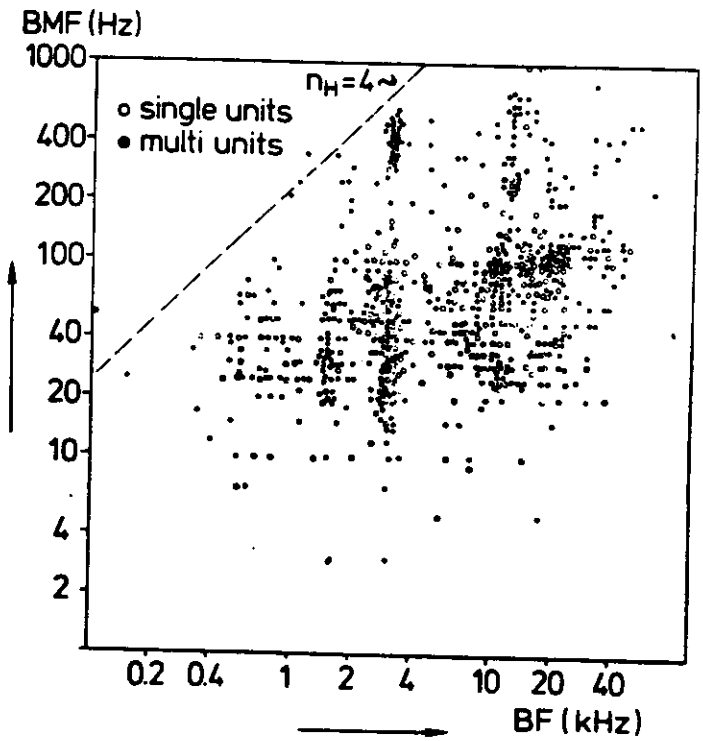

Figure 6. *BMFs of temporal modulation transfer functions of 226 single units (open circles) and 536 multiple units (filled circles) in the IC of anesthetized cats as a function of the CF of their spectral tuning curves.* (The apparent clustering of spectral CFs is due to a sampling bias.) The *dashed line* marks a CF/BMF ratio of 4/1. (From Langner and Schreiner, 1988.)

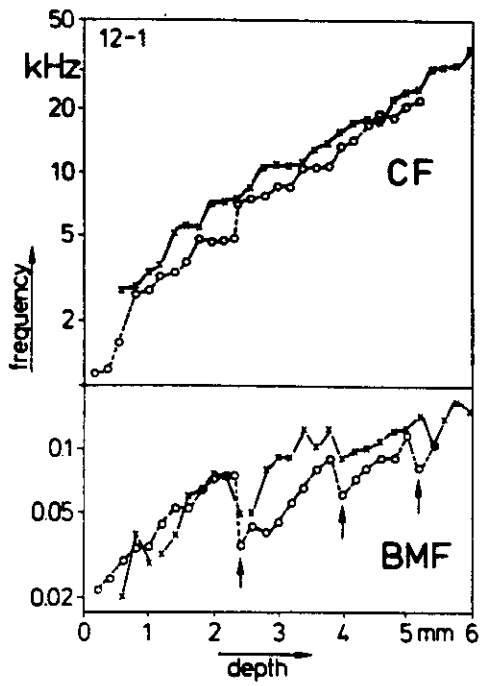

Figure 7. *CF and BMF profile for two dorsoventral recording tracks in the ICC of a cat. Arrows* mark steplike decreases in the BMFs encountered with increasing recording depth. (From Langner and Schreiner, 1988.)

these steps were not observed in all recording tracks. Overall, similar systematic relationships between the CF and BMF were found for most of the recording tracks along the tonotopic gradient.

The finding of a systematic change in the BMF with recording depth in the IC led to the question: What is the spatial relationship of the BMF to the other two functionally significant dimensions of the nucleus, that is, over the isofrequency laminae of this tonotopically organized nucleus? To explore this question, several maps of amplitude-modulated representation within isofrequency planes of the IC were obtained. Figure 8 shows an example of the distribution of BMFs in the 3-kHz plane of an IC—all single or multiple unit responses were tuned to a 3-kHz (±500 Hz) carrier tone. The mapped area measured about 1.6 mm in the rostrocaudal dimension of the nucleus and 3 mm in the lateromedial dimension. The X- and Y-axes of the graphs in Figure 8 represent these dimensions. Responses of neurons at 44 evenly distributed recording sites were analyzed. The right-hand graph in Figure 8 is a three-dimensional reconstruction of the BMF distribution in the isofrequency lamina with the height of the surface (Z-axis) as a measure of the BMF. The peak of the surface corresponds to the highest BMFs of about 400 Hz encountered in this particular isofrequency lamina. From a circumscribed center of high BMFs, the BMFs encountered in the isofrequency lamina monotonically decreased with increasing distance. The left graph in Figure 8 is a contour plot of the BMF distribution. Points of equal BMF are connected and can be called iso-BMF contours. As indicated by the three-dimensional plot, the iso-BMF contours appear to be concentrically arranged and the diameter of an iso-BMF contour increases with decreasing BMF. This example and data from

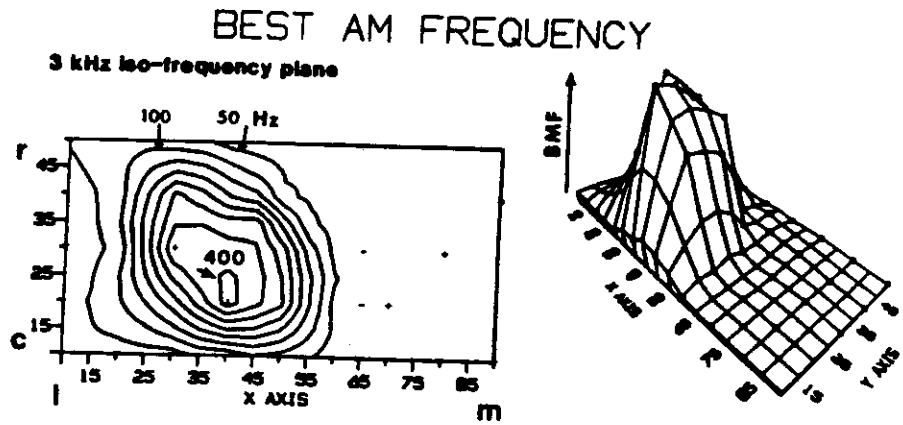

Figure 8. *Distribution of BMFs in the 3-kHz isofrequency lamina of the ICC.* The map was derived from 44 parallel recording tracks that were oriented approximately orthogonal to the isofrequency lamina. The mapped area measured around 4 mm in the rostrocaudal dimension and about 8 mm in the lateromedial dimension. The maps were reconstructed from 44 evenly separated recording locations with CFs of 3 kHz (± 500 Hz). At *left* is a contour plot of the BMF distribution. Interpolated *points* of equal BMF were connected by *lines* (iso-BMF contours). Iso-BMF contours representing 50 Hz, 100 Hz, and 400 Hz are indicated. At *right* is a three-dimensional reconstruction of the BMF distribution is shown. The height of the surface corresponds to the value of the BMF at any given location. The peak of the surface corresponds to BMFs of approximately 400 Hz. (From Schreiner and Langner, 1988.)

other similar maps constitutes strong evidence for a highly organized representation of temporal signal aspects within the isofrequency laminae of the IC.

The relationship of the organization of temporal parameters between different isofrequency planes is illustrated by the examples shown in Figure 9. The distribution of BMFs in the 3-kHz and the 12-kHz isofrequency planes of a cat are shown in a manner similar to Figure 8. The spatial location of the areas of maximal BMFs are approximately the same for both planes. However, the elevation of the BMF plane of the 12-kHz map is generally higher than for the 3-kHz map. That means, on the average, that the BMFs encountered in the 12-kHz map are slightly higher than those in the 3-kHz map, in accordance with the increase of BMF with depth/CF as shown in Figures 6 and 7. As a consequence of the overall increase of BMFs with CF, the diameter of an iso-BMF contour has to expand with increasing CF. The 500-Hz BMF contour is marked in both maps and illustrates the expansion of the high BMF area with increasing CF. With regard to the whole CF range in the nucleus, the expansion of iso-BMF contours with the CF leads to a topographical distribution of similar BMFs in a conical arrangement. Figure 10 schematically illustrates the surface connecting all locations with equal BMFs and its orientation within the IC. Examples for a low and a high BMF are given.

From these preliminary results, the following hypotheses about the internal organization of the IC with regard to temporal signal parameters can be drawn:

1. The ICC of the cat contains a highly systematic topographic representation of stimulus parameters of the temporal domain (e.g., amplitude modulation).

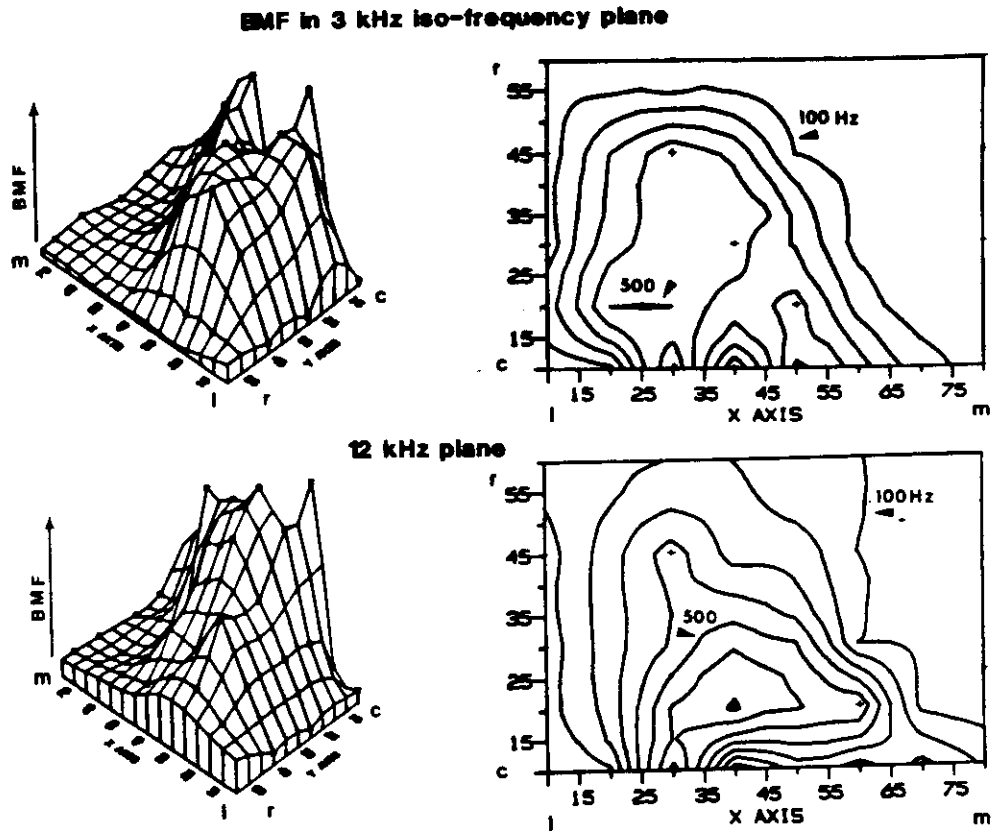

Figure 9. *Distributions of BMFs in the 3-kHz and 12-kHz isofrequency laminae of the IC in a single cat.* At *left* are three-dimensional reconstructions of the BMF map. At *right* are the interpolated iso-BMF contour maps. Iso-BMF contours of 100 Hz and 500 Hz are indicated. (From Schreiner and Langner, 1988.)

2. The topographic representation of temporal parameters is orthogonal to the spatial organization of spectral parameters (tonotopicity) in the sense that the main temporal gradient is present within each isofrequency lamina.
3. The topographic representation of BMFs within isofrequency laminae is realized through a concentric arrangement of iso-BMF contours, with the highest BMFs located at its center.

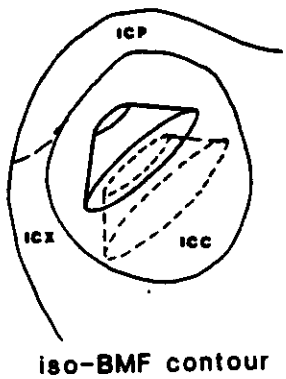

Figure 10. *Schematic representation of iso-BMF contours in the ICC.* Locations with similar BMFs are distributed on a conical surface. BMF distributions are shown for a high BMF (*dashed lines*) and for a lower BMF (*solid lines*).

4. For a given BMF, the diameter of the corresponding concentric BMF contour within an isofrequency lamina increases with increasing CF (although the steps in the BMF function with depth shown in Figure 7 indicate some discontinuities in this relationship).
5. Along the spectral gradient (across isofrequency laminae), sites of equal BMF are located on a conically shaped surface.
6. The frequency range and the topographic representation of BMFs in the IC are compatible with an interpretation of its function as a spatial reference or representation utilized for constructs of periodicity or residue pitch perception. Details of the neuronal tuning properties (Schreiner and Langner, 1984; Langner and Schreiner, 1988) including a close relationship between BMF and onset latency (Langner and Schreiner, 1985; Langner et al., 1987; Schreiner and Langner, 1988) indicate that intrinsic oscillations and coincidence detection underlie the creation of a spatial representation of periodicity information (see Langner, 1981, 1983, 1985; Langner and Schreiner, 1988).

REPRESENTATION OF AMPLITUDE MODULATION IN THE AUDITORY CORTEX OF THE CAT

Several studies of the auditory cortex have found some evidence that the ability of cortical neurons to follow successive temporal changes in the input signal is more limited than that found at more peripheral auditory levels (Whitfield and Evans, 1965; Ribaupierre et al., 1972; Evans, 1974; Creutzfeldt et al., 1980). However, the ability to represent the course of rapid but infrequent changes in the spectrotemporal composition of the input signal (transients) appears to be well preserved in the spatiotemporal representation of the signal across the cortical field (Creutzfeldt et al., 1980).

The reduction of temporal resolution in a neuron of the auditory cortex of an awake guinea pig as compared to a neuron in the MGB is demonstrated in Figure 11 (Creutzfeldt et al., 1980). Both unit responses were recorded simultaneously. The CFs of both neurons were identical and a high percentage of "spontaneous" spikes in the cortical neuron were preceded by a spontaneous spike in the thalamic unit, indicating synaptic connections between the two. Inspection of the response of the two units to amplitude-modulated tones revealed a dramatic difference in their ability to follow amplitude changes in the stimulus. Whereas

Figure 11. ***Responses of a thalamic and a cortical neuron in an unanesthetized guinea pig to rectangularly amplitude-modulated tones.*** **The spontaneous activity of these two neurons was positively correlated. The CF for both units was identical (2 kHz). The pulse duration and interstimulus interval were 800 msec; the rise time of the trapezoidal signal envelope was 10 msec. The PSTHs of responses to different modulation frequencies are displayed in parts *a–k* (20 signal presentations; 2-msec bin width). Parts *i–l* show the autocorrelation functions of the thalamic response for four different modulation frequencies. Peaks in the autocorrelation function (only the negative half is shown; the positive half of the autocorrelation function is a mirror image of the negative part) indicate synchronization of the spike occurrences with the modulation frequency. For 200 Hz, no peaks were present in the autocorrelation function, that is, the response was not significantly phase-locked to the modulation frequency. (From Creutzfeldt et al., 1980.)**

oral Patterns

ntric BMF
ng CF (al-
n Figure 7

s of equal

MFs in the
l reference
idue pitch
and Lang-
lationship
; Langner
scillations
esentation
ngner and

DITORY

the ability
t signal is
tfield and
al., 1980).
hanges in
ears to be
across the

rtex of an
l in Figure
aneously.
ntaneous"
ke in the
pection of
a dramatic
. Whereas

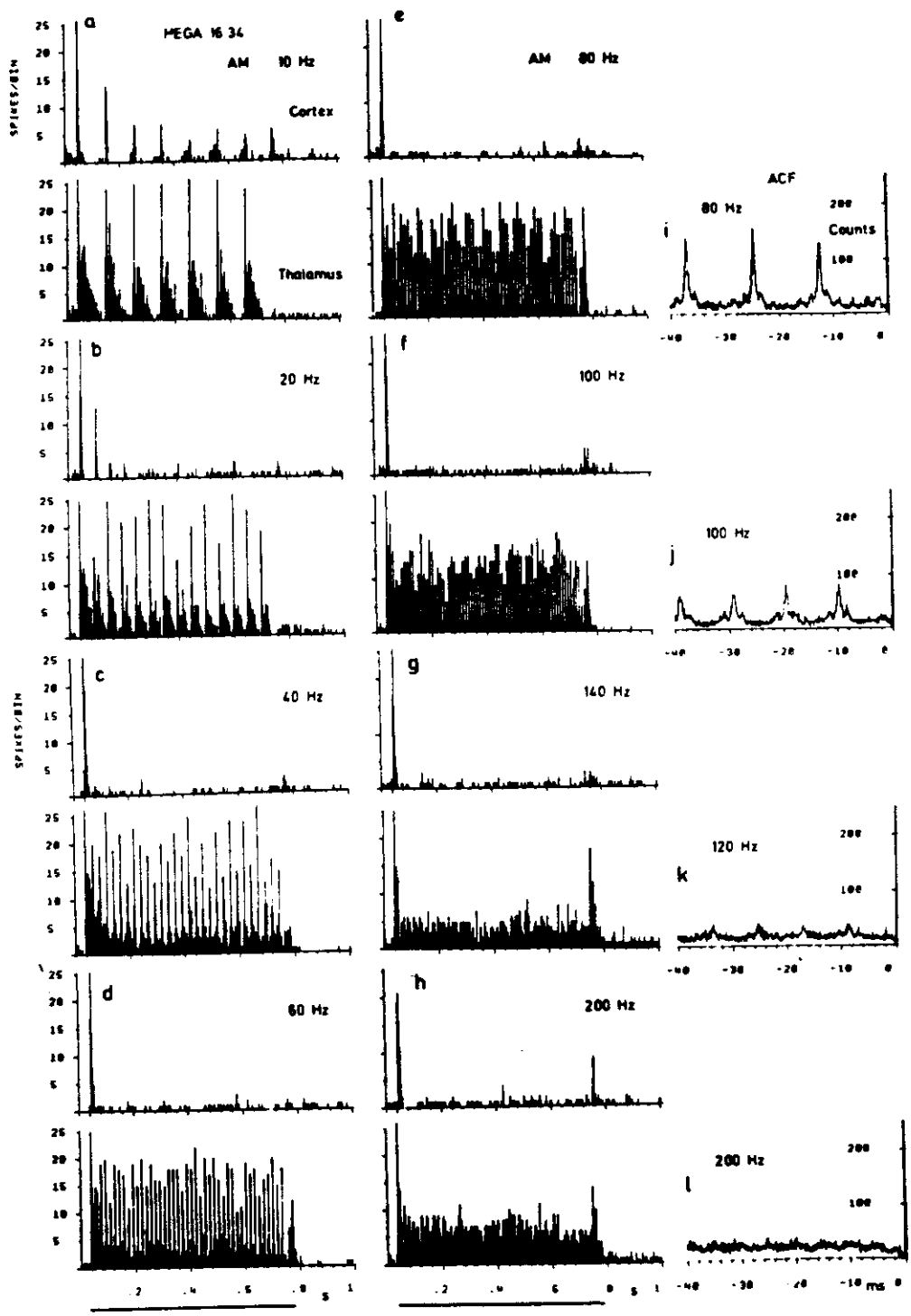

rectangularly
ly correlated.
nterval were
of responses
ions; 2-msec
nse for four
negative half
egative part)
For 200 Hz,
significantly

the thalamic responses showed synchronization with the stimulus envelope up to 150 Hz, the cortical unit ceased to follow modulation frequencies above 20 Hz. In other words, the temporal resolution of the cortical neuron appeared to be strongly diminished.

To gain a more systematic overview of the properties of the cortical representation of such temporal stimulus aspects, the response of cortical neurons to amplitude-modulated tones has been investigated in anesthetized cats (Schreiner and Urbas, 1984, 1986, 1988). For this survey, the multiunit recording technique was applied to obtain the overall characteristics of several auditory cortical fields. For about 88% of 172 cortical locations, the MTFs had a bandpass characteristic and BMFs could be determined. The BMFs covered a modulation range from 3 to 100 Hz. The other 12% showed a low-pass characteristic with a maximum at the lowest modulation frequency used in this study (2.2 Hz).

Figure 12 shows the BMFs of rate MTFs as function of CF for locations in five auditory cortical fields. The stimuli were sinusoidally amplitude-modulated CF tones (100% modulation). The majority of BMFs in the second auditory cortical field (AII), the posterior auditory field (PAF), and the ventroposterior auditory field (VPAF) were found to be equal to or below 10 Hz. This low modulation range corresponds well to earlier reports of a low temporal resolution in the auditory cortex (Evans, 1974; Creutzfeldt et al., 1980). The primary auditory field (AI) and, in particular, the anterior auditory field (AAF) showed a higher temporal resolution than the aforementioned fields. The average BMF was found to be approximately 15 Hz (±20 Hz SD) for AI and approximately 28 Hz (±27 Hz) for AAF, distinguishing AAF as the cortical field with the highest temporal resolution. Another property differentiating AAF from other investigated fields was a significant correlation between CF and BMF: BMFs tended to increase with increasing CF. However, no other fundamental organization in the spatial distribution of the cortical BMFs could be resolved; for example, there was no apparent organization reminiscent of or in any way equivalent to the orderly spatial representation of BMFs within isofrequency laminae in the IC.

In the bar graphs in Figure 13, the average temporal resolutions—expressed as BMF—of five cortical fields are summarized for two different stimulus conditions (sinusoidal and rectangular modulation waveform) and for two response measures (rate and synchronization). In general, it can be concluded that the shape of the modulating waveform had only minor influences on the estimate of the temporal resolution. This means that the repetition rate of transients plays a more prominent role in the cortical representation of signals than do details in the envelope shape of the transients or onsets. The fact that rate and synchronization measures yielded similar estimates for the temporal resolution of cortical neurons indicates that the marking of temporal events in the auditory cortex is accomplished by a robust activity pattern, usually a phasic onset response (see Figure 3).

Stimulation with unmodulated tone bursts produced periodic fluctuations of the evoked neural response at about 75% of the investigated cortical locations in AAF and AI. The frequencies of these "intrinsic oscillations" were usually closely related to the BMFs obtained at those locations. Duration and frequency of the intrinsic oscillations reflect the filter characteristics of the envelope filters in at least some of the auditory cortical fields (Schreiner and Urbas, 1986, 1988).

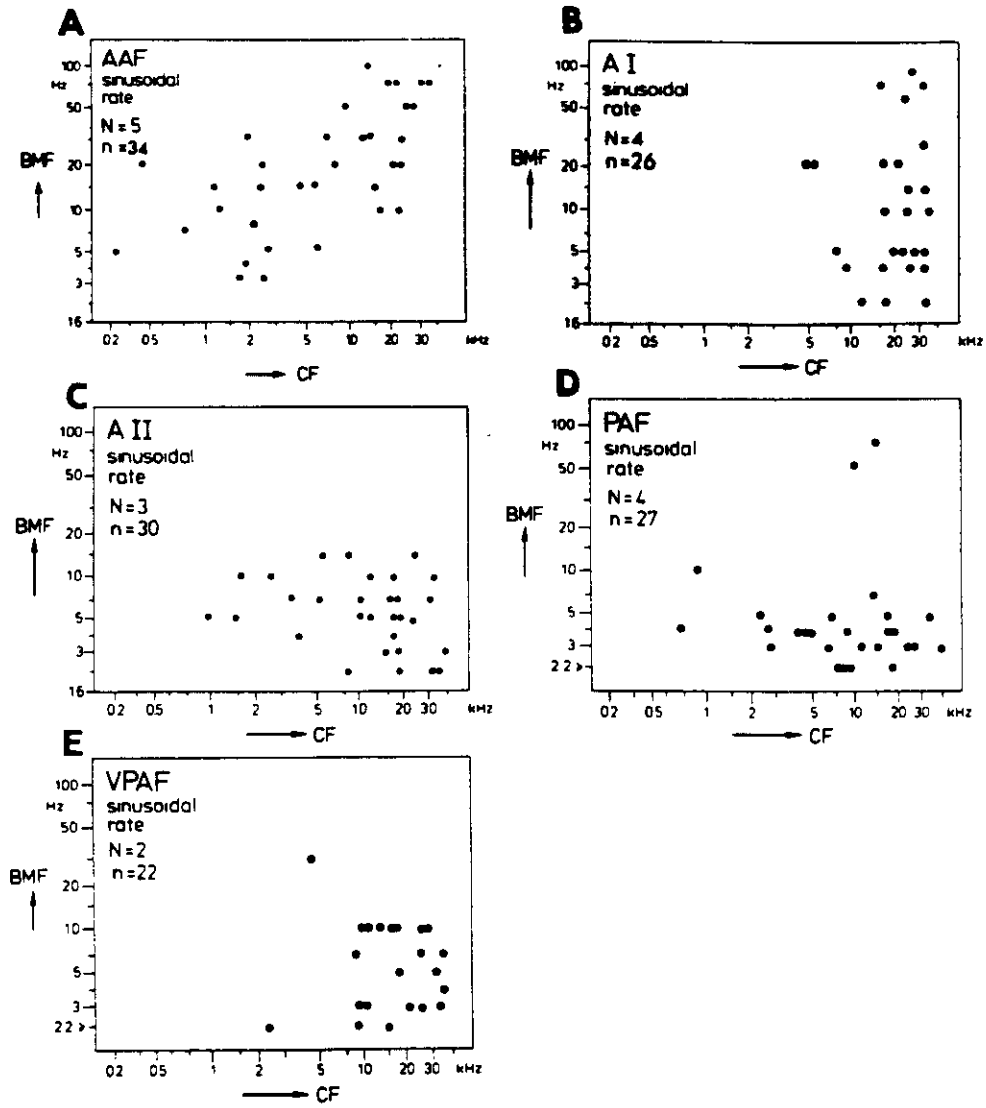

Figure 12. *Distribution of BMFs in five auditory cortical fields in the anesthetized cat.* The BMFs were derived from rate MTFs for sinusoidal modulation (see Figures 3 and 4B). The investigated cortical fields were the anterior auditory field (AAF); the primary auditory field (AI); the second auditory field (AII); the posterior auditory field (PAF), and the ventroposterior auditory field (VPAF). (From Schreiner and Urbas, 1988.)

Previous observations of the temporal characteristics of cortical neurons have been made in unanesthetized animals (Ribaupierre et al., 1972; Evans, 1974; Goldstein and Abeles, 1975; Creutzfeldt et al., 1980). A comparison of those results with results obtained in anesthetized cats provides no evidence that anesthesia exerts a strong detrimental influence on the cortical representation of amplitude-modulated signals.

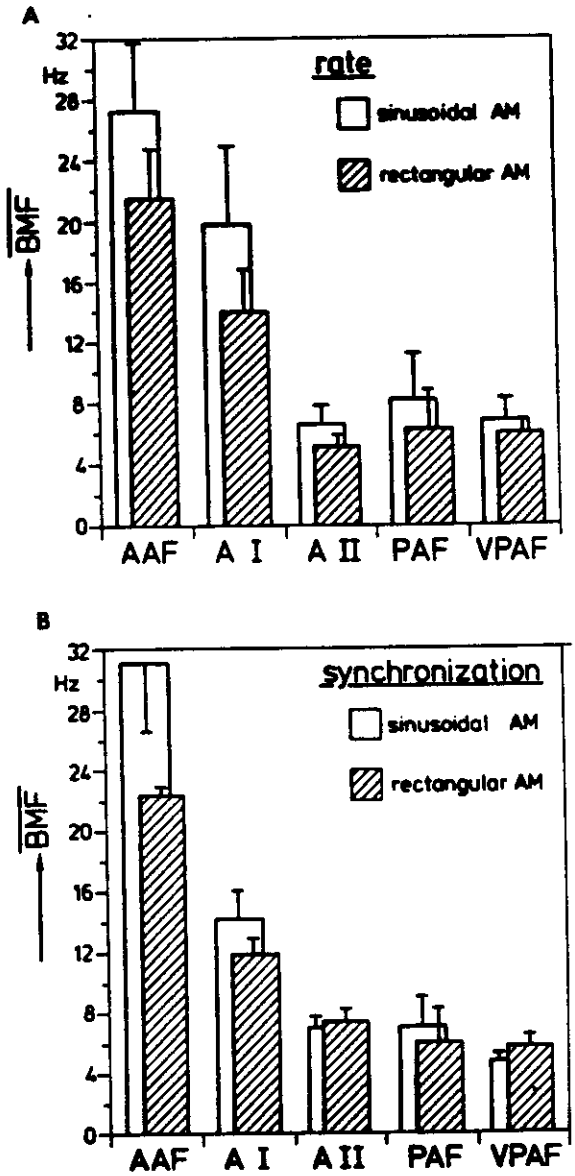

Figure 13. *Averaged BMFs for five auditory cortical fields. A:* BMFs derived from rate MTFs for sinusoidal (*white bars*) and rectangular (*hatched bars*) amplitude modulation of CF tones. *B:* BMFs derived from synchronization MTFs. The SEM is indicated by the *error bars*. (From Schreiner and Urbas, 1988.)

From the preliminary results of this study the following conclusions are drawn: (1) In the auditory cortex of the cat, a spatial segregation of response characteristics to temporal envelope features exists. Cortical fields with predominantly higher temporal resolution (AAF, AI) can be statistically distinguished from a group of cortical fields with predominantly low temporal resolution (AII, PAF, VPAF). (2) Within AAF, the cortical field with the highest temporal resolution, a gradient of BMFs across isofrequency lines has been observed. (3) The average temporal

resolution in all investigated cortical fields, with the possible exception of AAF, is far below the overall temporal resolution described for the IC and more peripheral stations.

CONCLUSIONS AND HYPOTHESES

From the experimental data available at present on the representation of temporal signal envelope aspects in the central auditory system, some conclusions and general hypotheses about organizational features of the auditory system and their functional significance with regard to the processing of temporal signal features may be drawn.

Organizational Features of the Central Auditory System Related to Processing of Signal Aspects in the Time Domain

At least three different levels of organization related to the processing and neural representation of temporal envelope features can be distinguished in the ascending auditory pathway.

Organization Across Different Auditory Stations. A general reduction of the overall temporal range of stimulus variations preserved in the temporal activity patterns of neural elements along the auditory pathway (Rees and Møller, 1983) can be described as the most basic temporal organizational feature ("first level of temporal organization"). Figure 14 summarizes the overall temporal resolution

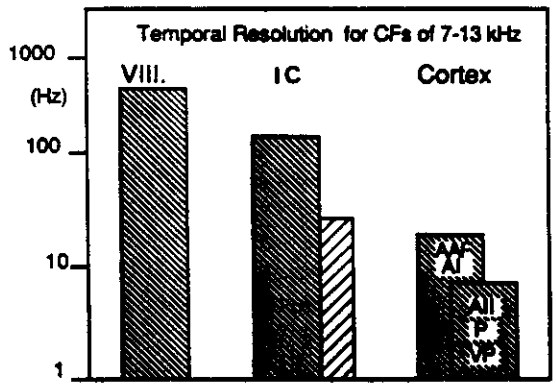

Figure 14. *Schematic representation of the temporal resolution at different levels of the mammalian auditory system.* Temporal resolution is expressed as either the average BMF found for MTFs with bandpass characteristic, or by the average cutoff frequency for MTFs with low-pass characteristic (the latter is especially the case for the VIIIth nerve data). The estimate of average BMFs was limited to units with CFs between 7 and 13 kHz in order to avoid influences from a possible functional relationship of BMF and CF. The estimate of the average temporal resolution of the auditory nerve (VIII) is based on results from Palmer (1982). Two estimates of temporal resolution are given for the IC. The *finely hatched bar* represents an estimate based on data collected by Schreiner and Langner (1984; Langner and Schreiner, 1985) in the cat. The *hatched bar* represents combined estimates of the temporal resolution given by Rees and Møller (1983) and by Gersuni and Vartanyan (1975). The estimates for different cortical fields are based on results from Schreiner and Urbas (1984, 1986, 1988).

found at different levels of the auditory system. The temporal resolution of the auditory nerve (Palmer, 1982) appears to be higher than at any other processing level. All estimates of the average temporal resolution in the IC (Nelson et al., 1966; Vartanyan, 1969; Gersuni and Vartanyan, 1973; Rees and Møller, 1983; Schreiner and Langner, 1984; Langner and Schreiner, 1988) are clearly lower than those given for the auditory nerve. The highest BMFs found in the IC (Schreiner and Langner, 1984; Langner and Schreiner, 1988) are still comparable with the temporal resolution of auditory nerve fibers. However, the majority of units in the IC are tuned to modulation frequencies well below the upper frequency limit given by the auditory nerve. Differences between our estimate of the temporal resolution in the IC (Schreiner and Langner, 1984; Langner and Schreiner, 1985, 1988; Langner et al., 1987) and previous estimates (Gersuni and Vartanyan, 1973; Rees and Møller, 1983) are probably related to differences in the applied sampling strategies.

Despite differences between the estimates of the temporal resolution of the IC, all of them are higher than the overall estimates for either high or low temporal resolution areas of the auditory cortex (see Figure 14), supporting the notion of a general decrease in temporal resolution within the ascending auditory pathway (Rees and Møller, 1983).

Organization Within Auditory Stations. The next organizational level of the temporal processing is reflected by differences found in various subdivisions of a given auditory station of the mainline auditory projection system ("second level of temporal organization"). Within the auditory cortex—the sixth level of the auditory projection system—clear differences between some of the cortical subdivisions were described for temporal resolution (Schreiner et al., 1983; Schreiner and Urbas, 1984, 1986, 1988). A hierarchy of temporal resolution was established, with the highest resolution in AAF; a somewhat lower resolution in AI; and an even lower resolution in AII, PAF, and VPAF (see Figure 13). This notion of a hierarchy of temporal resolution is quite different from the serial order hierarchical processing implied by the loss of temporal resolution between successive levels of processing, referred to as the first level of temporal organization. Each of the cortical fields receives information through a multicomponent, parallel projection system, feeding different combinations of information-bearing parameters to different cortical representational fields (Anderson et al., 1980; Merzenich and Kaas, 1980). Thus differences in the temporal resolution between cortical fields are most likely a consequence of task-intrinsic properties optimal for the field-specific representation or processing of acoustical information (Merzenich and Kaas, 1980; Suga, 1982, 1984).

In other nuclei, a similar segregation of temporal response characteristics has not been reported, although our studies in the IC derived some evidence suggesting a lower temporal resolution in the pericentral nucleus of the IC than in the ICC.

Organization Within a Subdivision. The next higher level of organized representation of temporal signal properties would be an organization confined to a single subdivision of a nucleus or cortical area ("third level of temporal organization"). The best example available for this level of temporal organization is found in the ICC. As demonstrated above, the ICC appears to contain a highly ordered representation of amplitude-modulated frequencies. That is, neural ele-

ments tuned to different frequency ranges of envelope modulations are arranged in topographic fashion within a coordinate system for the representation of certain temporal signal features. This kind of orderly map would appear to represent the ultimate neural representation of a particular signal feature by spatial distribution of neural activity, as proposed by Suga (1982, 1984) based on observations of highly specialized maps in the auditory cortex of the mustached bat.

At this time, no other station in the auditory pathway has been seen to have a similarly highly organized representation of temporal signal aspects. There are some subdivisions of the auditory pathway that include a far more limited but still somewhat systematic representation of temporal features. The auditory nerve and the anterior auditory cortical field are examples. Both show a significant correlation of the CF with the BMF. However, there is no evidence that this kind of weak temporal organization is of high functional significance.

In summary, it can be stated that the auditory system contains several levels of systematic topographical organization with respect to response characteristics that convey temporal modulation aspects of the input signal. These different levels of organization range from a general trend of changes in the temporal resolution along the ascending auditory axis to a highly systematically organized map of BMFs within a subdivision of the IC.

Most subdivisions of auditory nuclei probably lack the highly organized representations of temporal signal parameters seen in the IC. However, it is justified to assume that each nucleus and its subdivisions will have its own characteristic range of temporal resolution, reflecting a certain aspect of its properties of signal representation and coding. Oversimplifying, it could be said that different aspects of temporal signal characteristics are emphasized in their representation in different parts of the auditory system. It is sufficient to conclude that temporal signal aspects such as envelope variations represent a major organizational principle of the auditory system in addition to the well-established spectral (tonotopic) and binaural organization of the auditory system.

Functional Significance of Temporal Organization in the Central Auditory System

The interpretation of functional consequences based on the temporal organizations described above can only be of a speculative nature, since establishing functional connections between morphological structures and perceptual attributes is difficult. Nevertheless, a few obvious consequences for the representation of complex auditory signals in the central auditory system, most notably in the IC and the auditory cortex of the cat, are outlined here.

The relatively low temporal resolution found in the investigated auditory cortical fields implies that, on a first order, signal representation at the cortical level is characterized by the spectral content of transients, marking relatively infrequent variations in the input. The spectral properties of a sequence of transients are spatially distributed across the tonotopic organization of different fields (Creutzfeldt et al., 1980). In addition, this spatiotemporal distribution of transients will be affected by other functional aspects of cortical fields such as binaural characteristics (Imig and Adrian, 1977; Middlebrooks et al., 1980; Jenkins and Merzenich, 1984; Brugge, 1985), which are largely still poorly defined (with

the exception of the highly parameterized cortical maps found in bats; see Suga, 1982, 1984, and this volume). Differences in the temporal resolution of various cortical fields suggest that each field may emphasize, in its representation, a specific type of transient information.

The frequency range of temporal signal aspects covered by the auditory cortical fields is centered around the repetition or sequencing range found in speech (syllable, phoneme, and word sequencing; see Figure 1; Plomp, 1983) and probably also in cat vocalizations (G. Ehret, personal communication). In combination with results from cortical ablation studies, which showed a severe impairment of the discrimination of temporal signal properties (such as duration and sequential tone patterns; Whitfield, 1971; Neff et al., 1975), these data suggest that the auditory cortex plays a major role in the coding and processing of sequences of short and relatively infrequent events in complex signals.

Since the upper frequency limit of temporal resolution for the majority of auditory cortical neurons is below 100 Hz (Goldstein et al., 1971; Ribaupierre et al., 1972), and since the majority of neurons are tuned to modulation frequencies well below 50 Hz, most signals with periodicity or residue pitch above 100 Hz (including, for example, most music and speech signals) appear to have no direct temporal correlates of their pitch aspects represented in the cortex. On the other hand, a station that does display in its signal representation at least most of the temporal range that constitutes the periodicity pitch range (Schouten, 1970; Small, 1970; Viemeister, 1979) is the ICC. The orderly representation of modulation frequencies in concentric arrangements within isofrequency laminae and also in a systematic fashion across the tonotopic organization of the IC suggests a major role of the nucleus in the extraction or representation of temporal signal aspects in the periodicity pitch range. Our present results—including coding properties of units in the IC that have not been discussed in this chapter—are consistent with a model of a correlation analysis in the time domain based on periodicity coding (Langner, 1981, 1983, 1985). This model is suitable for explaining the pitch effects observed with amplitude-modulated signals in human subjects (Schouten, 1970). Our hypotheses are: (1) periodicity pitch in mammals including humans is analyzed in the time domain; (2) a spatial representation of periodicities is generated by a correlational analysis in the time domain; and (3) periodicity pitch is thereby probably encoded by a spatial arrangement of periodicity-tuned units.

The importance of temporal signal aspects for a robust transmission and representation of complex sounds in the auditory system has been demonstrated for the auditory nerve (Sachs and Young, 1979; Young and Sachs, 1979; Delgutte, 1980). Those results in combination with the finding of temporal organization in the IC and the auditory cortex further emphasize the need to study the processing of temporal signal aspects in order to understand the coding of complex signals in the auditory system.

ACKNOWLEDGMENTS

This work was supported by National Institutes of Health Grants NS-10414 (Merzenich) and NS-16361 (Leake), Hearing Research Inc., the Coleman Fund,

and the Deutsche Forschungsgemeinschaft. The authors wish to thank Dr. Michael Merzenich for his valuable comments on the manuscript.

REFERENCES

Andersen, R. A., P. L. Knight, and M. M. Merzenich (1980) The thalamocortical and corticothalamic connections of AI, AII and the anterior auditory field (AAF) in the cat: Evidence for two largely segregated systems of connections. *J. Comp. Neurol.* 194:663–701.

Aitkin, L. M., D. R. F. Irvine, and W. R. Webster (1984) Central neural mechanisms of hearing. *Handb. Physiol.* 3:675–738.

Brugge, J. F. (1985) Patterns of organization in auditory cortex. *J. Acoust. Soc. Am.* 78:353–359.

Bullock, T. H., ed. (1977) *Recognition of Complex Acoustic Signals*, Springer-Verlag, Berlin.

Creutzfeldt, O. D., F.-C. Hellweg, and C. E. Schreiner (1980) Thalamocortical transformation of responses to complex auditory stimuli. *Exp. Brain Res.* 39:87–104.

Delgutte, B. (1980) Representation of speech-like sounds in the discharge patterns of auditory-nerve fibers. *J. Acoust. Soc. Am.* 68:843–857.

Evans, E. F. (1974) Neural processes for the detection of acoustic patterns and for sound localization. In *The Neurosciences: Third Study Program*, F. O. Schmitt and F. G. Worden, eds., pp. 131–145, MIT Press, Cambridge, Massachusetts.

Evans, E. F., and I. C. Whitfield (1964) Classification of unit responses in the auditory cortex of the unanesthetized and unrestrained cat. *J. Physiol. (Lond.)* 171:476–493.

Fay, R. R. (1980) Psychophysics and neurophysiology of temporal factors in hearing by the goldfish: Amplitude modulation detection. *J. Neurophysiol.* 44:312–332.

Gersuni, G. V., and I. A. Vartanyan (1973) Time-dependent features of adequate sound stimuli and the functional organization of central auditory neurons. In *Basic Mechanisms in Hearing*, A. R. Møller, ed., Academic, New York.

Goldstein, M. H., Jr., and M. Abeles (1975) Single unit activity of the auditory cortex. *Handb. Sensory Physiol.* 5:199–218.

Goldstein, M. H., Jr., F. de Ribaupierre, and G. H. Yeni-Komishian (1971) Cortical coding of periodicity pitch. In *Physiology of the Auditory System*, M. B. Sachs, ed., pp. 299–306, National Education Consultants, Baltimore.

Imig, T. J., and H. O. Adrian (1977) Binaural columns in the primary field (AI) of cat auditory cortex. *Brain Res.* 138:241–257.

Javel, E. (1980) Coding of AM tones in the chinchilla auditory nerve: Implications for the pitch of complex tones. *J. Acoust. Soc. Am.* 68:133–146.

Jenkins, W. M., and M. M. Merzenich (1984) Role of cat primary auditory cortex for sound localization behavior. *J. Neurophysiol.* 52:819–847.

Johnson, D. H. (1980) The relationship between spike rate and synchrony in response of auditory-nerve fibers to single tones. *J. Acoust. Soc. Am.* 68:1115–1122.

Langner, G. (1981) Neuronal mechanisms for pitch analysis in the time domain. *Exp. Brain Res.* 44:450–454.

Langner, G. (1983) Evidence for neuronal periodicity detection in the auditory system of the guinea fowl: Implications for pitch analysis in the time domain. *Exp. Brain Res.* 52:333–355.

Langner, G. (1985) Time coding and periodicity pitch. In *Time Resolution in Auditory Systems*, A. Michelsen, ed., pp. 108–121, Springer-Verlag, Berlin.

Langner, G., and C. E. Schreiner (1985) Response latencies in the inferior colliculus of the cat: Another evidence for an auditory periodicity mechanism. *Soc. Neurosci. Abstr.* 11:248.

Langner, G., and C. E. Schreiner (1988) Periodicity coding in the inferior colliculus of the cat. I. Neuronal mechanisms. *J. Neurophysiol.* (in press).

Langner, G., C. E. Schreiner, and M. M. Merzenich (1987) Covariation of response latency and temporal resolution in the inferior colliculus of the cat. *Hear. Res.* 31:197–202.

Merzenich, M. M., and J. Kaas (1980) Principles of organization of sensory-perceptual systems in mammals. In *Progress in Psychobiology and Physiological Psychology*, J. M. Sprague and A. N. Epstein, eds., pp. 1–42, Academic, New York.

Merzenich, M. M., and M. D. Reid (1974) Representation of the cochlea within the inferior colliculus of the cat. *Brain Res.* 77:397–415.

Merzenich, M. M., P. L. Knight, and G. L. Roth (1976) Representation of cochlea within primary auditory cortex in the cat. *J. Neurophysiol.* 38:231–249.

Merzenich, M. M., W. M. Jenkins, and J. C. Middlebrooks (1984) Observations and hypotheses on special organizational features of the central auditory nervous system. In *Dynamic Aspects of Neocortical Function*, G. M. Edelman, W. E. Gall, and W. M. Cowan, eds., pp. 397–424, Wiley, New York.

Middlebrooks, J. C., R. W. Dykes, and M. M. Merzenich (1980) Binaural response-specific bands in primary auditory cortex (AI) of the cat: Topographical organization orthogonal to isofrequency contours. *Brain Res.* 181:31–48.

Møller, A. R. (1972) Coding of amplitude and frequency modulation in the cochlear nucleus of the rat. *Acta Physiol. Scand.* 86:233–238.

Møller, A. R. (1974) Responses of units in cochlear nucleus to sinusoidally amplitude modulated tones. *Exp. Neurol.* 45:104–107.

Møller, A. R. (1976) Dynamic properties of excitation and two-tone inhibition in the cochlear nucleus studied using amplitude-modulated tones. *Exp. Brain Res.* 25:307–321.

Neff, W. D., I. T. Diamond, and J. H. Casseday (1975) Behavioral studies of auditory discrimination: Central nervous system. *Handb. Sensory Physiol.* 5:307–400.

Nelson, P. G., S. D. Erulkar, and J. S. Bryan (1966) Responses of units of the inferior colliculus to time-varying acoustic stimuli. *J. Neurophysiol.* 29:834–860.

Palmer, A. R. (1982) Encoding of rapid amplitude fluctuations by cochlear-nerve fibres in the guinea pig. *Arch. Otorhinolaryngol.* 236:197–202.

Plomp, R. (1983) The role of modulation in hearing. In *Hearing—Physiological Bases and Psychophysics*, R. Klinke and R. Hartman, eds., pp. 270–275, Springer-Verlag, Berlin.

Reale, R. A., and T. J. Imig (1980) Tonotopic organization in auditory cortex of the cat. *J. Comp. Neurol.* 192:265–291.

Rees, A., and A. R. Møller (1983) Responses of neurons in the inferior colliculus of the rat to AM and FM tones. *Hear. Res.* 10:301–330.

Ribaupierre, F. de, M. H. Goldstein, Jr., and G. Yeni-Komishian (1972) Cortical coding of repetitive acoustic pulses. *Brain Res.* 48:205–225.

Rose, G. J., and R. R. Capranica (1984) Processing amplitude-modulated sounds by the auditory midbrain of two species of toads: Matched temporal filters. *J. Comp. Physiol.* 154:211–219.

Rose, J. E., J. L. Brugge, D. J. Anderson, and J. E. Hind (1967) Phase-locked response to low-frequency tones in single auditory nerve fibers of the squirrel monkey. *J. Neurophysiol.* 30:769–793.

Sachs, M. B., and E. D. Young (1979) Encoding of steady-state vowels in the auditory nerve: Representation in terms of discharge rate. *J. Acoust. Soc. Am.* 66:470–479.

Schouten, J. F. (1970) The residue revisited. In *Frequency Analysis and Periodicity Detection in Hearing*, R. Plomp and G. F. Smoorenburg, eds., pp. 41–54, Sijthoff, Leiden.

Schreiner, C. E., and G. Langner (1984) Representation of periodicity information in the inferior colliculus of the cat. *Soc. Neurosci. Abstr.* 10:395.

Schreiner, C. E., and G. Langner (1988) Periodicity coding in the inferior colliculus of the cat. II. Topographic organization. *J. Neurophysiol.* (in press).

Schreiner, C. E., and J. V. Urbas (1984) Functional differentiation of cat auditory cortex areas demonstrated using amplitude and modulation. *Neurosci. Lett. (Suppl.)* 14:S334.

Schreiner, C. E., and J. V. Urbas (1986) Representation of amplitude modulation in the auditory cortex of the cat. I. Anterior auditory field. *Hear. Res.* 21:227–241.

Schreiner, C. E., and J. V. Urbas (1988) Representation of amplitude modulation in the auditory cortex of the cat. II. Comparison between cortical fields. *Hear. Res.* 32:49–64.

Schreiner, C. E., J. V. Urbas, and S. Mehrgardt (1983) Temporal resolution of amplitude modulation and complex signals in the auditory cortex of the cat. In *Hearing—Physiological Bases and Psychophysics*, R. Klinke and R. Hartman, eds., pp. 169–175, Springer-Verlag, Berlin.

Schroeder, M. R. (1981) Modulation transfer functions: Definition and measurement. *Acustica* 49:179–182.

Small, A. M., Jr. (1970) Periodicity pitch. In *Foundations of Modern Auditory Theory*, J. V. Tobias, ed., pp. 1–54, Academic, New York.

Smith, R., and M. Brachman (1980) Response modulation of auditory nerve fibres by AM stimuli: Effects of average intensity. *Hear. Res.* 2:123–133.

Suga, N. (1982) Functional organization of the auditory cortex: Representation beyond tonotopy in the bat. In *Cortical Sensory Organization*, Vol. 3; *Multiple Auditory Areas*, C. N. Woolsey, ed., pp. 157–218, Humana, Clifton, New Jersey.

Suga, N. (1984) The extent to which biosonar information is represented in the bat auditory cortex. In *Dynamic Aspects of Neocortical Function*, G. M. Edelman, W. E. Gall, and W. M. Cowan, eds., pp. 315–373, Wiley, New York.

Symmes, D. (1981) On the use of natural stimuli in neurophysiological studies of audition (review). *Hear. Res.* 4:203–214.

Vartanyan, I. A. (1969) Unit activity in inferior colliculus to amplitude-modulated stimuli. *Neurosci. Transl.* 10:17–26.

Viemeister, N. F. (1979) Temporal modulation transfer functions based upon modulation thresholds. *J. Acoust. Soc. Am.* 66:1364–1380.

Whitfield, I. C. (1971) Auditory cortex: Tonal, temporal, or topical? In *Physiology of the Auditory System*, M. B. Sachs, ed., pp. 289–298, National Education Consultants, Baltimore.

Whitfield, I. C., and E. F. Evans (1965) Responses of auditory cortical neurons to stimuli of changing frequency. *J. Neurophysiol.* 28:655–672.

Woolsey, C. G., and E. M. Walzl (1942) Topical projection of nerve fibers from local regions of the cochlea to the cerebral cortex of the cat. *Bull. Johns Hopkins Hosp.* 71:315–344.

Young, E. D., and M. B. Sachs (1979) Representation of steady-state vowels in the temporal aspects of the discharge patterns of populations of auditory nerve fibers. *J. Acoust. Soc. Am.* 66:1318–1403.

M.M.MERZENICH

Chapter 12

Observations and Hypotheses on Special Organizational Features of the Central Auditory Nervous System

MICHAEL M. MERZENICH
WILLIAM M. JENKINS
JOHN C. MIDDLEBROOKS

ABSTRACT

Recent studies in the somatosensory system of the monkey have revealed that cortical representations of the skin surface are dynamically maintained and are altered as a function of skin use in adults. In this chapter, we describe some of the unique features of the organization of the auditory nervous system and then interpret their significance with reference to somatosensory cortical map dynamics. Special auditory system organizational features include the following: (1) a re-representation of the sensory epithelium in an extra nuclear and extra cortical dimension; (2) nervous-system-derived representations of sound location and sound spectra, not present as a simple map of either domain at the first order; (3) additional levels of information processing, with the primary auditory cortex (AI) on the sixth order, as compared with visual (VI) or somatosensory (SI) cortical fields, which are on the fourth order; (4) a remarkable multinuclear convergence from 12 or more functionally distinctive brainstem sources into the main-line forebrain auditory nuclei and cortical fields; and (5) an extraordinary divergent–convergent organization of projections in the isofrequency dimensions of auditory nuclei and cortical fields.

Recent studies of the functional organization of the main-line auditory projection system have revealed that (1) the contralateral sound field is represented on one side, within the tonotopic (main-line) axis of the system, (2) frequency-specific deficits in sound localization result from lesions destroying the AI representations of those specific frequencies, (3) sound location representations must be alterable throughout life, (4) there is relatively little individual variability in the frequency-representational dimensions of auditory nuclei and cortical fields, and (5) there is, in contrast, substantial variability in their isofrequency dimensions. Differences in representational variability are hypothesized to reflect differences in the anatomical distributions of inputs across these different nuclear dimensions. That is, a relatively limited neuroanatomical overlap in the frequency-representational dimension can support little use-dependent alteration, and hence little individual variability is recorded, whereas alterations are supported by the nearly all-to-all projections in the isofrequency dimensions of nuclei and cortical fields, and hence wide individual variability is recorded across this representational dimension.

We conclude with the following hypotheses: (1) Sound location representations are created, maintained, and altered as required by experience, accommodating changes in physical cues throughout life; (2) the main-line tonotopic projection axis plays a fundamental role in sound location representation; (3) the relatively static frequency representation insures a complex and proportionally constant representation of the sound spectrum for binaural sound location representation; and (4) cortical

responses of neurons are not determined and invariant in this system, and features of the organization of this system are not consistent with an algorithmic machinelike model of higher brain function. To the contrary, the functional representations recorded at any time in the life of an adult must be consequences of an input selection process that creates one of a very great number of possible representations in this cortical zone—a representation that is, in detail, subject to alteration by accumulated experiences.

Recent studies on the dynamic aspects of the organization of the somatosensory nervous system in adult monkeys have important implications for the interpretation of neuroanatomical features and functionally defined maps in all sensory systems. There is a growing understanding of the structural and functional organization of the auditory nervous system, which has been demonstrated to have several very interesting and special organizational features. We shall propose below several hypotheses about the functional significance of some of the complex and unique features of the organization of this system, after considering it in the light of somatosensory studies revealing that details of cortical maps are dynamically maintained and modifiable as a function of use.

The argument will be initiated by a brief description of relevant studies of the dynamics of somatosensory cortical map structure. Then we shall review some of the unique neuroanatomical features of the central auditory nervous system. New functional evidence will be summarized indicating that (1) one half of the sound field is represented in each half of the auditory neuraxis, (2) the primary auditory cortex (AI) is requisite for normal binaural sound localization behavior, (3) mechanisms for binaural sound localization are necessarily present in the "main-line" tonotopic auditory projection system, and (4) sound location representations must be alterable throughout life. Recent neuroanatomical evidence for a highly restricted pattern of connection in the frequency-representational dimension and for a widely overlapping divergent–convergent projection in the isofrequency dimensions of auditory nuclei and cortical fields will be reviewed. Finally, we shall describe physiological results indicating that in one cortical dimension, a dynamic process of "selection" (Edelman and Mountcastle, 1978; Edelman, 1982; Merzenich et al., 1984a; Edelman and Finkel, this volume) must operate to account for the highly location-specific neuronal response characteristics arising from a highly overlapping (degenerate) neuroanatomical projection organization. As in the somatosensory system model, the details of representation within large sectors of AI, for example, must be determined in experience by correlative stimulation events, and the "maps" thereby created must be modifiable throughout life. In the orthogonal-representational (i.e., tonotopic) dimension, relatively little use-dependent alterability would appear to be possible.

We shall consider the overall significance of some intrinsic organizational features and dynamics of auditory cortical fields and relate them to the internal organizations and alterabilities of visual and somatosensory cortical fields in adult cats and primates. These comparisons indicate that in every instance (1) functional alterability is limited to the cortical dimensions of significant projection overlap of afferent inputs and (2) input overlapping is strictly limited, and therefore possible cortical map alteration is also limited in instances in which information handling would appear to require a limitation of territorial competition as a function of use.

SOMATOSENSORY CORTICAL MAPS ARE DYNAMICALLY MAINTAINED

Recent studies of the dynamic maintenance and use-dependent alteration of cortical maps of the hand in adult monkeys (Merzenich et al., 1983a,b; 1984b,c) have revealed the following:

1. *Functionally defined maps of the skin surface are highly variable in different individual adult owl and squirrel monkeys (Merzenich et al., 1984b).* For example, the magnifications of representation of different digits recorded in different individual adult monkeys vary by as much as sevenfold in area 1 and by severalfold in area 3b. Numerous and sometimes dramatic differences in the topographical order are seen among different adult owl and squirrel monkeys in both fields (Figure 1; Merzenich et al., 1984b). This striking variability must almost certainly reflect not only a genetic contribution to map structure, but also the individual animal's historical use of these skin surfaces.

2. *Many intrinsic map features are dynamically alterable in adult monkeys.* Marked alterations in map features have been observed as a consequence of nerve transection with and without subsequent nerve regeneration (Figure 2d,f; Merzenich et al., 1983a,b), of digit amputation (Figure 2e; Merzenich et al., 1984c), of restricted cortical lesions (Jenkins et al., 1982), and of behavioral training that demanded increased use of a portion of a hand (W. Jenkins, M. Merzenich, J. Zook, B. Fowler, and M. Stryker, unpublished observations). All of these experimental manipulations have resulted in changes in (a) cortical receptive field sizes and representational magnifications, (b) the skin surfaces represented at specific cortical loci or, conversely, the cortical site of representation of any given skin surface, and (c) the positions of lines of representational discontinuity in cortical maps. In other words, following a restricted peripheral or central loss of input or a modification of specific skin surface uses, functionally defined cortical maps expand or contract with roughly inverse changes in receptive field areas and with sometimes dramatic translocations of representational sites and discontinuities.

3. *There is a distance limit for movement of representational sites, probably dictated by limits of anatomical overlap.* In studies of cortical map reorganization following digit amputations, it was found that there was a distance limit to reorganization of about 600–700 μm (Merzenich et al., 1984c). That is, surrounding representations appeared to expand to occupy the cortical zone formerly representing the one or two amputated digits, but that reoccupation was limited to a zone about 600–700 μm across the original border of representation of the amputated digit. More distant unoccupied "silent" zones persisted, even after a relatively long (many months) postamputation survival time. Such studies indicate that the possible site for representation of any given skin surface in area 3b is an area about 1.2–1.4 mm in diameter. This limit is presumably dictated by the degree of the anatomical spread and the overlap of afferents in the somatosensory projection system (Merzenich et al., 1983b, 1984a; Edelman and Finkel, this volume). Estimations of the cortical distributions of ventrobasal neuron terminal arbors in areas 3b and 1 in cats and monkeys (and spreads of terminals at subcortical levels) are at least roughly consistent with this functionally defined distance

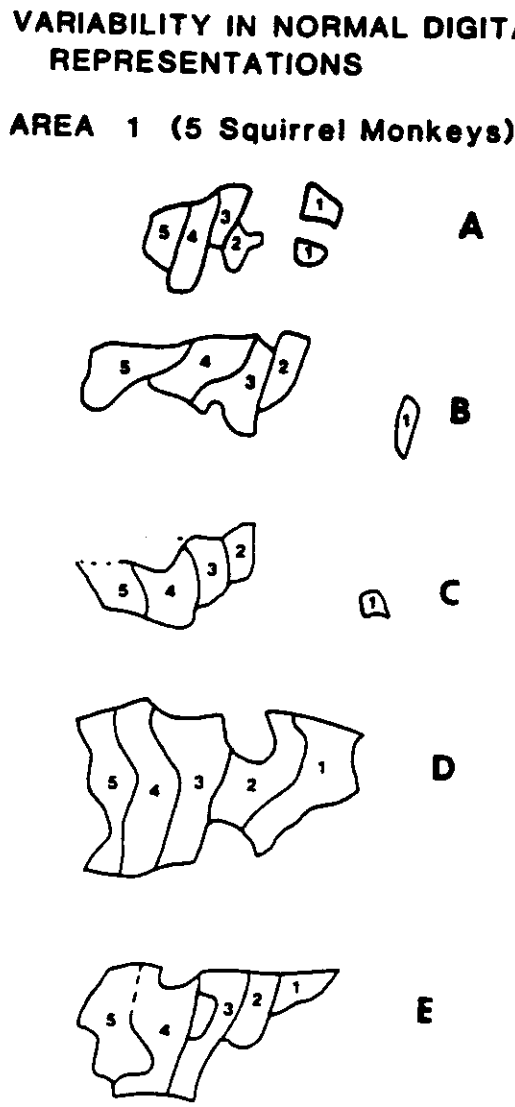

Figure 1. A–E: Representation of glabrous digital surfaces in cortical area 1 of five normal adult squirrel monkeys. The overall territory of the hand representation in area 1 was roughly the same in these five individuals; that is, the larger the digital representations in any monkey, the smaller the palmar representation. Note (1) the significant absolute and proportional differences in areas of glabrous surface representation of the different digits (and of the other hand surfaces) and (2) the significant differences in the topographic relationships of the digits (e.g., the relationships of the representations of digits 1 and 2) in different monkeys. These striking idiosyncratic differences are believed principally to reflect differences in hand use among these individuals.

limit for reorganization (Landry and Deschênes, 1981; Pons et al., 1981; Merzenich et al., 1984a).

Thus, somatosensory cortical maps are dynamically alterable in adult monkeys. The details of their representations are normally modified by experience; that is, there are myriad possible functional cortical maps, and the actual evident

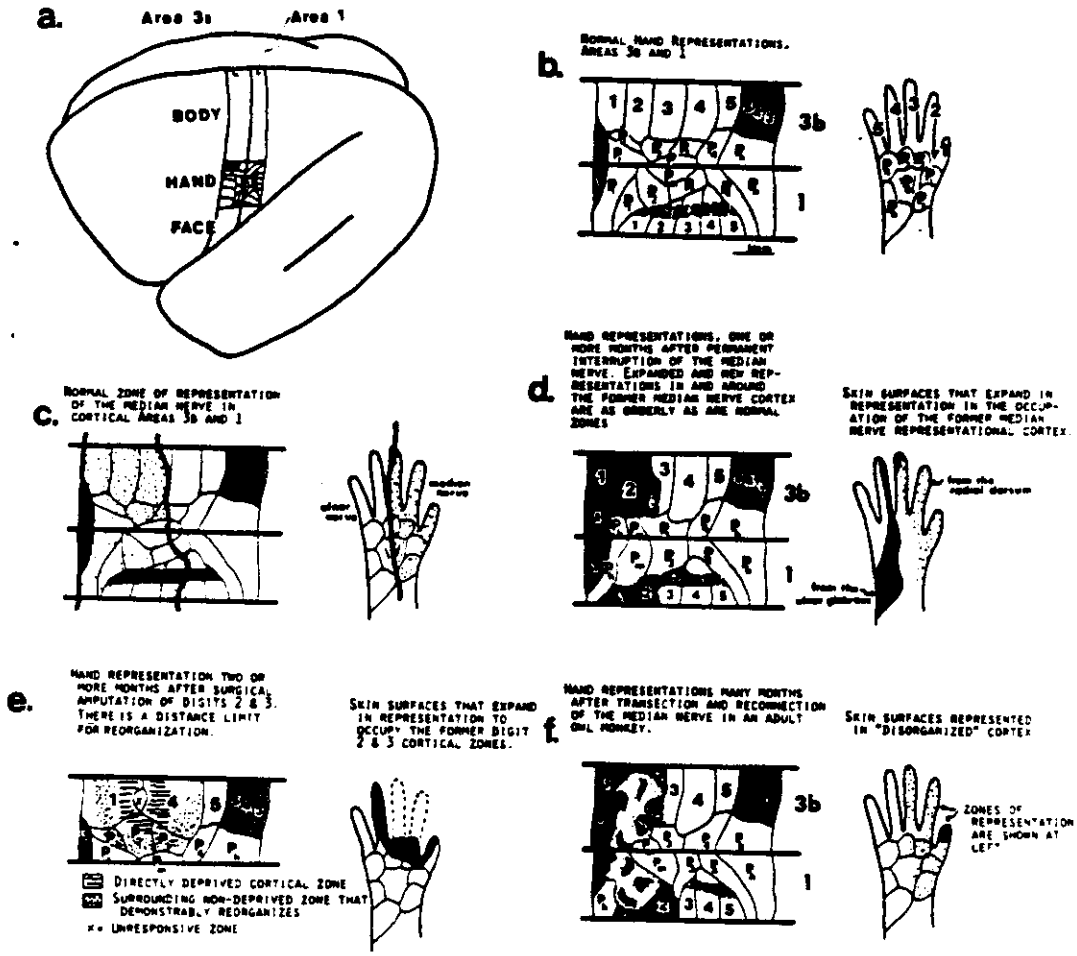

Figure 2. Some features of reorganization of hand representation in cortical areas 3b and 1 (a–c) following median nerve transection (d), amputation of digits 2 and 3 (e), and median nerve transection and regeneration (f). All drawings are schematic and represent common features of reorganization following these peripheral lesions. a: Locations of hand surface representations in cortical fields 3b and 1 in the adult owl monkey, as seen in a lateral view of the cortex. b: Topography of normal hand surface representations in these two cortical fields. Outlined labeled zones are cortical areas in which all cutaneous receptive fields for recorded neurons were centered on the corresponding areas of skin surface indicated in the hand drawing at right. Territories of dorsal hand surface representation are shaded. Note the double and roughly mirror-image representation of the hand surface in cortical areas 3b and 1 (Merzenich et al., 1978; 1981). These maps were derived from determination of receptive fields in 200–500 parallel penetrations across this cortical zone. c: Normal cortical territory of median nerve representation (*dotted*). The skin on the hand surface innervated by the median nerve is shown in the drawing at the right. d: Representative map derived one or more months after the median nerve was cut and tied to prevent regeneration. The former median nerve representational zone (shown in c) is occupied by new and expanded representations of surrounding skin surfaces innervated by the medial and ulnar nerves (see drawing of hand at right) (Merzenich et al., 1983a,b). Again, dorsal hand representational zones are shaded. e: Hand representation map in area 3b two or more months after amputation of digits 2 and 3. As in all other lesions, changes are seen in surrounding nondeprived (*dotted*) as well as in directly deprived (*wavy lines*) representational zones. The representations of significant hand surface areas (shown at the right) are translocated into the cortical sectors of represention of the amputated digits and come to be represented solely within that cortical zone. f: Hand surface representation in area 3b many months after transection and reconnection of the median nerve. In time, there is limited functional resorting of the hand representation, with any given skin surface (e.g., that shown in black at the right) represented over restricted, significant-sized patches in these fields. (Adapted from Merzenich et al., 1984a.)

maps reflect the history of a monkey's tactile experiences up to the time at which the maps are studied. Any specific new differential skin-surface use will lead to map alterations, with significant changes effected over a period of days or weeks. Those changes, we hypothesize, underlie and account for the acquisition of tactile skill.

In considering the mechanisms likely to underlie these functional dynamics (see Merzenich et al., 1983b, 1984a; Edelman and Finkel, this volume), the following principles appear to hold: (1) Map alterability is due to changes in synaptic effectiveness, but not to changes in the distributions of terminal arbors or of dendrites, that is, changes occur as a result of a dynamic process operating within a basically hard-wired projection system; (2) temporal correlation and neural activity levels must control the maintenance of local map structure; (3) an "overlap rule" is at least roughly enforced throughout reorganization, with the result that, from a relatively crude and highly overlapping anatomical mapping of the skin surface, highly detailed and functionally tailored maps of the skin surface are created.

These dynamic principles of organization must apply generally. As we have argued (Merzenich et al., 1984a), if identification of tactile images (recognition) and localization can arise from a somatosensory projection system with dynamically alterable maps, such alteration is almost certainly everywhere the case.

How might it apply to auditory or visual projection systems? Is there any reason to believe that they are not organized in a similar way? It has been argued that the locations of ocular dominance columns are established in early life and are thereafter not alterable by drastic changes in visual experience, for example, by monocular lid suture (see Hubel and Wiesel, 1977; LeVay et al., 1980; Movshon and Van Sluyters, 1981; Sherman and Spear, 1982). How is this observation consistent with the observed functional self-organizing properties of the adult somatosensory system? Is the auditory projection system more like the visual or the somatosensory projection systems in these respects? This final question constitutes the central question addressed in what follows.

SPECIAL FEATURES OF THE ORGANIZATION OF THE CENTRAL AUDITORY NERVOUS SYSTEM

Before discussing how the evident dynamics of functional somatosensory maps and the static neuroanatomical structure of visual maps might or might not apply to the auditory nervous system, it is important to understand the nature of a number of its unique organizational features (Merzenich et al., 1977, 1979, 1982; Merzenich and Kaas, 1980). An understanding of their significance is obviously central to any interpretation of the functional organization of the auditory system.

1. *There are "extra" levels of projection in the central auditory nervous system.* The primary auditory cortex is on the sixth order of the main-line auditory projection system (which consists of the spiral ganglion, ventral cochlear nucleus, superior olivary complex, central nucleus of the inferior colliculus, ventral division of the medial geniculate body, and AI). By contrast, primary visual and somatosensory cortical fields are on the fourth order of their respective systems (Figure 3B).

SOME UNIQUE ORGANIZATIONAL FEATURES OF THE CENTRAL AUDITORY SYSTEM

A. ADDITIONAL ISOREPRESENTATIONAL DIMENSION

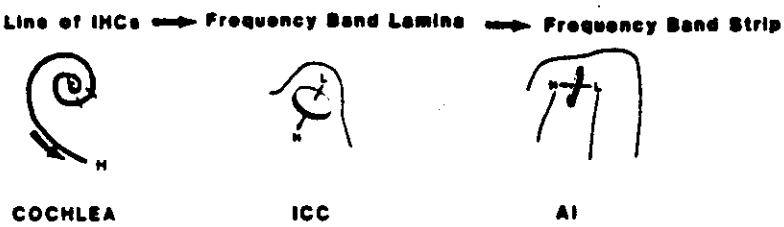

B. ADDITIONAL LEVELS OF PROCESSING IN THE MAINLINE CENTRAL AUDITORY SYSTEM

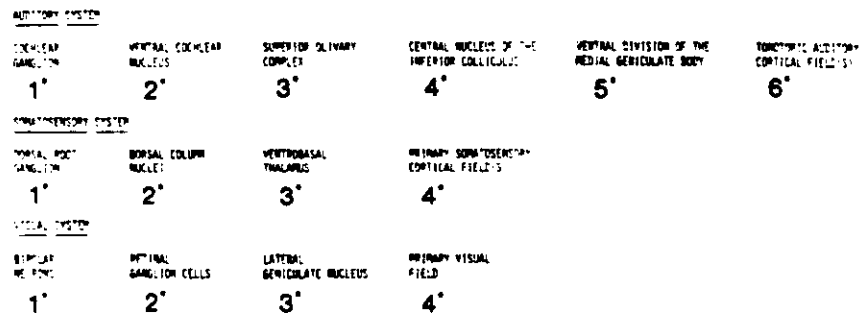

C. MORE COMPLEX CONVERGENCE OF INFORMATION FROM DIFFERENT SOURCES

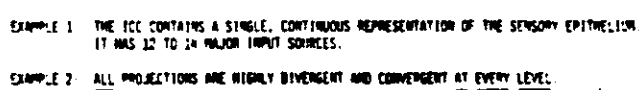

Figure 3. A–C: Summary of three unique organizational features of the central auditory nervous system. ICC, central nucleus of the inferior colliculus.

2. *There is a requisite extraction of information for creation of both sound location and spectral pattern representations in the central auditory nervous system.* The representation of the location of brief sounds in space is a result of comparisons of the intensities and times of arrival of the sounds at the two ears in central binaural nuclei. The principal binaural-comparing nuclei are the third-order medial and lateral superior olivary nuclei in the pons. Similarly, recent studies of the distributed auditory nerve array representations of the spectral components of complex sounds reveal that spectral component extraction must be the first step in the representation of such complexes (Young and Sachs, 1979; Sachs et al., 1983). The medial superior olive has been strongly implicated as the decoding site of complex sound components (e.g., speech elements), but the exact nature of this neural process is still unknown (see Loeb et al., 1983). Thus, in both the domain of sound pitch and that of sound location, psychological continua apparently originate directly in information-extracting machinery *on the third order.*

3. *There is an extra dimension of isorepresentation of the sensory epithelium (organ of Corti) within auditory nuclei and cortical fields.* Whereas somatosensory, visual, olfactory, and taste sensory epithelia are distributed over surfaces, the effective cochlear sensory epithelium is a single line of inner hair cells several thousand hair cells long. With a point-to-point representation anatomically similar to the representation of visual or somatic sensory epithelia, it could be represented by a narrow strip of cortex of insignificant width. Of course, auditory cortical fields and nuclei have another dimension, and the auditory sensory epithelium is re-represented across that dimension; that is, in auditory nuclei and cortical fields there is an additional isorepresentational dimension. Thus, any given small distance along the organ of Corti is represented within a slab of neurons of nearly constant thickness, extending across auditory nuclei from edge to edge (Merzenich and Reid, 1974; Merzenich et al., 1977, 1982; Figure 3A). By contrast, in visual or somatosensory nuclei, restricted loci are represented in columns of neurons (i.e., there is a single isorepresentational dimension). In AI or other "tonotopic" auditory cortical fields, any given short distance along the organ of Corti is represented within a strip of cortex (an "isofrequency strip"; see Merzenich et al., 1975) of approximately constant thickness that extends across the width of these fields from edge to edge. In visual and somatosensory cortical fields, by contrast, there is a point-to-point representational organization.

4. *There is a complex multinuclear convergence to the main-line midbrain auditory nucleus, the central nucleus of the inferior colliculus.* Information from the cochlea is distributed to a number of morphologically and functionally distinct regions of the ventral cochlear nucleus and to the distinctive cell laminae of the dorsal cochlear nucleus. From these nuclei it is distributed to the medial and lateral superior olives, the periolivary nuclei, and the ventral, intermediate, and dorsal nuclei of the lateral lemniscus. *All* of these nuclei (including all divisions of the ventral cochlear nucleus, several layers of the dorsal cochlear nucleus, and bilateral inputs from several other nuclear sources) project into the main-line midbrain auditory nucleus, the central nucleus of the inferior colliculus (Roth et al., 1978; Adams, 1979; Brunso-Bechtold et al., 1981; Figure 3C). Thus, the central nucleus of the cat, for example, has 12 or more functionally distinct sources of input. Although there is growing evidence for some regional segregation of inputs within this nucleus (Morest, 1964; Roth et al., 1978; Semple and Aitkin, 1979;

Brunso-Bechtold et al., 1981), nonetheless (1) several or many inputs are apparently convergent to any one region and (2) all inputs are apparently appropriately aligned in a single, large, continuous tonotopic representation (Merzenich and Reid, 1974).

5. *There is an extensive divergent–convergent level-to-level projection in the isorepresentation dimensions of auditory nuclei and cortical fields.* In many published studies of the interlevel connections of auditory nuclei and cortical fields, evidence for

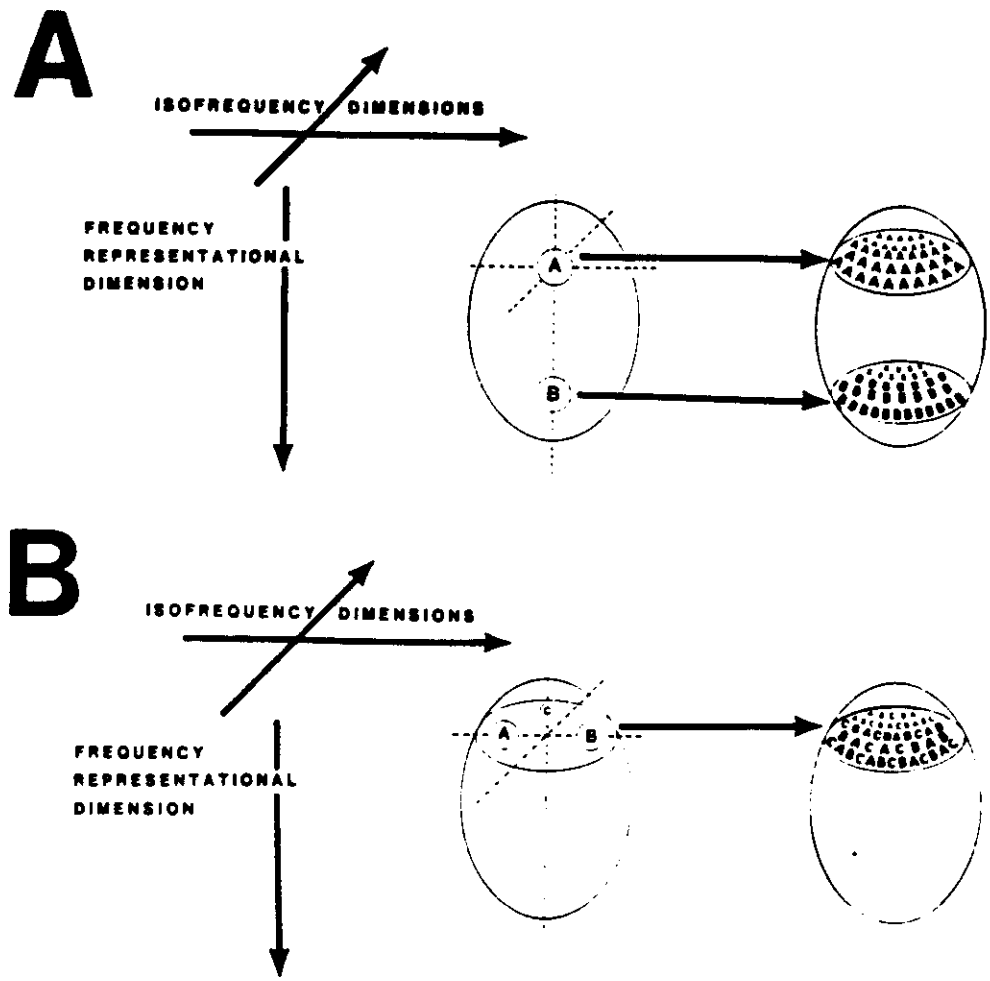

Figure 4. Diagrammatic illustration of the basic organization of the highly divergent and convergent level-to-level projections in the central auditory nervous system. Projecting arrays spread from restricted loci at one level (e.g., sites *A* or *B* or C in **B**) in nearly all-to-all projections across the isofrequency dimensions at the next higher level. Projections from different isofrequency laminae (e.g., sites *A* and *B* in **A**) are strictly segregated in the frequency-representational dimension of the target nucleus. This basic projection organization is seen at all six system levels in the main-line projection system, from the cochlear nucleus through the tonotopically organized auditory cortical fields. (See the text for specific details.)

an extraordinary divergent–convergent pattern of interconnection has been recorded in the isofrequency dimension (Figures 3C, 4; Sando, 1965; Osen, 1970, 1972; Colwell, 1977; Winer et al., 1977; Adams, 1979; Andersen et al., 1980a,b; Brunso-Bechtold et al., 1981; Merzenich et al., 1982; Zook and Casseday, 1982; Middlebrooks and Zook, 1983). Thus, for example, restricted injections of a retrograde tracer at any level lead to labeling of columns (in the two-dimensional sheetlike dorsal cochlear nucleus, lateral and medial superior olives, and auditory cortical fields) or sheets (in three-dimensional nuclei like the anteroventral cochlear nucleus, posteroventral cochlear nucleus, central nucleus of the inferior colliculus, etc.) of neurons in the source nuclei. Correspondingly, restricted injections into nuclei commonly lead to anterograde labeling across columns or sheets of neurons at higher levels. Thus, for example, neurons at any restricted locus in the medial superior olive receive inputs from neurons all across the isofrequency planes of the anteroventral cochlear nucleus (R. B. Masterton and K. Glendenning, personal communication). Neurons from all along the isofrequency dimension of the medial superior olive diverge in their projections to locations all across the corresponding isofrequency laminae of the medial-superior-olive-receiving sector of the central nucleus of the inferior colliculus. Conversely, an injection of a retrograde tracer into this sector of the central nucleus of the inferior colliculus leads to very equal labeling of neurons in a narrow column several cells across, all along the isofrequency dimension of the medial superior olive (Roth et al., 1978). Neurons in any restricted sector of the medial-superior-olive-recipient zone of the central nucleus of the inferior colliculus project forward to a sheet of neurons 1–4 mm^2 in area in the ventral division of the medial geniculate body (Andersen et al., 1980b). Similarly, neurons in restricted sectors of AI receive inputs from a corresponding thalamic neuronal sheet (Colwell, 1977; Andersen et al., 1980a; Merzenich et al., 1982). Thus, at every level, interlevel projections are highly divergent and convergent. Information is repeatedly combined and then widely redistributed in a complex, ascending, interlevel cascade.

Before discussing the possible functional significance of these special organizational features, it is important to consider some hitherto largely unappreciated functional features of the organization of the auditory forebrain.

FEATURES AND REQUIREMENTS OF A SOUND LOCATION REPRESENTATIONAL SYSTEM

The Contralateral Sound Field Is Represented on One Side of the Auditory Nervous System. The earliest ablation–behavioral studies in primates and carnivores indicated that a hemifield sound localization deficit results from unilateral lesions of the auditory cortex (Ferrier, 1876; Luciani, 1884). Similarly, several studies indicated that a hemifield localization deficit results from unilateral temporal lobe damage in humans (Wortis and Pfeffer, 1948; Sanchez-Longo and Forster, 1958; Klingon and Bontecou, 1966). However, in later animal and human studies employing different testing procedures and stimuli, no permanent sound localization deficits were recorded (Walsh, 1957; Neff, 1968; Strominger, 1969; Neff et al., 1975).

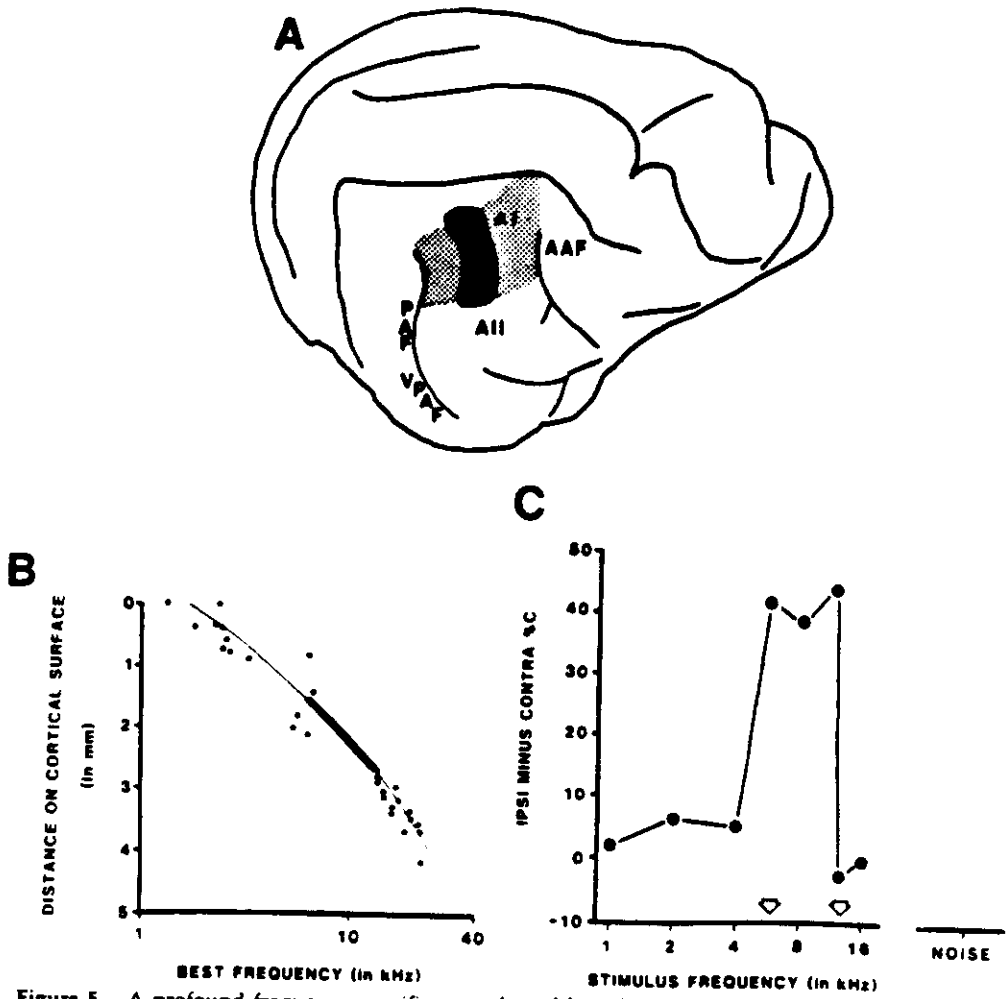

Figure 5. A profound frequency-specific contralateral hemifield sound localization deficit results from a restricted AI lesion. In this representative case, the lesion was induced by electrocoagulation of cortical surface vessels after mapping AI using sterile recording procedures. A: Location of a striplike lesion (*black*) with reference to the physiologically defined borders of AI (*shaded*) in an adult cat. B: Best frequency of neurons in penetrations into AI as a function of distance across the cortical surface in the frequency-representational dimension, defined 16 months after the induction of the lesion shown in A. Frequencies at which a profound sound localization deficit was observed are indicated by the heavy line segment of the curve fitting these data. In the zone of the lesion in this mapping experiment, the cortex was silent, and in histologically examined cases it has been found to be acellular. C: Ipsilateral minus contralateral sound localization performance for several frequencies in a seven-speaker test in this cat (180 trials per point), illustrating a profound deficit for localization of 40-msec tones at frequencies whose representation was destroyed by the lesion. Sound localization performance was normal with stimulation at higher or lower frequencies and with 40-msec noise bursts. Arrows along the abscissa mark the frequency range judged to be totally destroyed across AI in a detailed prelesion and immediately postlesion physiological map of the field in this cat. These deficits were permanent, and performance was surprisingly little affected by changes in stimulus intensity. (Adapted from Jenkins and Merzenich, 1984.)

Recent studies by Jenkins and his colleagues (Jenkins and Merzenich, 1981, 1983; Jenkins and Masterton, 1982) have explained at least some of the reasons for this contradictory evidence. Specifically, they have shown that a permanent, total hemifield localization deficit for brief sounds results from even a highly restricted lesion in AI. For example, an animal with a restricted lesion destroying the AI representation of an octave is unable to localize sound in the contralateral sound field at frequencies approximately corresponding to the range formerly represented in the lesioned sector (Figure 5). The frequency-specific deficit appears to be permanent, as judged in animals studied intensively for more than a year after the induction of such a lesion (Figure 5).

These results indicate that AI integrity is requisite for normal, binaural sound localization behavior. Why did earlier investigators come to a different conclusion? The sources of confusion have been reviewed elsewhere (Jenkins and Masterton, 1982; Jenkins and Merzenich, 1984). Suffice it to say here that (1) an animal can perform a two-speaker *lateralization* task accurately, even after a very large cortical ablation, but not a multispeaker *localization* task (Figure 6A), and (2) a profound deficit is recorded with brief stimuli, but no deficit is recorded when stimuli are of longer duration (sufficient for head turning) or are repeated (again with head turning) (Figure 6B). Thus, a substrate for true binaural localization but not lateralization or scanning abilities is present at higher levels in the main-line auditory projection system. (Studies by Neff and his colleagues have long demonstrated that there is a permanent deficit in scanning behavior consequent from a bilateral, but not from a unilateral, cortical lesion.)

Physiological studies have also indicated that half of the sound field is probably represented on one side of the projection system. Thus, for example, the contralateral ear is excitatory for intensity-difference-sensitive neurons in the main-line midbrain, thalamic, and cortical auditory areas. This is the case despite the fact that the intensity-difference-encoding lateral superior olives project bilaterally to each midbrain central nucleus; that is, intensity-difference-sensitive neurons respond as if only contralateral inputs drive higher-level neurons (Roth et al., 1978).

Additionally, interaural-time-difference-sensitive neurons almost invariably respond most strongly to interaural time differences that correspond to sounds located in the contralateral hemifield (Figure 7; Stillman, 1971; Roth et al., 1978;

Figure 6. Two sources of historical confusion about the behavioral consequences of unilateral lesions on sound localization in the cat. A: Behavioral performance of cats on two different tests after unilateral auditory lesions illustrates that a nearly profound deficit in the localization of clicks is observed in the contralateral hemifield following large unilateral lesions in the main-line auditory projection system. At the same time, no deficit in a two-speaker left–right (lateralization) task was seen in any lesioned animal. Each data point represents the mean of all data derived from an individual adult cat with large unilateral lesions at the following designated sites: L, lateral lemniscus; G, medial geniculate latency body; B, brachium of the inferior colliculus; I, inferior colliculus; C, auditory cortex. Seven-speaker test: 180 trials per point; two-speaker test: 60 trials per point. (Data from Jenkins and Masterton, 1982.) B: Sound localization performance in a seven-speaker apparatus in response to brief tones at a frequency falling within that of a striplike AI lesion as a function of stimulus duration. Improvements in localization ability as a function of stimulus duration are apparently dependent on orienting movements (scanning), which have a latency of about 40 msec (Thompson and Masterton, 1978). (Adapted from Jenkins and Merzenich, 1984.)

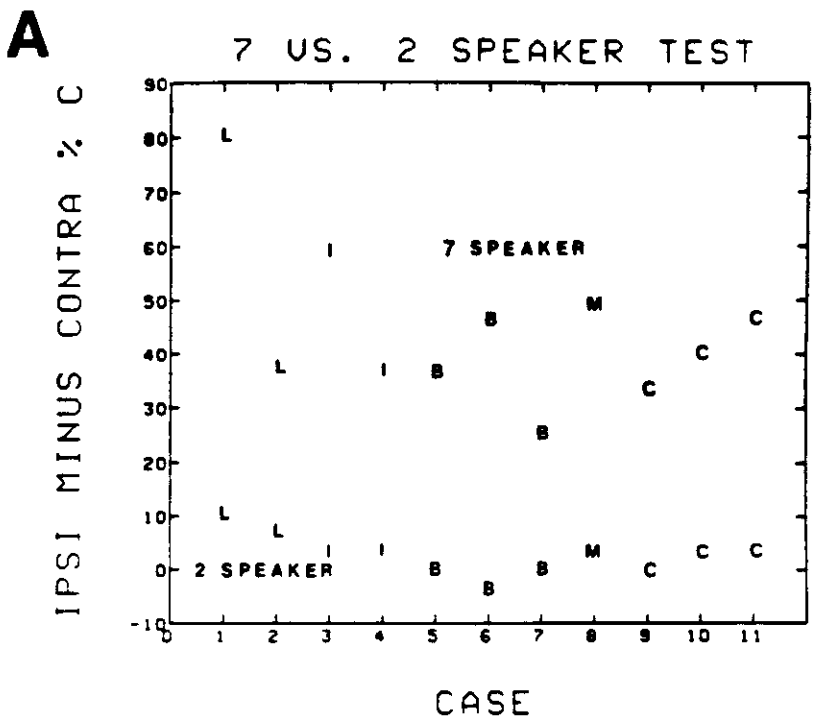
A
7 VS. 2 SPEAKER TEST
IPSI MINUS CONTRA % C
7 SPEAKER
2 SPEAKER
CASE

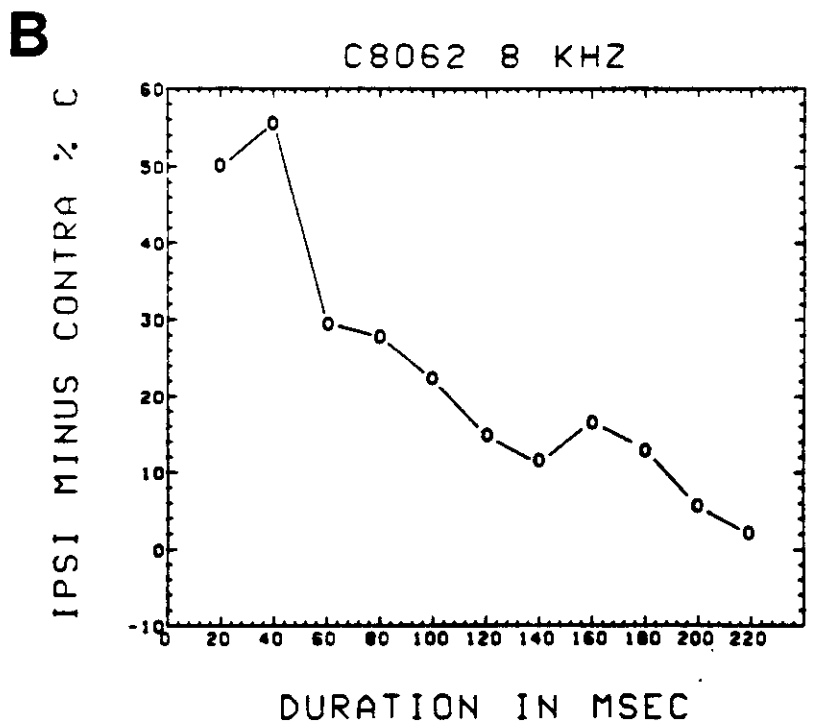
B
C8062 8 KHZ
IPSI MINUS CONTRA % C
DURATION IN MSEC

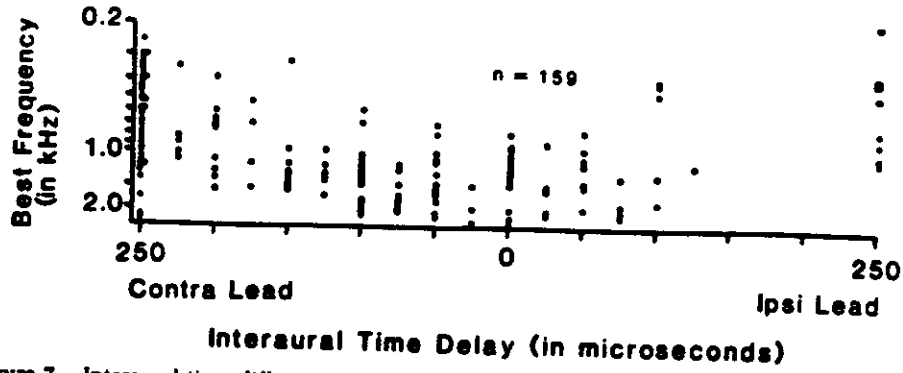

Figure 7. Interaural time differences at which 159 delay-sensitive neurons in the central nucleus of the inferior colliculus were most strongly driven. The physiological range of delays actually encompasses interaural time differences as great as 450–500 μsec in the adult cat (Roth et al., 1980). Note that few neurons were maximally responsive to delays in the ipsilateral hemifield greater than about 100 μsec. This corresponds to a free-sound-field location about 10–20° across the midline. This is one of a number of lines of circumstantial evidence indicating that the contralateral hemifield is represented on one side of the mainline auditory projection system. See the text for other examples. (Adapted from Roth, 1977.)

Semple and Aitkin, 1979; Chan and Yin, 1982; Yin and Kuwada, 1982). Relatively few neurons are optimally driven by stimuli corresponding to locations more than about 15–25° into the ipsilateral hemifield. This overlap zone, extending a few degrees into the ipsilateral field, is also manifested in cortical ablation–behavioral studies (W. Jenkins, unpublished observations).

Finally, the sensitivity of some neurons to location in the free sound field has been tested in the main-line nuclei of mammals. Of the neurons that are selective for sound locations, the great majority respond only to free-sound-field stimuli located contralaterally (Leiman and Hafter, 1972; Eisenman, 1974; Souvijari and Hyvärinen, 1974; Middlebrooks and Pettigrew, 1981).

The Form of a Sound Location Map in the Main-Line Projection System Is Unknown. A cortical map of sound source location has not yet been identified in any mammal except highly specialized echolocating bats. This failure may arise in part because the appropriate form of such maps has not been recognized. No highly directional space-selective neurons have been recorded in AI in the cat (see Middlebrooks and Pettigrew, 1981). At lower levels of the main-line (tonotopic) projection axis, no clear sound location maps or appropriately strict spatial distributions of interaural-time- or interaural-intensity-sensitive neurons have been recorded, although a weak time-difference topography has been noted in the central nucleus of the inferior colliculus and in AI (Brugge and Merzenich, 1973; Roth, 1977; Roth et al., 1978; Chan and Yin, 1982; Yin and Kuwada, 1982). Maps of sound locations have been found in the barn owl (Knudsen and Konishi, 1978; Knudsen, this volume), but not in structures homologous to the nuclei and cortical fields on the main-line auditory projection axis in mammals. As noted below, the forms of the maps described in owls are not appropriate for all aspects of binaural sound location behavior in mammals.

Binaural Localization of a Complex Sound Requires the Convergence of Interaural Time and Intensity Information across the Audible Spectrum. The interaural temporal, intensive, and spectral disparities between the two ears for any given sound source are highly nonlinear functions of both stimulus location and sound frequency (Wiener et al., 1966; Kuhn, 1977; Moore and Irvine, 1979; Roth et al., 1980; Middlebrooks and Pettigrew, 1981; Hafter, this volume). Moreover, interaural disparities undergo significant changes throughout the life of an animal as a consequence of the growth of the external ear, head, and body (see Hafter, this volume). Indeed, cues can change significantly with the donning of clothes or the growth of a winter pelt. Furthermore, mislocation errors and sound image changes resulting from ear canal blockage are compensated for almost completely over a period of several weeks in humans; when the blockage is removed, there is a mirror-image mislocation error, and a subsequent quicker return to normal, corrected performance (F. B. Simmons, unpublished observations). It should be emphasized that all of these factors (i.e., ear canal blockage; growth of head, ears, and body; etc.) have different effects for different small segments of the sound spectrum. In addition, the central auditory system must cope with common changes in the condition of the cochlea, for example, frequency-specific hearing losses consequent to aging. An animal's experience clearly must contribute to necessary lifelong adjustments and active maintenance (and almost certainly to the original development) of its central representations of sound space.

Sound Localization Is Frequency Specific and Requires Representation within a Projection System Resolving Spectral Components of Complex Stimuli. Thus, for example: (1) The locations of separately heard complex sounds (for example, different voices) are independently and simultaneously represented. Sound source locations are identified with the unique spectral features of these complex sound sources. (2) When sounds in different locations in space fall within a critical band, the sound location is the resultant of the combination of cues from the different sources (Scharf et al., 1976; see Hafter, this volume). However, with wider frequency separations, sounds of different frequencies sort into separate, independent locations. (3) Again, frequency-specific lesions in AI produce profound frequency-specific sound localization deficits (Jenkins and Merzenich, 1981). Moreover, the frequency ranges of these deficits are affected remarkably little by large changes in stimulus intensity (W. Jenkins, unpublished observations).

All of these data support the conclusion that sound localization in mammals is processed in a projection system that simultaneously resolves the spectral components of complex sounds. It is important to note that maps of sound localization like those described in the midbrain of the owl probably cannot account for human or other mammalian performance in this respect, because those maps are frequency nonspecific (see Knudsen, this volume).

Summary

1. Sound location must be represented in a tonotopically organized (spectral-component-resolving) part of the auditory nervous system.
2. Ablation–behavioral studies directly reveal this to be the case, with permanent frequency-specific deficits resulting from restricted lesions in a small part of the "tonotopic" main-line system.

3. Considered analytically, an extraordinarily complex and multidimensional feature extraction is required to derive sound location.
4. An extra dimension of isofrequency representation (representational degeneracy) is required to represent sound locations within a projection system map that also strictly resolves sound frequencies.
5. Given the complex, multidimensional and binaural origins of sound source identification, there must be a series of appropriate parallel feature-extractors; neuroanatomical studies indicate that there is a convergence of this information across the isofrequency dimensions of the tonotopically organized auditory thalamic nuclei and cortical fields.
6. Sound location maps must be alterable thoughout life.

ORGANIZATION OF ANATOMICAL PROJECTIONS: WHAT FUNCTIONAL FEATURES ARE DIRECTLY DETERMINED BY ANATOMICAL BOUNDARIES? WHAT FUNCTIONAL FEATURES ARE DYNAMIC?

Given these general conclusions, how is the auditory projection system, especially the auditory forebrain, organized (1) to accomplish the spectral processing required for sound location representation, and (2) to account for the apparent requirement for dynamic alterability of sound location maps? Before addressing this joint issue, it is necessary to review briefly several pertinent features of the anatomical organization of this projection system.

Variability in Internal Organization of the Auditory Nuclei and Cortical Fields

There are only very limited data on the functional variability of the organization of auditory structures. They indicate that the "best frequency" or tonotopic organization of nuclei and cortical fields is relatively constant and probably anatomically determined, whereas variability in the isofrequency dimension, by contrast, is substantial. In an earlier study of the best-frequency representation in the central nucleus of the inferior colliculus, we noted a remarkably constant and invariably complete representation of the cochlear sensory epithelium (Merzenich and Reid, 1974). When best frequency versus intranuclear position data from a series of experiments were combined, they fell onto the same basic function and varied little among individual cats (Figure 8A). When best-frequency

Figure 8. Graphs illustrating the relative constancy of frequency representation in the main-line auditory projection system. A: Best frequency for neurons at 976 sites along 49 penetrations across the central nucleus of the inferior colliculus, plotted as a function of penetration depth. Data were obtained from experiments conducted in seven adult cats. All penetrations were in the sagittal plane, directed caudally at angles ranging from about 20° to 35° out of the frontal stereotaxic plane. (Adapted from Merzenich and Reid, 1974.) B: Best frequency for neurons recorded in vertical penetrations in cortical field AI as a function of distance along the frequency-representational dimension of the field. Each symbol represents data from a different cat; data for each cat are artificially shifted along the ordinate so that they can be readily compared. (Adapted from Merzenich et al., 1976.)

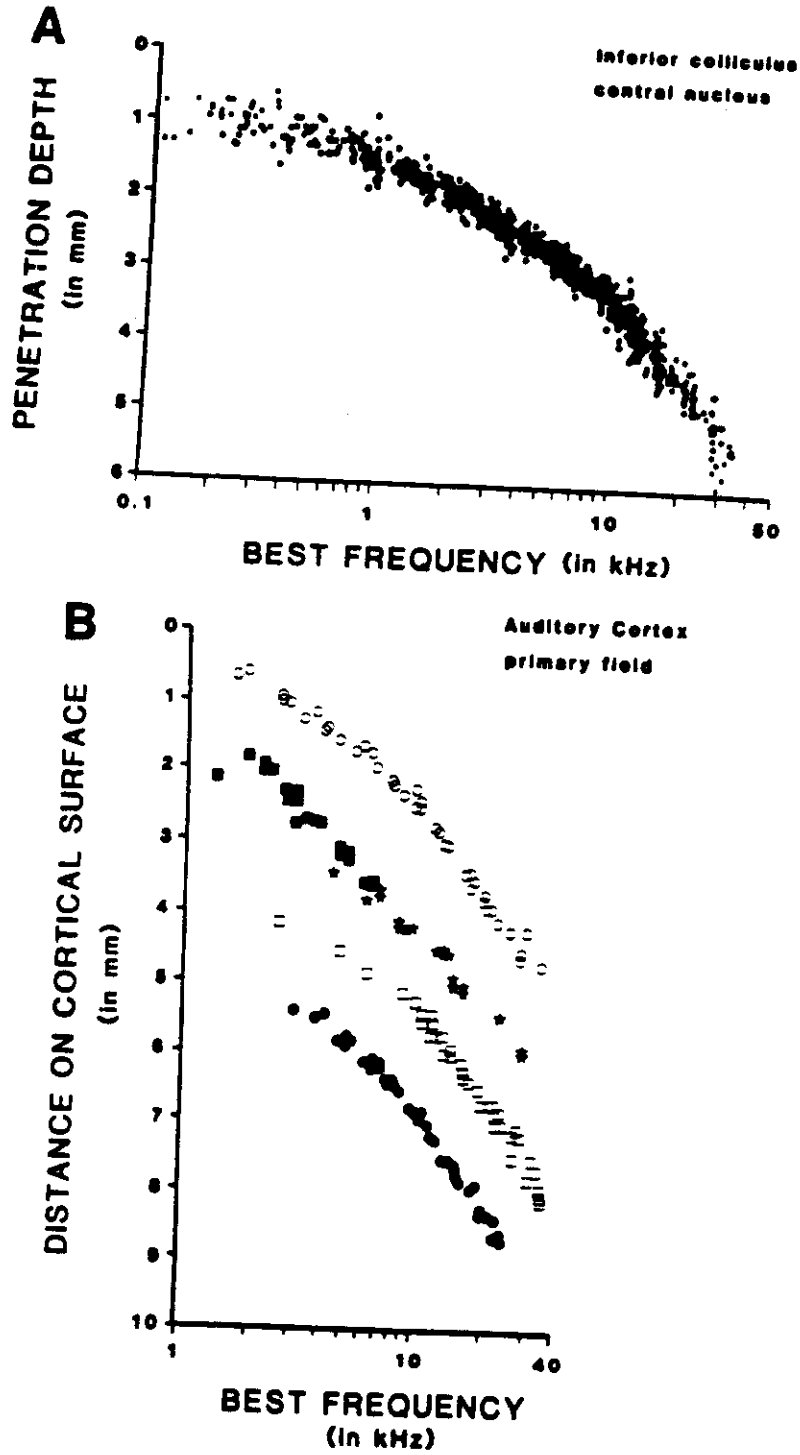
A
PENETRATION DEPTH
(in mm)
0
1
2
3
4
5
6
0.1
1
10
50
BEST FREQUENCY (in kHz)
Inferior colliculus
central nucleus
B
DISTANCE ON CORTICAL SURFACE
(in mm)
0
1
2
3
4
5
6
7
8
9
10
1
10
40
BEST FREQUENCY
(in kHz)
Auditory Cortex
primary field

data from cortical maps were considered, a similar analysis also revealed no special regional distortions in the proportional areas of representations, and frequency representations were complete (Figure 8B).

Several other lines of evidence indicate that the frequency organization of these main-line nuclei and cortical fields is established almost entirely by the projection system's anatomy. (1) There is a stepwise representation of frequency in auditory nuclei at all levels. When examined in very fine grain, the best frequencies for neurons recorded on any axis across the frequency-representational dimension change in steps encompassing a significant part of an octave (Merzenich et al., 1982). In terms of functional map detail, this feature is probably akin to the boundaries of ocular dominance columns in the sense that these are probably anatomically created functional discontinuities. They appear to contrast with the always-overlapping maps of somatosensory cortical fields. (2) The auditory cortex does not reorganize significantly to represent sound frequencies whose cortical representations are destroyed by a striplike cortical lesion (W. Jenkins and M. Merzenich, unpublished observations). Again, this is in apparent contrast to the somatosensory case. (3) Although there is a remarkable, nearly all-to-all projectional organization in the isofrequency dimension of auditory nuclei and cortical fields (as described above), projection arrays are relatively strictly delimited in the orthogonal, frequency-representational axis (see Sando, 1965; Colwell, 1977; Adams, 1979; Andersen et al., 1980a; Merzenich et al., 1982; Middlebrooks and Zook, 1983). (4) Reconstruction of afferent arbors in the main-line midbrain and thalamic auditory nuclei reveal that although neuronal terminations are widely distributed in the isofrequency axis, they remain restricted within the cellular laminae of these nuclei (Morest, 1964, 1965). (5) Frequency versus position functions are surprisingly similar in several different examined species of mammals (macaques, cats, and squirrels) (Merzenich et al., 1976).

Map Variability in the Isofrequency Dimensions of Nuclei and Cortical Fields

Although the frequency organization of nuclei and cortical fields is surprisingly constant, the isofrequency axis organization is (1) highly predictable with regard to its anatomically widespread convergence and divergence and (2) surprisingly variable in its evident functional organization. This latter point is illustrated by a series of maps of the binaural organization of AI and AII in the region of their common borders, from a study by Schreiner and Cynader (1984; Figure 9). In Figure 9, open regions represent intensively mapped sectors in which neurons were excitatory–excitatory (EE) in response character: The response of neurons to stimulation of both ears in this region was greater than the response to stimulation of either ear alone. In the dotted sectors, neurons were excitatory–inhibitory (EI): They were excited by stimulation of the contralateral ear and inhibited by stimulation of the ipsilateral ear. Note the remarkable variability in the spatial distributions of binaural-responsive neurons of these response classes in both fields. Indeed, since the discovery of "binaural bands" in AI (Imig and Adrian, 1977; Brugge and Imig, 1978; Imig and Brugge, 1978; Middlebrooks et al., 1980) we have mapped AI in many individual cats and have recorded an almost idiosyncratic subdivision of this field into its binaural bands. Moreover, response properties often vary markedly within these binaural bands, and the

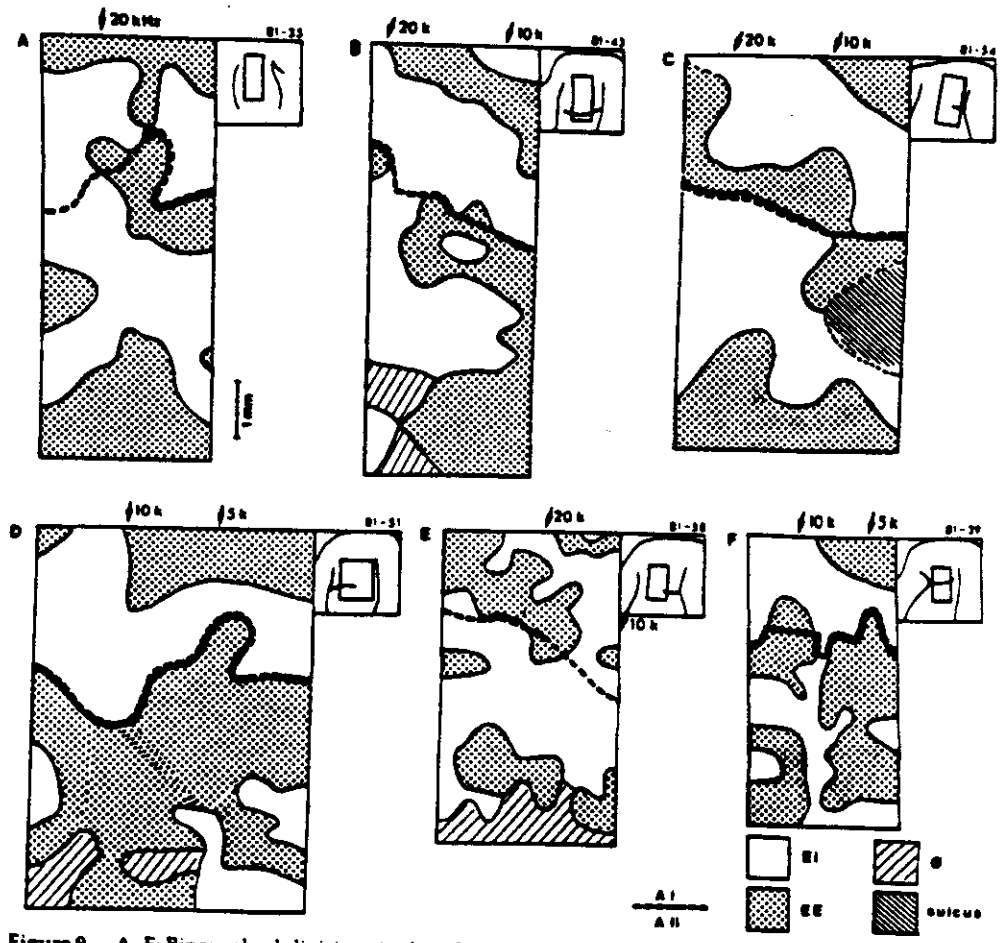

Figure 9. A–F: Binaural subdivisions in the AI–AII border region in six normal adult cats. Excitatory–inhibitory zones are dotted. Excitatory–excitatory zones are open. The dashed lines mark the approximate locations of the AI–AII border as defined by physiological criteria. Positions and orientations of some isofrequency axes in AI are shown at the top of each drawing. The approximate location of the mapped zone in relation to cortical surface features is shown at the upper right of each drawing. Note the remarkable individual differences in the functional binaural subdivision of both fields. Φ, contralateral-only zones. (From Schreiner and Cynader, 1984.)

same basic organization is not seen for the corresponding bands in different animals (or often even at different frequencies in the same animal). Thus, although across the isofrequency dimension of AI the functional response properties of neurons are highly site specific (see Abeles and Goldstein, 1971; Brugge and Merzenich, 1973; Merzenich et al., 1977; Kitzes et al., 1980), the binaural "maps" in this dimension exhibit very substantial intraband and interband variation among individuals.

The Nearly All-to-All Projection Organization in the Isofrequency Dimension in the Auditory Forebrain

Recent studies on the projection organization of the main-line auditory thalamic nucleus (the ventral division of the medial geniculate body) to AI indicate, again,

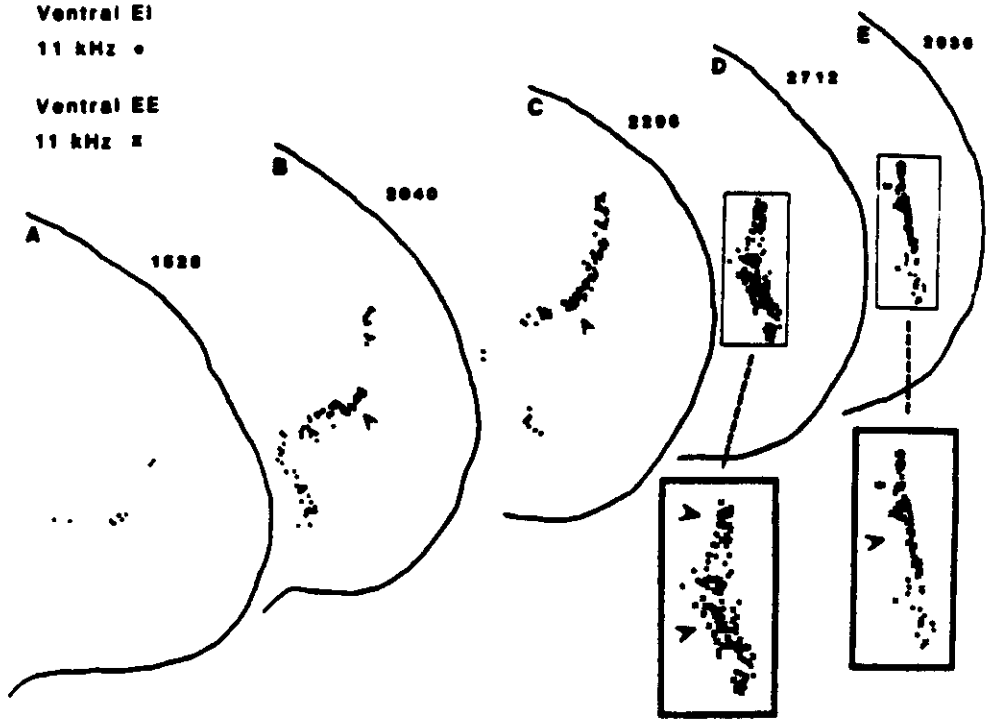

Figure 10. Neurons labeled by injection of nuclear yellow (*dots*) and propidium iodide (*X-marks*, pinpointed by *arrowheads* in each drawing) into the center of the adjacent excitatory–inhibitory (*EI*) and excitatory–excitatory (*EE*) bands in the higher-frequency sector of AI. Note that (1) injection anywhere along the isofrequency axis of either subdivision (or anywhere in any other subdivision of the same class) produces very similar labeled cell arrays; (2) the great convergence from these broken sheets of thalamic neurons into restricted (not more than 200 μm in diameter) loci in AI; and (3) the relatively sharp borders of the projecting neuronal array in the frequency-representational axis (left to right in the drawings). (From Middlebrooks and Zook, 1983.)

a remarkable convergent–divergent organization. When a highly restricted injection is introduced into AI, retrogradely labeled neurons projecting to that locus occupy a sheet roughly 1–4 mm^2 in area, which includes a very large proportion of all possible projecting neurons in the isofrequency dimension and extends across the thalamic nucleus from edge to edge (see Figures 10, 11). If the injection is at a low-frequency (below 4–5 kHz) representational site in AI, the sheet of projecting neurons is continuous. If it is at a higher-frequency representational site, the sheet of projecting neurons is usually discontinuous (Andersen et al., 1980a; Merzenich et al., 1982; Middlebrooks and Zook, 1983). This reflects the fact, recently discovered by Middlebrooks and Zook (1983), that in the higher-frequency part of the ventral medial geniculate body the sources of input destined for EE and EI AI sectors are segregated into separate laminae (Figures 10, 11).

Again, perhaps the most remarkable aspect of this organization is the extent of convergence from this complex structure into very restricted (100–200 μm wide) AI loci. In the higher-frequency, banded region of AI, a small injection results in the labeling of neurons distributed among all of the discrete EI layers of the thalamic source nucleus. A virtually identical pattern of projecting neurons

is labeled regardless of the location of injection within a given band and regardless of which EI band is labeled (Merzenich et al., 1982; Middlebrooks and Zook, 1983). In the projection to EE cortical zones, there is a more significant regional segregation of sources of input, but overlaps of projection are still enormous, with at least 50–60% of EE-projecting neurons across the isofrequency axis of the ventral division of the medial geniculate body projecting to any restricted EE locus in AI.

Thus, while the projection anatomy in the frequency-representational dimension preserves a relatively strict and rigidly defined functional tonotopic organization, in the isofrequency dimension there is a nearly all-to-all projection organization for neurons of each binaural (EE or EI) class. Nonetheless, detailed response properties of isofrequency neurons are highly site specific, and cortical "maps" across the isofrequency dimension are internally highly variable.

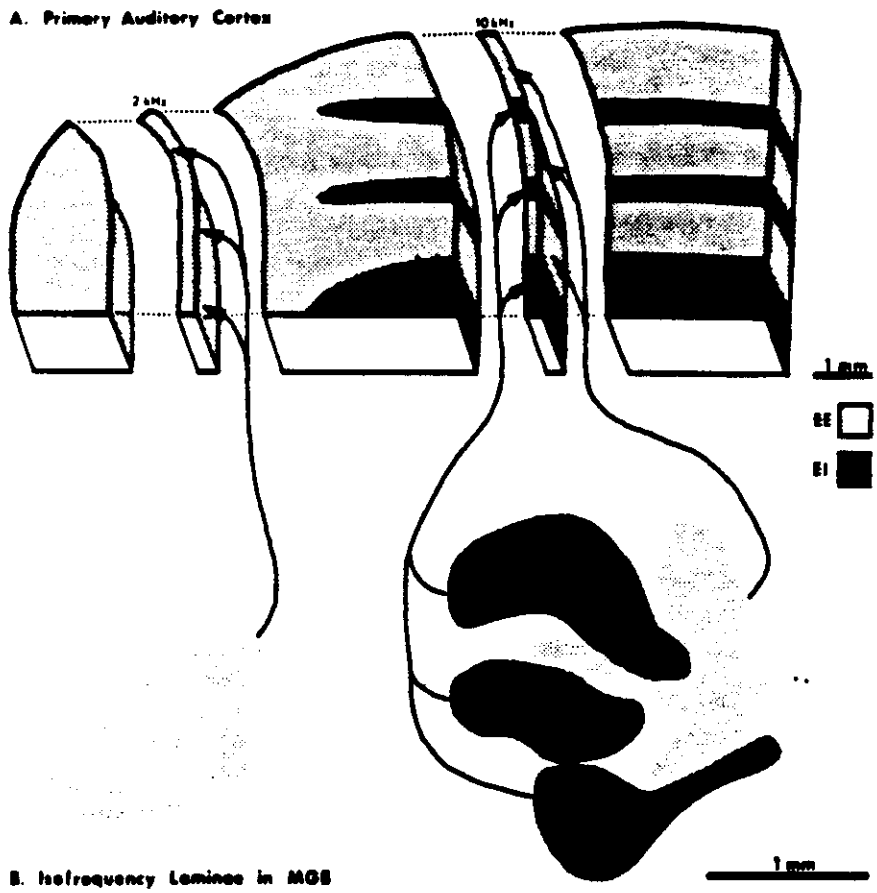

Figure 11. Topography of projection from the ventral division of the medial geniculate body to the primary auditory cortex (AI). A: Idealized binaural map of AI in the right hemisphere. The isofrequency contours representing 2 and 10 kHz are shown separately. B: Isofrequency laminae in the ventral division representing 2 and 10 kHz. The laminae, which normally are highly folded, are flattened on the plane of the page. Dark shading indicates excitatory–inhibitory (*EI*) bands in AI and their sources of input from the ventral division. Light shading indicates excitatory–excitatory (*EE*) bands and sources.

CONCLUSIONS AND HYPOTHESES

Given these observations on somatosensory representational map dynamics and auditory system organization, we would like to present a series of conclusions and hypotheses that together constitute an interpretation (at the first level) of the functional significance of special features of auditory system organization.

When Auditory Neuroscientists Have Been Faced with Understanding the Central Neural Basis of Sound Localization, They Have Promoted Several General Ideas That Are Now Subject to Serious Challenge. First, from the inception of the Jeffress (1948) model of sound localization representation, physiologists and anatomists have sought a brain stem map of sound location. Jeffress (1948) originally proposed that the geometries of projections onto the interaural-time-comparing nucleus, the medial superior olive, might provide for the genesis of a point-by-point map of interaural time differences. However, recent studies described above have revealed a highly divergent and convergent projection from the medial superior olive (MSO) to the central nucleus of the inferior colliculus (ICC), from the MSO-recipient part of the ICC to the main-line thalamic nucleus, and from that nucleus to AI. Thus, by the anatomical patterns of ascending connections alone, any map created at any of these levels is not projected forward in a point-to-point representational array (as in the representation of location in visual or somatosensory projection systems). This is another way of saying that if a map of sound location is recorded at any given level on this projection axis, it must be generated by a functional process of input selection at that level.

Second, auditory neuroscientists, like visual neuroscientists, have favored a computerlike algorithmic information-extraction model of sound location and spectral pattern representation. The projection system has been imagined as having a series of "sound analyzers" and comparators that process information about various aspects of sound stimuli in parallel—with the identification of sound location a compound product of this series of parallel representational systems ("feature extractors"). However, recent evidence indicates that a large number of functionally distinctive brain stem source nuclei (12 or more) converge in their projections to higher system levels. In this massive convergence, information is sorted out at main-line forebrain levels into two (from 12 or more) parallel systems in the higher-frequency sectors of these representations; in lower-frequency sectors, there is an anatomical convergence of *all* of these input sources. Thus, the complex pieces of information fed from numerous functionally distinctive brain stem sources to the main-line midbrain nucleus are not treated separately but, to the contrary, are anatomically superimposed at higher system levels.

Inherent in computerlike algorithmic models of information extraction is the requirement that connections in a machinelike, problem-solving, feature-extracting subsystem be hard-wired, with specific neurons having preassigned, functionally static roles. However, the site-specific nature of the responses of thalamic or cortical neurons in the face of a highly convergent anatomy, coupled with a requirement for functional dynamism, suggests that (as in the somatosensory system) there is no such functional rigidity in the higher levels of this system.

Third, sound location representations have not been clearly identified in the tonotopic projection axis. Indeed, in the elegant studies of Knudsen and Konishi (1978) cited earlier, a sound location representation has been recorded in the barn owl in nontonotopic fields. However, the recent studies of Jenkins and colleagues appear to associate unequivocally true binaural localization of brief sounds with the tonotopic projection axis. Moreover, there are strong psychophysical reasons to believe that binaural sound location is represented in a system also resolving sound frequency. The studies of Jenkins and Masterton (1982) also clearly demonstrate, once and for all, that a permanent, true, binaural contralateral hemifield localization deficit is incurred after unilateral lesions on this projection axis.

How Is the Main-Line Auditory Projection System Like the Visual System and How Is It Like the Somatosensory System in Its Capacity for Dynamic Self-Organization? Across one nuclear or cortical dimension, the representation of sound frequency is relatively constant when considered in the grain of the usual recorded maps. When examined in finer detail, there are small representational discontinuities in this dimension all across these maps. Furthermore, projecting arrays of neurons feeding any small cortical or nuclear locus are strictly delimited into a corresponding narrow band in the source nucleus, across the corresponding frequency-representational dimension. Thus we conclude that in this frequency-representational dimension, a relatively strict neuroanatomical projection organization insures a complete and proportionally constant frequency representation. Across this nuclear or cortical field dimension there is a relatively limited spread of thalamic projections accommodating little alterability. Again, for maps derived with this degree of resolution, this relatively strict neuroanatomical projection accounts for the limited individual variability in frequency representations.

In the other auditory map dimension(s), terminal spread is enormous, and the site-specific response properties of neurons at the forebrain level must be accounted for by dynamic selection of a few of many possible inputs (Edelman, 1982; Merzenich et al., 1984a; Edelman and Finkel, this volume). Because of the magnitude of the spread of inputs, individual variability in this dimension is great, because in this dimension (we hypothesize) the anatomical substrate supports substantial alterability as a function of use. We have argued that in the somatosensory system the dynamic generation and maintenance of detailed functional map structures involves selection of specific inputs from many possible ones, and that this selection must be determined and controlled by temporal correlations and input activity levels (Merzenich et al., 1983b, 1984a; see Edelman and Finkel, this volume). Moreover, internal map order is maintained because of the dynamic maintenance of a shifted overlap of selected responses. In the auditory case, information converges from various functionally distinctive sources. If input selection is based on the same principles in the auditory cortex, then cortical selection would be expected to be controlled by psychophysical continua, for example, by all neurally represented aspects of sounds across the free sound field. If the overlap rule is enforced, then adjacent cortical sites should be driven by stimuli in adjacent locations in the free sound field.

In all sensory systems, the capacity for self-organization resulting from experience is necessarily constrained by the organization of the anatomical projections. Within somatosensory areas 3b and 1, projection arbors from different skin surfaces overlap widely, supporting the movement of effective receptive field locations many hundreds of neurons in any direction. In area 17, lack of overlap of terminals along the borders of ocular dominance bands establishes barriers across which significant territorial competition is apparently not possible. However, functional processes of input selection are almost certainly in play within given ocular dominance columns (see Merzenich et al., 1984a). In the auditory cortical field AI, relatively limited overlap strictly limits territorial competition in the frequency-representation dimension, and segregation of projections to binaural bands of different classes in the high-frequency sector (representing 3–5 kHz and above) of the ventral division of the medial geniculate body and AI indicates that competition is limited to territories within these subdivisions. However, there are no such barriers to territorial competition in the lower-frequency sectors of these representations. Finally, nearly all-to-all projections within these binaural class subdivisions and all across lower-frequency subdivisions provide a greater substrate for use-dependent competition for territory than any recorded in the somatosensory projection system.

One implication of these results is that the constancy of the frequency representation may not of itself implicate the main-line projection system in pitch representation and recognition, per se. Indeed, its very limited modifiability in this dimension on the one hand insures a complete and nondistorted representation of the sound spectrum for sound location representation, and on the other possibly limits its potential significance in use-dependent acquisition of skills involving the recognition of complex sounds.

In this respect, we previously may have been considering this system in reverse. That is, seeing order in its spectral representations, it has been assumed that the tonotopic projection axis plays a primary role in frequency processing and spectral representation. However, given the somatosensory example, in which specific uses of restricted surfaces lead to dramatic changes in cortical representation with the consequent production of significant map variability, it is across this degenerately connected dimension that the projection system is most likely to be principally operating. The main-line auditory projection system appears to represent, in some as yet undefined way, binaural sound localization across this axis.

To summarize, we would like to propose a series of simple hypotheses about the functional significance of the special features of auditory system organization:

1. The auditory system creates sound location maps by experience.
2. The system retains this ability to some extent into adulthood and provides a substrate for the accommodation of changes in complex cues for localization resulting from aging, ear canal blockage, hearing loss with aging, and so forth.
3. Map detail is controlled by psychophysically coincident or closely sequenced inputs, that is, by simple real-world psychophysical continua.
4. Specific binaural response properties for neurons at any location at any moment are selected by experience, as governed by the enforced "rules" of dynamic organization (Merzenich et al., 1984a), from many alternatives.

5. Partial damage to this system should lead to map readjustments, with at least partial recovery of the damaged sector of the sound localization representation.
6. Although the auditory system has extra levels of processing, nonetheless cortical representations are still three levels above the level at which the information required for the creation of binaural sound location representations is generated—as are primary cortical representations in other systems.
7. Convergence of information from many brainstem sources into the mainline projection axis effects the convergence of the manifold spectral and binaural comparison cues required for sound location representation.
8. An extra dimension of isofrequency representation is requisite for representation of sound location on a projection axis also devolving sound frequencies, that is, for the observed frequency-specific treatment of sound location representation.
9. Finally, highly convergent and divergent projections provide appropriately degenerate connections (see Edelman, 1982; Merzenich et al., 1984a; Edelman and Finkel, this volume) necessary for use-dependent functional alteration of the representation throughout life.

Most of these hypotheses can be evaluated experimentally and should provide a focus for future studies of the higher levels of this highly specialized sensory system.

ACKNOWLEDGMENTS

The authors would like to thank their many collaborators in the studies described here. This manuscript was written in part while Dr. Merzenich was a Fellow of The Neurosciences Institute of the Neurosciences Research Program, 1230 York Avenue, New York, New York 10021. The authors gratefully acknowledge the assistance of Joseph Molinari in the preparation of this chapter. This research was supported by NIH grant NS-10414, the Coleman Fund, and Hearing Research, Inc.

REFERENCES

Abeles, M., and M. H. Goldstein, Jr. (1971) Functional architecture in cat primary auditory cortex: columnar organization according to depth. *J. Neurophysiol.* 36:172–187.

Adams, J. C. (1979) Ascending projections to the inferior colliculus. *J. Comp. Neurol.* 183:519–538.

Andersen, R. A., R. L. Snyder, and M. M. Merzenich (1980a) Thalamocortical and corticothalamic connections of AI, AII and AAF in the cat: evidence for two largely segregated systems of connections. *J. Comp. Neurol.* 194:663–701.

Andersen, R. A., G. L. Roth, L. M. Aitkin, and M. M. Merzenich (1980b) The efferent projections of the central nucleus and the pericentral nucleus of the inferior colliculus in the cat. *J. Comp. Neurol.* 194:649–662.

Brugge, J. F., and T. J. Imig (1978) Some relationships of binaural response patterns of single neurons of cortical columns and interhemispheric connections of auditory area AI of cat cerebral cortex.

In *Evoked Electrical Activity in the Auditory Nervous System*, R. G. Naunton and C. Fernandez, eds., pp. 487–503, Academic Press, New York.

Brugge, J. F., and M. M. Merzenich (1973) Responses of neurons in auditory cortex of the macaque monkey to monaural and binaural stimuli. *J. Neurophysiol.* 36:1138–1158.

Brunso-Bechtold, J. K., G. C. Thompson, and R. B. Masterton (1981) HRP study of the organization of auditory afferents ascending to central nucleus of inferior colliculus in cat. *J. Comp. Neurol.* 197:705–722.

Chan, J. C., and T. C. T. Yin (1982) Topographical relationships along the isofrequency laminae of the cat inferior colliculus: correlation with the anatomical lamination and representation of binaural response properties. *Soc. Neurosci. Abstr.* 8:348.

Colwell, S. A. (1977) *Reciprocal Structure in the Medial Geniculate.* Unpublished doctoral dissertation, University of California, San Francisco.

Edelman, G. M. (1982) Group selection as a basis for higher brain function. In *The Organization of the Cerebral Cortex*, F. O. Schmitt, F. G. Worden, G. Adelman, and S. G. Dennis, eds., pp. 535–563, MIT Press, Cambridge, Massachusetts.

Edelman, G. M., and V. B. Mountcastle (1978) *The Mindful Brain*, MIT Press, Cambridge, Massachusetts.

Eisenman, J. M. (1974) Neural encoding of sound location: an electrophysiological study in auditory cortex (AI) of the cat using free field stimuli. *Brain Res.* 75:203–214.

Ferrier, D. (1876) *The Functions of the Brain*, Smith, Elder, and Co., London.

Hubel, D. H., and T. N. Wiesel (1977) Functional architecture of macaque visual cortex. *Proc. R. Soc. Lond. (Biol.)* 198:1–59.

Imig, T. J., and H. O. Adrian (1977) Binaural columns in the primary field (AI) of cat auditory cortex. *Brain Res.* 138:241–257.

Imig, T. J., and J. F. Brugge (1978) Sources and terminations of callosal axons related to binaural and frequency maps in primary auditory cortex of the cat. *J. Comp. Neurol.* 182:637–660.

Jeffress, L. A. (1948) A place theory of sound localization. *J. Comp. Physiol. Psychol.* 41:35–39.

Jenkins, W. M., and R. B. Masterton (1982) Sound localization: effects of unilateral lesions in central auditory system. *J. Neurophysiol.* 47:987–1016.

Jenkins, W. M., and M. M. Merzenich (1981) Lesions of restricted frequency representational sectors within primary auditory cortex produce frequency dependent sound location deficits. *Soc. Neurosci. Abstr.* 7:392.

Jenkins, W. M., and M. M. Merzenich (1984) Role of cat primary auditory cortex for sound localization behavior. *J. Neurophysiol.* (in press).

Jenkins, W. M., M. M. Merzenich, J. M. Zook, B. C. Fowler, and M. P. Stryker (1982) The area 3b representation of the hand in owl monkeys reorganizes after induction of restricted cortical lesions. *Soc. Neurosci. Abstr.* 8:141.

Kitzes, L. M., K. S. Wrege, and J. M. Casseday (1980) Patterns of responses of cortical cells to binaural stimulation. *J. Comp. Neurol.* 192:455–472.

Klingon, G. H., and D. C. Bontecou (1966) Localization in auditory space. *Neurology (NY)* 16:879–886.

Knudsen, E. I., and M. Konishi (1978) Space and frequency are represented separately in auditory midbrain of the owl. *J. Neurophysiol.* 41:870–884.

Kuhn, G. F. (1977) Model for the interaural time differences in the azimuthal plane. *J. Acoust. Soc. Am.* 62:157–167.

Landry, P., and M. Deschenes (1981) Intracortical arborizations and receptive fields of identified ventrobasal thalamocortical afferents to the primary somatic sensory cortex in the cat. *J. Comp. Neurol.* 199:345–371.

Leiman, A. L., and E. R. Hafter (1972) Responses of inferior colliculus neurons to free field auditory stimuli. *Exp. Neurol.* 35:431–449.

LeVay, S., T. Wiesel, and D. H. Hubel (1980) The development of ocular dominance columns in normal and visually deprived monkeys. *J. Comp. Neurol.* 191:1–51.

Loeb, G. E., M. W. White, and M. M. Merzenich (1983) Spatial cross-correlation. A proposed mechanism for acoustic pitch perception. *Biol. Cybern.* 47:149–163.

Luciani, L. (1884) On the sensorial localizations in the cortex cerebri. *Brain* 7:145–160.

Merzenich, M. M., and J. H. Kaas (1980) Principles of organization of sensory-perceptual systems in mammals. *Prog. Psychobiol. Physiol.* 9:1–42.

Merzenich, M. M., and M. D. Reid (1974) Representation of the cochlea within the inferior colliculus of the cat. *Brain Res.* 77:397–415.

Merzenich, M. M., P. L. Knight, and G. L. Roth (1975) Representation of cochlea within primary auditory cortex in the cat. *J. Neurophysiol.* 38:231–249.

Merzenich, M. M., J. H. Kaas, and G. L. Roth (1976) Auditory cortex in the grey squirrel: tonotopic organization and architectonic fields. *J. Comp. Neurol.* 166:387–401.

Merzenich, M. M., G. L. Roth, R. A. Andersen, P. L. Knight, and S. A. Colwell (1977) Some basic features of organization of the central auditory system. In *Psychophysics and Physiology of Hearing*, E. F. Evans and J. P. Wilson, eds., pp. 485–495, Academic Press, New York.

Merzenich, M. M., J. H. Kaas, M. Sur, and C.-S. Lin (1978) Double representation of the body surface within cytoarchitectonic areas 3b and 1 in "SI" in the owl monkey (*Aotus trivirgatus*). *J. Comp. Neurol.* 181:41–74.

Merzenich, M. M., R. A. Andersen, and J. C. Middlebrooks (1979) Functional and topographic organization of the auditory cortex. *Exp. Brain Res. [Suppl.]* 2:61–75.

Merzenich, M. M., M. Sur, R. J. Nelson, and J. H. Kaas (1981) Organization of the SI cortex: multiple cutaneous representations in Areas 3b and 1 of the owl monkey. In *Cortical Sensory Organization. Vol. 1: Multiple Somatic Areas*, C. N. Woolsey, ed., pp. 47–66, Humana Press, Clifton, New Jersey.

Merzenich, M. M., S. A. Colwell, and R. A. Andersen (1982) Thalamocortical and corticothalamic connections in the auditory system of cat. In *Cortical Sensory Organization. Vol. 3: Multiple Auditory Areas*, C. N. Woolsey, ed., pp. 43–57, Humana Press, Clifton, New Jersey.

Merzenich, M. M., J. H. Kaas, J. T. Wall, R. J. Nelson, M. Sur, and D. J. Felleman (1983a) Topographic reorganization of somatosensory cortical areas 3b and 1 in adult monkeys following restricted deafferentation. *Neuroscience* 8:33–55.

Merzenich, M. M., J. H. Kaas, J. T. Wall, M. Sur, R. J. Nelson, and D. J. Felleman (1983b) Progression of change following median nerve section in the cortical representation of the hand in areas 3b and 1 in adult owl and squirrel monkeys. *Neuroscience* 10:639–665.

Merzenich, M. M., R. J. Nelson, J. H. Kaas, J. T. Wall, M. P. Stryker, M. Sur, J. M. Zook, M. S. Cynader, D. J. Felleman, and A. Schoppman (1984b) Variability in hand surface representations in areas 3b and 1 in adult owl and squirrel monkeys. *J. Comp. Neurol.* 224 (in press).

Merzenich, M. M., R. J. Nelson, M. P. Stryker, M. S. Cynader, A. Schoppman, and J. M. Zook (1984c) Somatosensory cortical map changes following digit amputation in adult monkeys. *J. Comp. Neurol.* 224:591–605.

Middlebrooks, J. C., and J. D. Pettigrew (1981) Functional classes of neurons in primary auditory cortex of the cat distinguished by sensitivity to sound location. *J. Neurosci.* 1:107–120.

Middlebrooks, J. C., and J. M. Zook (1983) Intrinsic organization of the cat's medial geniculate body identified by projections to binaural response-specific bands in the primary auditory cortex. *J. Neurosci.* 3:203–224.

Middlebrooks, J. C., R. W. Dykes, and M. M. Merzenich (1980) Binaural response-specific bands in primary auditory cortex (AI) of the cat: topographical organization orthogonal to isofrequency contours. *Brain Res.* 181:31–48.

Moore, D. R., and D. R. F. Irvine (1979) A developmental study of the sound pressure transformation by the head of the cat. *Acta Otolaryngol. (Stockh.)* 87:434–440.

Morest, D. K. (1964) The laminar structure of the inferior colliculus of the cat. *Anat. Rec.* 148:314.

Morest, D. K. (1965) The laminar structure of the medial geniculate body of the cat. *J. Anat.* 99:143–160.

Movshon, J. A., and R. C. Van Sluyters (1981) Visual neural development. *Annu. Rev. Psychol.* 32:477–522.

Neff, W. D. (1968) Localization and lateralization of sound in space. In *Hearing Mechanisms in Vertebrates*, A. V. S. de Reuck and J. Knight, eds., pp. 207–231, Little, Brown, Boston.

Neff, W. D., I. T. Diamond, and J. H. Casseday (1975) Behavioral studies of auditory discrimination: central nervous system. In *Handbook of Sensory Physiology*, Vol. 2, W. D. Keidel and W. D. Neff, eds., pp. 307–400, Springer-Verlag, New York.

Osen, K. K. (1970) Course and termination of the primary afferents in the cochlear nucleus of the cat: an experimental anatomical study. *Arch. Ital. Biol.* 105:21–51.

Osen, K. K. (1972) Projection of the cochlear nuclei on the inferior colliculus in the cat. *J. Comp. Neurol.* 144:355–372.

Pons, T., M. Sur, and J. H. Kaas (1981) Axonal arborizations in area 3b of somatosensory cortex in the owl monkey, *Aotus trivirgatus*. *Anat. Rec.* 202:151A.

Roth, G. L. (1977) Some features of the anatomical and physiological organization of the central nucleus of the inferior colliculus: implications for its role in the processing of auditory information. Unpublished doctoral dissertation, University of California, San Francisco.

Roth, G. L., L. M. Aitkin, R. A. Andersen, and M. M. Merzenich (1978) Some features of the spatial organization of the central nucleus of the inferior colliculus of the cat. *J. Comp. Neurol.* 181:661–680.

Roth, G. L., R. K. Kochlar, and J. E. Hind (1980) Interaural time differences: implications regarding the neurophysiology of sound localization. *J. Acoust. Soc. Am.* 68:1643–1651.

Sachs, M. B., E. D. Young, and M. I. Miller (1983) Speech encoding in the auditory nerve: implications for cochlear implants. *Ann. N.Y. Acad. Sci.* 405:94–113.

Sanchez-Longo, L. P., and F. M. Forster (1958) Clinical significance of impairment of sound localization. *Neurology (NY)* 8:119–125.

Sando, I. (1965) The anatomical interrelationships of the cochlear nerve fibers. *Acta Otolaryngol. (Stockh.)* 59:417–436.

Scharf, B., M. Florentine, and C. H. Meiselmann (1976) Critical band in auditory lateralization. *Sens. Proc.* 1:109–126.

Schreiner, C., and M. S. Cynader (1984) Basic functional organization of the second auditory cortical field (AII) of the cat. *J. Neurophysiol.* (in press).

Semple, M. N., and L. M. Aitkin (1979) Representation of sound frequency and laterality by units in central nucleus of cat inferior colliculus. *J. Neurophysiol.* 42:1626–1639.

Sherman, S. M., and P. D. Spear (1982) Organization of visual pathways in normal and visually deprived cats. *Physiol. Rev.* 62:738–855.

Souvijari, A. R. A., and J. Hyvärinen (1974) Auditory cortical neurons in the cat sensitive to the direction of sound source movement. *Brain Res.* 73:455–471.

Stillman, R. D. (1971) Characteristic delay neurons in the inferior colliculus of the kangaroo rat. *Exp. Neurol.* 32:404–412.

Strominger, N. L. (1969) Localization of sound in space after unilateral and bilateral ablation of auditory cortex. *Exp. Neurol.* 25:521–533.

Thompson, G. C., and R. B. Masterton (1978) Brain stem auditory pathways involved in reflexive head orientation to sound. *J. Neurophysiol.* 41:1183–1202.

Walsh, E. G. (1957) An investigation of sound localization in patients with neurological abnormalities. *Brain* 80:222–250.

Wiener, F. M., R. R. Pfeiffer, and A. S. N. Backus (1966) On the sound pressure transformation by the head and auditory meatus of the cat. *Acta Otolaryngol. (Stockh.)* 61:255–269.

Winer, J. A., I. T. Diamond, and D. Raczkowski (1977) Subdivisions of the auditory cortex of the cat: the retrograde transport of horseradish peroxidase to the medial geniculate body and posterior thalamic nuclei. *J. Comp. Neurol.* 176:387–418.

Wortis, S. B., and A. Z. Pfeffer (1948) Unilateral auditory-spatial agnosia. *J. Nerv. Ment. Dis.* 108:181–186.

Yin, T. C. T., and S. Kuwada (1982) Characteristic delays in the cat inferior colliculus. *Soc. Neurosci. Abstr.* 8:348.

Young, E. D., and M. B. Sachs (1979) Representation of steady-state vowels in the temporal aspects of the discharge patterns of populations of auditory nerve fibers. *J. Acoust. Soc. Am.* 66:1318–1403.

Zook, J. M., and J. H. Casseday (1982) Origin of ascending projections to inferior colliculus in the mustached bat (*Pteronotus parnellii*). *J. Comp. Neurol.* 207:14–28.

M.M.MERZENICH

Neural Ontogeny of Higher Brain Function;

Implications of Some Recent Neurophysiological Findings

By:

Dr. Michael M. Merzenich
Dr. Terry T. Allard[1]
Dr. William M. Jenkins

From:

Coleman Laboratory
University of California at San Francisco
San Francisco, CA 94143-0732

[1]Present address: Cognitive and Neural Sciences Division, Office of Naval Research, 800 N. Quincy, Arlington, VA 22217-5000

INTRODUCTION

Despite substantial experimental interest in the processes of "development" of the nervous system, there is surprisingly little direct understanding of neurophysiological processes underlying cognition and its ontogeny. There are several obvious reasons for this lack of progress. First, neuroscience has largely dealt with the issues of development in the terms of prenatal or early postnatal maturation of anatomical structures and connections, and of the origins of response primitives principally within "primary" cortical fields as they relate to anatomical maturation. Second, studies in animals beyond the first weeks of life have largely focused on examination of static anatomical and functional properties of sensory and motor systems. There has been very little study of the young or adult mammalian forebrain through a period of acquisition of new behaviors. Third, examination of complexly coupled flesh and blood neuronal networks, in which dynamic processes underlying progressive development of new perceptual abilities and motoric skills are resident, has been very limited. The dynamics of the complexly interconnected forebrain machinery cannot be reconstructed from data generated by the predominant neurophysiological method, i.e., by recording the activity of usually-unidentified network elements one at a time (see Mountcastle, this volume).

Developmental psychologists have a common lament that learning theories are largely based on the results of studies in adult animals and humans. Understanding of the origins of neural mechanisms of complex behaviors by neurophysiologists are also plagued by the fact that, with few exceptions, either: a) samples of neural responses are derived in adult "untrained" animals with unknown behavioral histories examined for a specific response detail over a period of a few hours in their life; or b) studies are conducted in over-trained animals, after their behavioral training has resulted in a high performance level --- in other words, just when consideration of mechanisms underlying the acquisition of those behaviors are no longer very evident or open to study.

While progress for understanding the neural origins of complex human behaviors has been painfully slow, there has, of course, been an increasingly extensive description of the sequenced development of human visual and

somatosensory and auditory perception and cognition, of motor behaviors, of speech and language, of recognition and memory, of personality, and so forth. Each of these and other related behavioral subfields constitutes an organized area of study, and has generated a major literature in its own right. From this vast behavioral literature, the necessary accomplishments of the neural machine are defined in ever-increasing detail. In parallel, there is a rapidly developing understanding of basic physical changes in the nervous system through its ontogeny, although that understanding is superficial and is certainly incomplete. For example, changes in neuron dendrites, of synapse numbers, of rates of synaptic turnover, of pyramidal cell spine numbers, of the absolute or proportional volumes of neuropil, of neural soma sizes, of the spreads of input arbors, of the microvasculature and metabolism, of the degree of myelination of axons of afferents or efferents or intrinsic axons --- to cite some examples --- have been described as a function of the age of postnatal animals including humans.

What is lacking is: a) a clear understanding of the neural origins of progressively more complex behaviors; and b) any deep understanding as to how even the general, described morphological changes in the forebrain of the growing child might relate to the basic processes underlying observable, experience-driven development of progressively more complex behaviors.

In this report, we make an initial attempt to posit a general model of the neural origins of complex human behaviors (considered on the first level of understanding), and then attempt to illustrate how observed, sequenced morphological maturation of the nervous system would be expected to relate to the generation of behavioral products by this intrinsic neocortical machinery. This model will satisfy no one. A general theory of the ontogenetic neural origins of complex behaviors has a tremendous body of developmental phenomenology to account for, and descriptions and models of higher brain functions are by no means agreed on by specialists in any of the subdisciplines of child development. At this point there can be no very compelling assignment of specific function or behaviorally defined developmental stage made to any specific neural forebrain field. Considerations of the control and operation of this machine in a crucial intermediate domain of time (hundreds of milliseconds to seconds) is a present subject of experimental investigation, and requires special treatment not possible here. Finally, in this brief review we can only superficially consider the interplay of the affective and decision making aspects of the machine with its operations under input drive.

What is presented is a point of view, based upon electrophysiological observations, of the kind of neural machine that must underly the development of complex behaviors and their individual evolution.

BACKGROUND

In a long series of neurophysiological experiments, we have described the basic nature of intrinsic self-organizing processes in functional subdivisions of the primate neocortex (see Merzenich, et al., 1984a; 1984b; 1988; 1990; for review). Most experiments have been conducted within the body surface representations in the somatosensory cortical domain, which we have considered to be a relatively easily documentable model system for studying neocortical representational plasticity across a significant cortical network sector. These and other related experiments have

revealed that the specific details of cortical "representations" - -- of the distributed, selective responses of cortical neurons --- are established and are continually remodelled BY OUR EXPERIENCES throughout life. This constitutes an important challenge to a widely prevailing view that the details of distributed cortical neuron response specificities of the eye or ear or skin or movements are established in early life by the anatomical maturation of the nervous system, and are thereafter functionally static.

1. Some Rules of This "Cortical Representational Plasticity"

An understanding of the operational rules of these self-organizing neocortical processes are at the heart of understanding how they might relate to and account for neurobehavioral development. They have been outlined in several recent reviews (see Merzenich, et al., 1984a; 1988; 1990). First and foremost among them, it was argued (Merzenich, et al., 1984a; also see Edelman and Finkel, 1984; von der Malsburg and Singer, 1988) then demonstrated experimentally (Clark, et al., 1987; 1988; Allard, et al., 1990; Jenkins, et al., 1990; Dinse, et al., 1990; Recanzone, et al., 1991e) that the temporal structures of inputs must be important for the input selection by which cortical map details are established by use --- and by which they are remodelled by use throughout life. Considered in terms of representational detail, cortical somatosensory maps are not simple anatomically-based representations of the skin surface receptor array, as has long been believed. Rather, cortical areas spatially map TEMPORAL continua. There is no mystery about the origins of this cortical network input-selection behavior. Our and other cortical network modeling studies (see Grajski and Merzenich, 1990a; 1990b; Merzenich, et al., 1991) indicate that any competitive neuronal network: a) with realistic spreads and convergences and divergences of inputs, b) whose inputs and network connections are subject to plastic changes by an appropriate learning rule, and c) that has an appropriate integrative time constant will behave in this way.

Other major conclusions about processes underlying the cortical input selection that underlie these behaviorally driven cortical representational changes include the following:

a) Behaviorally emergent neural responses are generated from anatomically-always-present extrinsic and intrinsic cortical inputs (see Merzenich, et al., 1984a; 1988; 1990; Edelman and Finkel, 1984; Edelman, 1987). Changes in synaptic effectivenesses underlie this behaviorally- driven neuron response remodelling.

b) This remodeling of selected, distributed cortical neuron responses is the accomplishment of columnarly arrayed, cooperative (i.e., coupled) groups of neurons --- cortical "minicolumns" --- that are on the order of a few tens of microns up to a few hundreds of microns in horizontal extent (see Mountcastle, 1978; Merzenich, et al., 1988; 1990). There are of the order of one or two hundred million of these small parallel processing machines in the human neocortex.

c) The remodeling of cortical representations by experience is a competitive process. The effective inputs of these cortical processing machines are shaped by the relative quantities of coincident or nearly coincident inputs that also result in the continual reshaping of these coupled cortical cell assemblies (see Willshaw and von

der Malsburg, 1975; Edelman and Mountcastle, 1978; Edelman, 1987; Edelman and Finkel, 1984; Pearson, et al., 1987; von der Malsburg and Singer, 1988; Dinse, et al., 1990; Merzenich, et al., 1990; Recanzone, et al., 1991e; Merzenich, et al., 1991). There is a continual competition between neuronal groups for the domination of neurons on their mutual borders.

It should be emphasized that competitive use-driven changes in functional cortical cell assemblies are not mysterious or surprising. If experience-driven modification of the effectivenesses of horizontal cortical network connections (e.g., of intracortical pyramidal cell axon collaterals) is allowed, and if, again, this process is marked by a relatively short integrative time constant, then a specific pattern of coincident or nearly-coincident behaviorally-significant extrinsic inputs should result in a selective remodeling of both afferent input effectivesses and the strength of positive coupling of intrinsic network neurons forming positively-coupled cortical neuronal groups (see Edelman and Finkel, 1984; Pearson, et al., 1987; von der Malsburg and Singer, 1988; Merzenich, et al., 1991). That neuronal group remodelling has been directly studied in several recent experiments (e.g., see Merzenich, et al., 1990; Dinse, et al., 1990; Recanzone, et al., 1991d-e; Merzenich, 1991)

We hypothesize that the same coincidence-based intrinsic self-organizing processes are general across the neocortex. Although some field-specific neuron population differences are recorded between cortical areas and of course constitute the basis of their cytoarchitectonic distinction between cortical areas, studied cortical fields have distributions of anatomically identified neuron populations similar to those recorded in our principal model cortical zone, somatosensory area 3b. In general, neocortical cell populations and their distributions are more noteworthy for their commonalities than for their differences across the forebrain. In our own experiments, distributed use-driven response remodelling paralleling that recorded in area 3b has also been documented in somatosensory cortical fields 3a (Recanzone, et al., 1991c) and 1 (e.g., see Merzenich, et al., 1990), in the movement representations of area 4 (Merzenich, et al., 1988; 1990) and in the primary auditory cortex (G. Recanzone, M. Merzenich, W. Jenkins and C. Schreiner, unpublished observations; also see Kitzes, et al., 1978; Diamond, 1985). Other investigators have documented similar or spatially more dramatic behaviorally-driven representational changes in a number of other cortical areas (for example, see Woody and Engel, 1972; Buchhalter, et al., 1978; Disterhof and Stuart, 1976; Kitzes, et al., 1978; Weinberger and Diamond, 1988; Miyashita, 1988; Miyashita and Chang, 1988; Spitzer, et al., 1988; Diamond and Weinberger, 1989; Rolls, et al., 1989). In a nonbehavioral context, a widespread capacity for lifelong cortical representational plasticity has also been demonstrated a) following restricted losses of peripheral sensory inputs in all examined somatosensory (e.g., see Kalaska and Pomeranz, 1978; Franck, 1980; Rasmusson, 1982; Merzenich, et al., 1983a,b; 1984; Kelahan and Deutsch, 1984), auditory (Robertson and Irvine, 1989), visual (Kaas, et al., 1990), and motor (Sanes, et al., 1990) cortical fields; b) following restricted SI cortical lesions expressed by representational reorganization in SI (Cole and Glees, 1954; Jenkins, et al., 1987) and in SII (Pons, et al., 1988) somatosensory cortical fields; c) following direct cortical network stimulation, in motor (Graham Brown and Sherrington, 1912; Graham Brown, 1915; Leyton and Sherrington, 1917; Nudo, et al., 1990) and somatosensory (Dinse, et al., 1990; Recanzone, et al., 1991) cortical fields; and d) in motor cortex, following direct stimulation of sensory cortex (Sakamoto, et al., 1987).

It should be emphasized that the intrinsic self-organization in any given cortical field is necessarily limited by field-specific sources of anatomical inputs and by the spreads of the inputs specific to that cortical zone (see Merzenich and Kaas, 1980; Merzenich, et al., 1984; 1988). We hypothesize that each field has a static anatomical construct that is ordinarily topographically far more crude than is its emergent functional map (also see Edelman, 1981; 1987). This cruder anatomical map represents the input repertoire from which experience-refined input-timing-based functional maps can be generated. In many cortical fields, anatomical inputs are arrayed in an orderly topography. In others, this anatomical topography can be weakly expressed or absent: special posterior parietal, inferior and anterior temporal, frontal and medial-wall cortex zones have virtually all-to-all distributions of projections from their multiple input sources.

2. Distributed Cortical Systems and Limited Cortical Representational Hierarchies

There are of the order of a hundred representational regions within the neocortex in man. Each is marked by: a) field-specific sources of inputs; b) field-specific internal spreads of inputs; and c) field-specific functional response properties of resident neurons (see Merzenich and Kaas, 1980; Merzenich, et al., 1988; 1990; Kaas, 1988; Van Essen, et al., 1990; Felleman and Van Essen, 1990). On this basis alone, it is clear that each of these many cortical zones has a specific functional role.

Cortical fields are complexly interconnected in each sensory and motor domain (e.g., see Merzenich and Kaas, 1980; Felleman and Van Essen, 1990). A number of 3- to 6- or 7- stage hierarchies can be traced within the neocortex in which inputs are a) progressively more complex as to source; and b) progressively more divergent and convergent in their spreads. By operation of general self-organizing process(es) described above, each of these cortical fields will create a field-specific functional construct, by use. The use-derived "maps" of the koniocortical ("primary") cortical zones will vary the least because the anatomical spreads of inputs are the most constrained within these zones. At higher hierarchical levels, convergence and divergence of connections is far greater, and on this basis alone, these cortical areas should be correspondingly more adaptive. This is borne out in numerous experiments that reveal that highly specific neural responses can be relatively quickly generated in highly divergently-convergently connected cortical fields in animals trained to recognize or to manipulate simple or complex stimulanda in simple or complex behavioral contexts (e.g., see Miyashita, 1988; Miyashita and Chang, 1988; Spitzer, et al., 1988; Weinberger and Diamond, 1988; Rolls, et al., 1989). Because of their more complex input combinations and wider input spreads, progressively more idiosyncratic constructs can be expected to arise by operation of these processes at progressively "higher" hierarchical levels. Object recognition ultimately require representation across highly convergently-divergently connected forebrain projection areas.

3. Behaviorally Contingent Control of Input Effectivenesses for Creating Representational Changes

Recent experiments reveal that experience-driven changes in cortical input effectivenesses and the experience-driven reshaping of cortical neuronal groups that

together underly generation of representational changes are modulated as a function of behavioral state or context. Thus, neuron response changes (Woody and Engel, 1972; Disterhof and Stuart, 1976; Buchhalter, et al., 1978; Kitzes, et al., 1978; Nudo and Merzenich, 1987; Weinberger and Diamond, 1988; Spitzer, et al., 1988; Jenkins, et al., 1990; Recanzone, et al., 1991b-d) and distributed cortical field representational changes (Nudo and Merzenich, 1987; Jenkins, et al., 1990; Recanzone, et al., 1991a-d) have been recorded in an animal performing a behaviorally controlled task that engages specific cortical areas, but not when equivalent differential stimulation is delivered passively, or after a learned behavior is extinguished. We hypothesize that the rules of this modulation of input effectiveness will parallel the rules of modulation of effective inputs recorded in training, learning, recognition, memory, et alia. The modulatory control systems that produce and distribute these cognitive inputs are a present subject of intense study.

Experience-based alteration of distributed responses in given cortical fields can also be subject to contingent external gating control. For example, neurons in the hand area of cortical area 3b are responsive throughout periods of active exploration of the hand, while neurons in cortical area 1 are inhibited during periods of active hand exploration (inputs from other skin areas are unaffected; see Nelson and Douglas, 1989). This observation presumably accounts in large part for the entirely different detailed forms of the cortical map generated in cortical area 1 as compared with cortical area 3b in the same individual monkeys (Merzenich, et al., 1978; 1987). Similarly, responses of auditory cortical fields in alert monkeys are profoundly suppressed during periods of head movement (Brugge and Merzenich, 1973). These and a growing number of other examples of context-dependent gating of cortical responses suggest that inputs from sensory epithelia generated during specific movements can be gated as they enter a competition matrix. Certainly a functional input-time-based representation of the skin or sound field created with inputs entering the cortical network during movement will differ substantially from a representation created from inputs derived with the body surface or head or eye maintained in a static position.

It is probable that such "gating" of inputs entering cortical network competition matrices is commonplace, and should by not be expected to be limited to motor-sensory gating. Thus, while one principal role of cortico-cortical connections is to provide cortically processed input to competition matrices at higher hierarchical levels or in parallel streams, an important second role for elaborate cortical field-to-field connections is to provide for location-specific, behavioral-context-dependent input gating.

A discussion of other possible roles of these complex field-to-field projections, e.g., in coordinating field-to-field changes to minimize errors of association, to provide topographically specific inputs not directly entering the network competition matrices that enable or facilitate or disable or disfaciliitate self-organization in downstream cortical areas, or to provide fed-back "error signals" or "efference copies" or "sequence plans", are beyond the scope of this brief review.

4. STABILIZATION OF DYNAMIC CORTICAL REPRESENTATIONS

Finally, there is evidence for in-place stabilizing machinery for self-organizing neocortical fields, operating at least to a large extent during periods of sleeping. In

rapid eye movement (REM) sleep, inputs are fed from a brain stem nucleus widely across thalamic nuclei, and there relayed onto input lines feeding cortical fields over most of the forebrain (see Hopson, 1989, 1990, for review). This special off-line input consists of spatially widely distributed and temporally synchronous activity. This is an especially powerful form of input to this self-organizing machinery. It has been crudely modeled by us in experiments in which peripheral nerves innervating large skin fields have been chronically electrically stimulated, thereby generating nearly synchronous inputs to large cortical zones (Recanzone, et al., 1990). Such input operates antagonistically to the processes by which effective inputs are selected and by which coupled neuronal groups are refined, and we hypothesize that the bouts of broad-field spiking occuring during periods of REM sleep would have the effect of erasing specifically non-stored inputs. A similar proposal was earlier advanced by Crick and Mitchison (1983).

To more explicitly explain this hypothesis, one might reflect on the time sequence of treatment of stored changes indicated by cognitive studies (e.g., see Lashley, 1951). We have earlier stated that the effectivenesses of inputs for producing enduring changes must be modulated as a function of behavioral state. Input-induced changes must be conserved over the short term (minutes to hours), as it can be behaviorally "recorded" post-hoc, albeit with declining fidelity over time. Principally within the limits of a day, a permanent (strongly reinforced = long-term potentiated) record of inputs can be created over a broad range of post-hoc time. Considered in this context, broadly synchronous inputs generated in REM sleep would be important for the elimination of weakly stored --- i.e., behaviorally non-reinforced or weakly-reinforced --- inputs.

In our peripheral nerve stimulation studies, it is important to note that the power of the creating changes of representational detail is a direct function of stimulus number. Similarly, the "erasing power" of REM sleep should be a function of the duration of daily REM sleep periods.

We have also hypothetized that there is a stabilizing role for non-REM sleep, during which stored changes in coupled cell assemblies generated within cortical fields during periods of waking might be stabilized (see Merzenich, et al., 1984a; Merzenich, 1987; Hopson, 1990). A discussion of the mechanisms by which this could be achieved is beyond the scope of this brief review.

INTRINSIC SELF-ORGANIZING NEOCORTICAL PROCESSES AS THEY RELATE TO THE ONTOGENY OF HUMAN COGNITION

1. Summary of Premises

To begin this discussion, we summarize our basic conclusions:

a) There is a field-by-field self-organization of functional representations in cortical fields.

b) Use-derived cortical representations map temporal input continua by an intrinsic neocortical process(es) that operates with a relatively short time constant.

c) This self-organization of each of the more than 100 cortical areas is qualitatively limited by field-specific sources of input.

d) This self-organization is limited in scope in each cortical area by the extents of spreads of inputs. At progressively higher levels on limited subsystem hierarchies, more complex input-source combinations and more extensive internal spreads of inputs result in the generation of progressively more representational (more abstract), and progressively more idiosyncratic functional constructs.

e) Powerful cortico-cortical projections can provide input sources that are the product of cortical input selection process which directly entering competition matrices (where they converge with subcortical inputs), or can profoundly and selectively gate effectivenesses of inputs to prevent them from generating behaviorally context-specific changes in cortical network competition matrices. This latter function extends the range of possible forms of experience-generated representational constructs, and can specifically couple or discouple sensory and motor activities.

f) Effectivenesses of inputs for creating enduring changes in representational constructs are modulated as a function of behavioral state. It is hypothesized that the rules for generating these enduring changes will be synonomous with the rules for learning reinforcement and memory.

How can these representations be expected to develop and stabilize over time in a young animal or child?

2. Neurological Bases of Delayed Functional Neocortical Self-Organization

Cortical fields are a tabula rasa at birth, in the sense that there can initially be only limited, stored experience-derived constructs. Cortical fields are not a tabula rasa at birth, in the sense that genetically or epigenetically defined sources and distributions of inputs are limited in every field, and thereby constrain the possible use-derived products of each of the more than a hundred functional cortical areas. Moreover, basic neocortical adaptive mechanisms are genetically prescribed, and so limited.

If the cortical competition matrices were operating in a young child as in an adult, early inputs would be inordinately powerful in establishing initial representations and in determining the specific early directions of change by use. In fact the cortical machinery is highly constrained in the plasticity permitted in early life. There are several features of organization of the neocortex that obviously impact on the rate and time of onset of the self-organization of its component fields, and hence on their ontogenic products. They insure the requisite deliberate pace of stable and progressive neurobehavioral development.

First, as noted above, the self-organizing machinery of cortical fields is obviously morphologically immature in the early stages of post-natal development. Dendrites increase in the richness of their local arborizations, and synapse numbers first increase in early postnatal life, then decline substantially (e.g., see Rakic, et al., 1986; Diamond, et al., 1987; Scheibel, 1989; Zecevic, et al., 1989). The complexities of dendritic arborizations and the rates of synaptic turnovers are to some extent themselves a function of the intensity of early experiences (e.g., see Diamond,

1987; Sirevaag, et al., 1987; 1988; Venable et al., 1989; Scheibel, et al., 1990). For these self-organizing processes, the delay of full myelination (see Fleschig, 1920; Yakolev and Lecours, 1967) is probably the single most important feature of childhood cortical immaturity. For process(es) a) whose experienced-derived constructs are created by the temporal synchronicity of inputs, and b) that has a relatively short integrative time constant, an increase in myelination is equivalent to a decrease in input noise, and should profoundly impact on the possible effectivenesses of inputs entering these cortical networks.

Second, for the orderly development of complex behaviors, use-created representations must be created in sequence. A creation of a refined representation of the skin surface and several constructs required for producing requisite fine hand movements must predate the generation of still higher level cortical constructs required for recognition of object shape in the haptic domain. A detailed representation of the loading of muscles of the limb and of the three-dimensional visual world are among the more fundamental representational continua that must predate generation of a representation of visually-guided limb reach. A representation of phonetic elements must predate a creation of an organized motor speech area in which they represent movement targets. And so forth. Representations must be created and consolidated in orderly developmental sequences. Or to put it another way, representations requiring convergence from functional, use-generated repertoires must obviously await their creation and stabilization.

That is not to say that these requisite representations are not subject to further modification. Thus, for example, the skin surface expands substantially and positional relationships and predominant stimulation modes change greatly over it, requiring fine tuning of skin input source maps throughout life; loading repertoires of muscles of the limb change inexorably with growth and its accompanying changes in masses and resistances; sound location representations must be continually redefined as basic cues change with head and body growth, and so forth. Each basic use-derived repertoire will slowly evolve, within the limits of anatomical constraints and as predominant use patterns evolve, with age. Each has the capacity to modify itself, as relevant physical continua change with growth or environmental circumstances.

Third, the weight of experience controls the pace of cortical field representations, because it determines the robustness of source representations. The statistics of the outputs from these representations is a measure of their power for modifying the cortical representations to which they deliver their experience-refined outputs. They become more reliable and predictable input sources with more and more behavioral experience, in no small part because their own progressive consolidation also contributes to the definition of predominant use patterns.

Fourth, the progressive myelination of successively "higher" neocortical levels (see Flechsig, 1920; Yakolev and Lecours, 1967) over time would have the effect of delaying self-organization of their input-coincidence-based constructs until the use-derived representations within their prospective source fields are consolidated. The myelination sequence must necessarily impact on the effectiveness of inputs for the idiosyncratic organization of the details of representations of fields. Again, gradual myelination, usually occupying months of time for given cortical zones, should have a profound impact in gradually consolidating the created representation of the self-organizing field, and delaying effective delivery of information from that

use-created repertoires to higher processing levels.

Fifth, the proportionally long periods of REM sleep should contribute to a prolongation of the acquisition of inputs effective in inducing permanently stored change. As the child matures, these REM sleep periods progressively decline, from about 9 hours a day at birth to about 5 hours a day at age 2 to about 3 hours a day at age 5 to about 1.5-2 hours a day after age 10 (e.g., see Roffwarg, et al., 1866; Hopson, 1990). As self-organizing cortical fields are progressively and sequentially consolidated, the cortical network requirements for noise reduction would be expected to decline correspondingly.

3. Developmental "Stages"

The orderly path of cognitive development has often been described in terms of the "developmental stage" or "level". An expecially relevant earlier description of programmed, staged development driven by experience is that of Piaget and his colleagues (Piaget, 1970; Piaget and Inhelder, 1969; also see Hunt, 1969). Piaget's concept of a development stage has obvious parallels with our characterization of progressive sequential neurological development as suggested by our models of a self-organizing neocortex operating by these simple process rules. As a product of a self-organizing machine of this type, complex human behavior necessarily evolves from the simple to the complex; our model neocortex is necessarily staged in development. An anatomical sequence of maturation probably controls the sequences of field-by-field development of functional repertoires in cortical subsystems. The "primary" cortical areas, with the most topographic and restricted anatomical connections, are the first to completely myelinate and to mature morphologically (e.g., see Fleschig, 1920; Scheibel, 1989). These more primary areas are responsible for our most fundamental behavioral source repertoires --- i.e., for what might be termed "cortically generated response primitives". Development of the first-order functional constructs by experience in the more primary areas are requisite for creation of second-order, convergence-based repertoires; second-order for production of third-order, and so forth. The lower the order of the functional repertoire, the more that anatomical constraints insure a relatively constant and predictable product; for higher-order repertoires, great idiosyncratic variability in experienced-generated constructs is possible.

Piaget's models encompass most aspects of this forebrain self-organization model. By his view, there is a foreordained sequence of cognitive development initiated with an innate neural representation of stimulus and response primitives. Development occurs in from a few to up to about a dozen (in different cognitive or motor spheres) clearly definable stages. Experience drives the machine, which makes a progressive "accommodation" (Piaget and Inhelder, 1969; Hunt, 1969) to novel inputs --- in neurological terms, a progressive refinement of cortical representational constructs. There must be a "consolidation" and an "equilibration" at each stage, by which the "accommodation" of new inputs gradually results in stabilized, statistically-predictable constructs which enable generation of functional constructs created by higher-level combinations.

SIGNIFICANCE; CONCLUSIONS

These models of the neocortical self-organizing processes explain how a simple, general, intrinsic neocortical process might be expressed sequentially and progressively more powerfully field by field self-organization, to generate the complex neural representational constructs underlying human perception and cognition. They indicate that the innate in development would include:

a) the treatment of information in projection systems feeding different neocortical zones, which impose limits on the constructs that can be created by quantities of behaviorally important, temporally-correlated inputs within those zones;

b) the anatomically limited sources and convergences and divergences of inputs within each cortical zone; and

c) the intrinsic process machinery and its inbuilt "rules", which strictly limits the achievable products of this system in operation.

Experience is, of course, the primary fuel for this engine. It first generates relatively predictable but nonetheless idosyncratic representational constructs in the first-myelinated, more- primary cortical zones. As the weight of experiences is played out across the cortex and as cortical areas are anatomically refined on the local scale of effective synapses and local dendrite morphology, more and more robust functional representations emerge. As the statistics of these more-primary field outputs become more and more predictable, and as myelination and cell maturation progress to successively higher hierchical levels, effective self-organization can then be achieved within them. Successively more powerful combinations and constructs are progressively generated by experience, over the succession of years of a human childhood, and are ultimately fully expressed across 4- or 5- or 6- or 7-level system hierarchies. And hence, from a relatively simple cortical processing machine, the functional cortical minicolumn of Vernon Mountcastle, multiplied in the neocortex one or two hundred million times and delivered rich inputs in more than a hundred field-specific forms, comes the behavioral commonalities and limitations as well as the rich array of experience-derived abilities and talents and knowledge that mark humankind.

ACKNOWLEDGMENTS

Experimental studies described in this review were supported by NIH Grant NS-10414, the Coleman Fund, and HRI. The authors thanks numerous colleagues who have contributed to these studies, and to the development of these models. This manuscript is dedicated to Dr. Vernon Mountcastle, an inspiring mentor (for MMM) and scientist whose insights into the dynamical operations of the neocortex have provided crucial underpinnings for our studies.

REFERENCES CITED

Allard, R.A., S. A. Clark, W. M. Jenkins and M. M. Merzenich (1990) Reorganization of somatosensory area 3b representation in adult owl monkeys following digital syndactyly. J. Neurophysiol. (in press).

Buchhalter, J., Brons, J., and C. Woody (1978) Changes in cortical neuronal excitability after presentations of a compound auditory stimulus. Brain Res. 156:162-167.

Brugge, J. F., and M. M. Merzenich (1973) Responses of neurons in auditory cortex of the macaque monkey to monaural and binaural stimulation. J. Neurophysiol. 36:1138-1158.

Clark, S.A., Allard, T., Jenkins, W.M., and M. M. Merzenich (1988) Syndactyly results in the emergence of double digit receptive fields in somatosensory cortex in adult owl monkeys. Nature 332:444-445.

Clark, S.A., Allard, T., Jenkins, W.M., and M. M. Merzenich (1986) Cortical map reorganization following neurovascular island skin transfers on the hands of adult owl monkeys. Soc. Neurosci. Abstr. 12:391.

Cole, J., and P. Glees (1954) Effects of small lesions in sensory cortex in trained monkeys. J. Neurophysiol. 1:1-13.

Crick, F., and Mitchison, G. (1983) The function of dream sleep. Nature 304:111-114.

Diamond, M.C., Greer, E.R, York, A., Lewis, D., Barton, T., and Lin, J. (1987) Rat cortical morphology following crowded-enriched living conditions. Exptl. Neurol. 96:241-247.

Diamond, D.M., and Weinberger, N.M. (1989) Role of context in the expression of learning-induced plasticity of single neurons in auditory cortex. Behav. Neurosci. 103:471-494.

Dinse, H.R., Recanzone, G.H., and M. M. Merzenich (1990) Direct observation of neural assemblies during neocortical representational reorganization. IN: Parallel Processing in Neural Systems and Computers. (eds. R. Eckmitler, G. Hartmann and G. Hauske). Elsevier, North Holland, pp. 65-70.

Disterhof, J. F.and D. K. Stuart (1976) Trial sequence of changed unit activity in auditory system of alert rat during conditioned response acquisition and extinction. J. Neurophysiol. 39:266-281

Edelman, G.M. (1987) Neuronal Darwinism: The Theory of Neuronal Group Selection. Basic Books, New York.

Edelman, G.M. (1981) Group selction as the basis for higher brain function. IN: Organization of the Cerebral Cortex. (eds. F. O. Schmitt, F. G. Worden, G. Adelman and S. G. Dennis). MIT Press, Cambridge, pp. 51-100.

Edelman, G. M., and Finkel, L. H. (1984) Neuronal group selection in the cerebral cortex. IN: Dynamic Aspects of Neocortical Function. (eds. G. M. Edelman, W. E. Gall and W. M. Cowan). Wiley, New York, pp. 653-695.

Edelman, G.M. and V.B. Mountcastle, (1978) The Mindful Brain: Cortical

Organization and the Group-Selective Theory of Higher Brain Function. MIT Press, Cambridge, MA.

Franck, J.I. (1980) Functional reorganization of cat somatic sensory-motor cortex (SmI) after selective dorsal root rhizotomies. Brain Res. 186:458-462.

Felleman, D. J., and D. C. Van Essen (1990) Distributed hierarchical processing in primate cerebral cortex. Cerebral Cortex (in press).

Fleschig, P. (1920) Anatomie des menschlichen Gehirns und Ruckenmarks auf myelogeneti- schen Grundlage. Georg Thieme, Liepzig.

Graham Brown, T., and C. S. Sherrington (1912) On the instability of a cortical point. Proc. Royal Soc. Lond. B. 85:250-277.

Graham Brown, T. (1915) Studies in the physiology of the nervous system. XXII: On the phenomenon of facilitation. 1: Its occurence in reactions induced by stimulation of the motor cortex of the cerebrum in monkeys. Quart. J. Exp. Physiol. 9:6-99.

Grajski, K.A., and M. M. Merzenich (1990) Hebb-type dynamics is sufficient to account for the inverse magnification rule in cortical somatotopy. Neural Computation 2: 74-81.

Grajski, K.S., and M. M. Merzenich (1990) Neuronal network simulation of somatosensory representational plasticity. IN: Neural Information Processing Systems, Vol. 2. (ed. D. L. Touretzky). Morgan Kaufman, San Mateo, CA (in press)

Hopson, J.A. (1990) Sleep and Dreaming. J. Neurosci. 10:371-382

Hopson, J.A. (1989) The Dreaming Brain. Basic Books, New York.

Hunt, J. McV. (1969) The impact and limitations of the giant of developmental psychology. IN: Studies of Cognitive Development. (eds. D. Elkind and J. H. Flavell). Oxford U. Press, New York, pp. 3-66.

Jenkins , W.M., and M. M. Merzenich (1987) Reorganization of neocortical representations after brain injury: A neurophysiological model of the bases of recovery from stroke. Prog. Brain Res. 71:249-266.

Jenkins, W.M., Merzenich, M.M., Ochs, M., Allard, T.T., and E. Guic-Robles (1990) Functional reorganization of primary somatosensory cortex in adult owl monkeys after behaviorally controlled tactile stimulation. J. Neurophysiol. 63:82-104.

Kaas, J.H. (1988) Why does the brain have so many visual areas? J. Cogn. Neurosci. 1:121-135.

Kaas, J.H., Krubitzer, L.A., Chino, Y.M., Langston, A.L., Polley, E.H., and N. Blair (1990) Reorganization of retinotopic maps in adult mammals after lesions of the retina. Science 228:229-231.

Kalaska, J., and B. Pomeranz (1979) Chronic paw denervation causes an age-dependent appearance of novel responses from forearm in "paw cortex" of kittens and adult cats. J. Neurophysiol. 42:618-633.

Kelahan, A.M., and G. S. Deutsch (1984) Time-dependent changes in the functional organization of somatosensory cerebral cortex following digit amputation in adult raccoons. Somatosens. Res. 2:49-81.

Kitzes, L.M., Farley, G.R., and K. A. Starr. (1978) Modulation of auditory cortex unit activity during the performance of a conditioned response. Exptl. Neurol. 2:678-697.

Lashley, K.S. (1951) The problem of serial order in behavior. IN: Cerebral Mechanisms in Behavior. (ed. L. Jeffress). Wiley, New York.

Leyton, A.S. F., and C. S. Sherrington (1917) Observations on the excitable cortex of the chimpanzee, orang-utan, and gorilla. Quart. J. Exp. Physiol. 11:135-222.

Merzenich, M.M. (1987) Dynamic neocortical processes and the origins of higher brain functions. IN: Neural and Molecular Bases of Learning. (eds. J. P. Changeux and M. Konishi). Wiley, New York, pp. 337-358.

Merzenich, M.M., and J. H. Kaas (1980) Principles of organization of sensory-perceptual systems in mammals. Prog. Psychobiol. Physiol. Psychol. 9: 1-42,

Merzenich, M.M., Kaas, J.H., Sur, M., and C.-S. Lin (1978) Double representation of the body surface with cytoarchitectonic areas 3b and 1 in "SI" in the owl monkey (Aotus trivirgatus) J. Comp. Neurol. 181:41-74.

Merzenich, M.M., Kaas, J.H., Wall, J.T., Nelson, R.J., Sur, M., and D. J. Felleman (1983a) Topographic reorganization of somatosensory cortical areas 3b and 2 in adult monkeys following restricted deafferentation. Neurosci. 10:33-55

Merzenich, M.M., Kaas, J.H., Wall, J.T., Sur, M., Nelson, R.J., and D. J. Felleman (1983b) Progression of change following median nerve section in the cortical representation of the hand in areas 3b and 1 in adult owl and squirrel monkeys. Neurosci. 10:639-665.

Merzenich, M.M., Jenkins, W.M., and J. C. Middlebrooks (1984a) Observations and hypotheses on special organizational features of the central auditory nervous system. IN: Dynamic Aspects of Neocortical Function. (eds. G. M. Edelman, W. E. Gall and W. M. Cowan). Wiley, New York, pp. 397-424.

Merzenich, M.M., Nelson, R.J., Stryker, M.P., Cynader, M.S., Schoppmann, A., and J. M. Zook (1984b) Somatosensory cortical map changes following digital amputation in adult monkey. J. Comp. Neurol. 224:591-605.

Merzenich, M.M., Nelson, R.J., Kaas, J.H., Stryker, M.P., Jenkins, W.M., Zook, J.M.Cynader, M.S., and A. Schoppmann (1987) Variability in hand surface representations in areas 3b and 1 in adult owl and squirrel monkeys. J. Comp.

Neurol. 258:281-296.

Merzenich, M.M., Recanzone, G.H., Jenkins, W.M., Allard, T.T., and R. J. Nudo (1988) Cortical representational plasticity. IN: Neurobiology of Neocortex. (eds. P. Rakic and W. Singer). Wiley, New York, pp. 41-67.

Merzenich, M.M., Recanzone, G.H., and Jenkins, W.M. (1990) How the brain functionally constructs its representations. IN: Natural and Artificial Parallel Computations. (eds. M. Arbib and J. A. Robinson) MIT Press, New York (in press)

Merzenich, M.M., Grajski, K.A., Jenkins, W.M., Recanzone, G.H., and B. Peterson (1991) Functional cortical plasticity. Cortical network origins of representational changes. Cold Spring Harbor Symp. Quant. Biol. 55 (submitted, 9/90)

Miyashita, Y (1988) Neuronal correlate of visual associative long-term memory in the primate temporal cortex. Nature 335:817-820.

Miyashita, Y., and H. S. Chang (1988) Neuronal correlate of pictorial short-term memory in the primate temporal cortex. Nature 331:68-70

Mountcastle, V.B. (1978) IN: The Mindful Brain: Cortical Organization and the Group Selective Theory of Higher Brain Function. G. M. Edelman and V. B. Mountcastle, MIT Press, Cambridge, MA.

Nelson, R. J., and V. D. Douglas (1989) Changes in premovement activity in primary somatosensory cortex differ when monkeys make hand movements in response to visual vs vibratory cues. Brain Res. 484:43-56.

Nudo, R.J., W. M. Jenkins and M. M. Merzenich (1990) Repetitive microstimulation alters the cortical representation of movements in adult rats. Somatosen. Motor Res. (in press)

Pearson, J.C., Finkel, L.H., and G. M. Edelman (1987) Plasticity organization of adult cerebral cortical maps: a computer simulation based on neuronal group selection. J. Neurosci. 7:4209-4233.

Pons, T.P., Garraghty, P.E., and M. Mishkin (1988) Lesion-induced plasticity in the second somatosensory cortex of adult macaques. Proc. Natl. Acad. Sci. 85:4279-5281.

Rakic, P., Bourgeois, J.P., Eckenhoff, M.F., Zecevic, N., and P. S. Goldman-Rakic (1986) Concurrent overproduction of synapses in diverse regions of the primate cerebral cortex. Science 232:232-235.

Recanzone, G., Allard, T.T., Jenkins, W.M., and M. M. Merzenich (1990) Receptive field changes induced by peripheral nerve stimulation in S1 of adult cats. J. Neurophysiol. 63:1213-1225

Recanzone, G.H., Jenkins, W.M., Hradek, G.H., and M.M. Merzenich (1991a) Progressive improvement in discriminative abilities in adult owl monkeys performing

a tactile frequency discrimination task. J. Neurophysiol. (submitted)

Recanzone, G.H., M.M. Merzenich, W. M. Jenkins, Grajski, K.A., and H. A. Dinse (1991b) Topographic reorganization of the hand representational zone in cortical area 3b paralleling improvements in frequency discrimination performance. J. Neurophysiol. (submitted)

Recanzone, G.H., M.M. Merzenich and W.M. Jenkins (1991c) Frequency discrimination training engaging a restricted skin surface results in an emergence of a cutaneous response zone in cortical area 3a. J. Neurophysiol. (submitted)

Recanzone G.H., M.M. Merzenich and C. S. Schreiner (1991d) Changes in the distributed temporal response properties of SI cortical neurons reflect improvements in performance on a temporally-based tactile discrimination task. J. Neurophysiol. (submitted)

Recanzone, G.H., H.A. Dinse and M. M. Merzenich (1991e) Expansion of the cortical representation of a restricted skin field in primary somatosensory cortex following intracortical microstimulation. Cerebral Cortex (submitted)

Robertson, D., and D. R. F. Irvine (1989) Plasticity of frequency organization in auditory cortex of guinea pigs with partial unilateral deafness. J. Comp. Neurol. 282:456-471

Rolls, E.T., Baylis, G.C., Hasselmo, M.E., and V. Nalwa (1989) The effect of learning on the face selective responses of neurons in the cortex in the superior temporal sulcus of the monkey. Exptl. Br. Res. 76:153-64.

Rollwarg, H.P., Muzio, J.N., and W. C. Dement (1966) Ontogenetic development of the human sleep-dream cycle. Science 152:604-607.

Sakamoto, T., Porter, L., and H. Asanuma (1987) Long-lasting potentiation of synaptic potentials in the motor cortex produced by stimulation of the sensory cortex in the cat: a basis of motor learning. Brain Res. 413:360-364.

Sanes, J.N., Sunder, S., and J. P. Donaghue (1990) Dynamic organization of primary motor cortex output to target muscles in adult rats. I. Long-term patterns of reorganization following motor or mixed peripheral nerve lesions. Exptl. Br. Res. 79:479-491.

Scheibel, A., Conrad, T., Perdue, S., Tomiyasu, U., and A. Wechsler (1990) A quantitative study of dendrite complexity in selected areas of the human cerebral cortex. Brain and Cognition 12:85-101

Sirevaag, A.M., and W. T. Greenough (1987) Differential rearing effects on rat visual cortex synapses. III. Neuronal and glial nuclei, boutons, dendrites and capillaries. Brain Res. 424:320-332.

Spitzer, H., Desimone, R., and Moran, J. (1988) Increased attention enhances both behavioral and neuronal performance. Science 140:338-340.

Van Essen, D., Felleman, D.J., DeYoe, E.A., Olavarria, J., and J. Knierim (1990)

Modular and hierarchical organization of extrastriate visual cortex in the macaque monkey. Cold Spring Harbor Symp. Quant. Biol. 55 (in press)

Venable, N., Fernandez, V., Diaz, E., and T. Pinto-hamuy (1989) Effects of preweaning environmental enrichment on basilar dendrites of pyramidal cells in occcipital cortex: A Golgi study. Devel. Br. Res. 49:140-144.

von der Malsburg, C., and Singer, W. (1988) Principles of cortical network organization. IN: Neurobiology of Neocortex. (eds. P. Rakic and W. Singer) John Wiley and Sons, New York. pp. 69-99.

Weinberger, N. M. and D. M. Diamond (1988) Dynamic modulation of the auditory system by associative learning. IN: Auditory Function: Neurobiological Bases of Hearing. (eds. G. M. Edelman, W. E. Gall and W. M. Cowan). Wiley, New York, pp. 485-512

Wilshaw, D.J., and C. von der Malsburg (1975) How patterned neural connections can be set up by self-organization. Proc. Royal Soc. Lond. B 194:432-445.

Woody, C.D., and J. Engel (1972) Changes in unit activity and thresholds to electrical microstimulation at coronal-pericruciate cortex of cat with classical conditioning of different facial movements. J. Neurophysiol. 35:230-241.

Yakolev, P.I., and A. R. Lecours. (1967) The myelogenetic cycles of regional maturation of the brain. IN: Regional Development of the Brain in Early Life. (ed. A. Minkowski). Blackwell Sci., Oxford, pp. 3-70.

Zecevic, N., Bourgeois, J.P. and P. Rakic (1989) Changes in synaptic density in motor cortex of rhesus monkey during fetal and postnatal life. Devel. Brain Res. 50:11-32.